EJNMMI Radiopharmacy and Chemistry 2024, **9**(Suppl 1):65
https://doi.org/10.1186/s41181-024-00294-8

EJNMMI Radiopharmacy and Chemistry

MEETING ABSTRACTS

Open Access

Meeting abstracts from the 21st European Symposium on Radiopharmacy and Radiopharmaceuticals

Coimbra, Portugal. 18-21 April 2024

Published: 18 September 2024

OP01

Improved PET imaging of NETs with [^{61}Cu]Cu-NOTA-TATE: a straightforward comparison with [^{61}Cu]Cu-/[^{68}Ga]Ga-DOTA-TATE

Alexandra I. Fonseca[1], Sara Almeida[1], José Sereno[2], Hugo Ferreira[3,4], Ivanna Hrynchak[1], Célia Gomes[3,4], Francisco Alves[2,5], Antero Abrunhosa[2]
[1]ICNAS Pharma, Ed. ICNAS, Polo das Ciências da Saúde, University of Coimbra, Coimbra, Portugal. [2]CIBIT/ICNAS, Institute for Nuclear Science Applied to Health, University of Coimbra, Coimbra, Portugal. [3]Faculty of Medicine, Coimbra Institute for Clinical and Biomedical Research (iCBR), University of Coimbra, Coimbra 3000-548, Portugal. [4]Center for Innovative Biomedicine and Biotechnology Consortium (CIBB), University of Coimbra, Coimbra 3000-548, Portugal. [5]Instituto Politécnico Coimbra, ESTeSC - Coimbra Health School, Coimbra, Portugal
EJNMMI Radiopharmacy and Chemistry 2024, **9(1)**: OP01

Aim: Copper-61 has attracted wide attention from both physicists and radiochemists in recent years due to its favorable physical decay properties (3.33 h half-life, 61.5% β+, Emax 1.22 MeV) and ease of production for PET imaging, as well as potential for radionuclide therapy with its therapeutic counterpart radionuclide copper-67 [1]. Herein, we performed a comparison of the stability, in vitro uptake, in vivo pharmacokinetic and imaging characteristics of the [^{61}Cu]Cu-labeled DOTA-TATE and NOTA-TATE compared with the clinical standard [^{68}Ga]Ga-DOTA-TATE in a preclinical model of a neuroendocrine tumor (NET).
Materials and methods: Copper-61 was produced via natural zinc liquid target irradiation using an IBA Cyclone 18/9 cyclotron, followed by post-processing [2,3]. The DOTA-TATE and NOTA-TATE conjugated peptides were labeled with copper-61, and the radiopharmaceuticals stability was assessed up to 6 h after EOS in both final formulation (15% EtOH/NaCl) and mice serum. In vitro evaluation of the cell uptake of the radiolabeled peptides was performed in pancreatic tumoral cell line AR42J to prove the specificity of the peptides towards the SST receptors (SSTr). Control and primary tumor-bearing mice were i.v. injected with the radiolabeled peptides and imaged in a micro-PET/MRI.
Results: The radiolabeling process of [^{61}Cu]Cu-DOTA-TATE and [^{61}Cu]Cu-NOTA-TATE resulted in high molar activity (18.5–37 GBq/μmol) and high radiochemical purity over 95%. Both gallium-68 and copper-61 labeled peptides exhibited increasing cellular uptake with time in AR42J cells that overexpress SSTr. Both [^{61}Cu]Cu-NOTA-TATE and [^{61}Cu]Cu-DOTA-TATE accumulated in AR42J tumors but to different extents. [^{61}Cu]Cu-DOTA-TATE show high uptake in non-targeted organs, such as the liver and gastrointestinal tract. Whereas [^{61}Cu]Cu-NOTA-TATE showed fast, primarily renal, clearance and low uptake in non-targeted organs at 1 h p.i. Tumor detectability was visually improved at 4 h p.i. for [^{61}Cu]Cu-NOTA-TATE, at this time point all the activity has cleared with only significant uptake in the tumor. Ex vivo biodistribution data confirmed the PET/MRI images, [^{61}Cu]Cu-NOTA-TATE have recorded the highest tumor uptake seen at 4 h p.i. (12.81 ± 0.99%ID/g, n = 3).
Conclusion: [^{61}Cu]Cu-NOTA-TATE had significant better biodistribution profile and imaging properties than [^{61}Cu]Cu-DOTA-TATE and showed similar biodistribution and pharmacokinetics to [^{68}Ga]Ga-DOTA-TATE at 1 h p.i., while showing enhanced imaging characteristics for late time point imaging. [^{61}Cu]Cu-NOTA-TATE showed to have promising characteristic to be translated to human clinical trials.

References

1. Fani M, Nicolas GP. 61Cu-Labeled Radiotracers: Alternative or Choice? J. Nucl. Med. 2023; 64(12): 1855–1857.
2. do Carmo SJC, Alves VH, Alves F, Abrunhosa AJ. Fast and cost-effective cyclotron production of 61Cu using a natZn liquid target: An opportunity for radiopharmaceutical production and R&D. Dalton Trans. 2017; 46: 14556–60.
3. Fonseca AI, Alves VH, Do Carmo SJC, Silva M, Hrynchak I, Alves F, et al. Production of GMP-Compliant Clinical Amounts of Copper-61 Radiopharmaceuticals from Liquid Targets. Pharm. 2022; 15(6).

OP02

Development of SPECT agent [^{99m}Tc]Tc-BQ0413 for PSMA visualization: preclinical evaluation and preliminary results of Phase I clinical study

Anna Orlova[1], Ekaterina Bezverkhniaia[1], Panagiotis Kanellopoulos[1], Anna Medvedeva[2], Mariia Larkina[3], Ruslan Varvashenya[3], Ayman Abouzayed[1], Anastasia Rybina[2], Maryam Oroujeni[1], Anzhelika Vorobyeva[1], Ulrika Rosenström[1], Vladimir Tolmachev[1], Vladimir Chernov[3]
[1]Uppsala University, Uppsala, Sweden. [2]Tomsk National Research Medical Center, Tomsk, Russia. [3]Siberian State Medical University, Tomsk, Russia
EJNMMI Radiopharmacy and Chemistry 2024, **9(1)**: OP02

Aim: Radionuclide imaging using radiolabelled inhibitors of prostate-specific membrane antigen (PSMA) can be used for staging of prostate cancer. We have designed a molecule BQ0413, which contains Glu-urea-Lys binding moiety, optimized linker structure including 2-napthyl-L-alanine and L-tyrosine [1], and mercaptoacetyl-triglutamate chelator for labelling with Tc-99m. The purpose of this study was to evaluate the imaging properties of [^{99m}Tc]Tc-BQ0413.
Materials and methods: Synthetically produced pseudo-peptide BQ0413 was labeled with technetium-99m. PSMA-transfected PC3-pip cells were used to evaluate [^{99m}Tc]Tc-BQ0413 target specificity and affinity. A whole body planar scintigraphy and SPECT/CT imaging were performed 2, 4, and 6 h after injection of 50 µg (680 ± 140 MBq) of [^{99m}Tc]Tc-BQ0413 in five patients with prostate cancer. Trial registration: ClinicalTrials.gov: NCT05839990
Results: [^{99m}Tc]Tc-BQ0413 bound specifically to PSMA-expressing cells with affinity 33 ± 15 pM. In tumor-bearing mice, the tumor uptake of [^{99m}Tc]Tc-BQ0413 (38 ± 6%IA/g in PC3-pip 3 h after injection of 40 pmol) was dependent on PSMA expression (0.9 ± 0.3%IA/g in PSMA-negative SKOV-3 tumors). The co-injection of 5 nmol of unlabeled BQ0413 enabled blocking of [^{99m}Tc]Tc-BQ0413 uptake in normal PSMA-expressing tissues without blocking the uptake in tumors that resulted in an appreciable increase in the tumor-to-organ ratios. In patients all injections of [^{99m}Tc]Tc-BQ0413 were well tolerated, no adverse events were registered. The stable physiological uptake of [^{99m}Tc]Tc-BQ0413 was observed in the lacrimal glands, salivary glands (2 h pi SUVmean 16 ± 8), liver (13 ± 2), spleen (12 ± 5), kidneys (21 ± 6), the elimination was predominantly renal. Activity uptake in clinicaly relevant organs (bones and muscles) was low and decreased with time (SUVmean < 1). An average effective dose was 0.007 ± 0.001 mSv/MBq. With the given activity, the radionuclide-associated dose burden per patient is 4-7 mSv/study. Uptake of [^{99m}Tc]Tc-BQ0413 in primary tumors was identified in 5/5 patients (2 h pi SUVmean 3.4 ± 1.4 [1.15–4.82]). Uptake in LN metastases was detected in four patients (SUVmean 6 ± 4 [1.72–10.19]), in bone metastases—in 2 patients (14 ± 16 [2,39-25,11]). Physiological uptake and uptake in cancer lesions did not changed with time significantly.
Conclusion: [^{99m}Tc]Tc-BQ0413 demonstrated specific binding to PSMA with binding affinity in low picomolar range. The intermediate results of the Phase I study show that injections of [^{99m}Tc]Tc-BQ0413 are well-tolerated, safe and associated with low absorbed doses. Imaging using [^{99m}Tc]Tc-BQ0413 enables visualization of primary prostate cancer lesions, as well as LN and bone metastases.
Reference

1. Lundmark F, Olanders G, Rinne SS, et al. Design, Synthesis, and Evaluation of Linker-Optimised PSMA-Targeting Radioligands. Pharmaceutics 2022, 14, 1098.

OP03

Folate-targeted polymeric micelles for image-guided drug delivery of an anticancer gold complex

Joana F. Santos[1*], Francisco Silva[2], Rafaela A.L. Silva[1], Dulce Belo[1,3], Lurdes Gano[1,3], Fernanda Marques[1,3], Célia Fernandes[1,3]
[1]C2TN Centro de Ciências e Tecnologias Nucleares, Instituto Superior Técnico, Universidade de Lisboa, Loures, Portugal. [2]Nuclear Medicine – Radiopharmacology, Champalimaud Foundation, Lisbon, Portugal. [3]Departamento de Engenharia e Ciências Nucleares, Instituto Superior Técnico, Universidade de Lisboa, Lisboa, Portugal
[*]**Corresponding author**: joana.f.santos@ctn.tecnico.ulisboa.pt

EJNMMI Radiopharmacy and Chemistry 2024, **9(1)**: OP03
Aim: The gold bisdithiolate complex, nBu$_4$N[Au(cdc)$_2$] (**1**), showed potential as a cytotoxic agent against ovarian cancer (OC) cells, demonstrating significantly less cross-resistance when compared with cisplatin[1]. However, its limited water solubility poses a challenge for clinical applications. To overcome this, a strategy involving the encapsulation of **1** in polymeric micelles (PMs) has been developed, increasing solubility and half-life blood circulation[2]. Moreover, to enhance specificity, the outer shell of the micelles can be functionalized with targeting ligands. Furthermore, radionuclides can be incorporated either in the outer shell or in the core of the micelles, for image-guided drug delivery. The most widely used technique involves the chemical modification of the micelles' shell with chelating agents (e.g.,DOTA, DTPA), conferring high stability[3]. However, this modification may impact the biodistribution and pharmacokinetics of the PMs. Therefore, a new strategy has been developed, in which the radionuclide is entrapped in the micellar core by forming a complex with a hydrophobic substance (e.g.,8-hydroxyquinoline), enabling in vivo imaging without altering the chemical structure of the nanoparticle[4]. Thus, we have designed PMs functionalized with folic acid (FA) carrying **1** and the [^{111}In]In/[^{67}Ga]Ga-oxine complex, for OC theranostics (Fig. 1).
Materials and methods: PMs with and without FA were synthesized by the thin-film hydration method, characterized by DLS/HPLC/UV-Vis and the release of [Au(cdc)$_2$]$^-$ was evaluated. MTT assays were performed to evaluate the cytotoxicity of the PMs in different OC cell lines, both sensitive (A2780, OVCAR3) and resistant (A2780CisR) to cisplatin. The micelles were labeled with [^{111}In]In/[^{67}Ga]Ga-oxine and their stability was evaluated. Biodistribution studies in normal mice were conducted.
Results: The PMs were obtained with suitable hydrodynamic diameter (< 200 nm) and high loading contents. Release studies demonstrated a controlled release of [Au(cdc)$_2$]$^-$ over time. Cytotoxicity studies revealed significant antiproliferative effects of the PMs towards OC cells, comparable to the free [Au(cdc)$_2$]$^-$. The [^{111}In]In/[^{67}Ga]-oxine complexes were obtained with high radiolabeling yield (≈80%) and radiochemical purity (RCP > 99%). Both functionalized and non-functionalized radiolabeled PMs were obtained with high yield (> 90%) and stability, retaining above 80% of [^{111}In]In/[^{67}Ga]Ga-oxine up to 72h in PBS and in cell culture medium. Biodistribution studies indicated slow blood clearance and prolonged circulation half-life in vivo. Cellular uptake studies with the radiolabeled micelles are underway.
Conclusion: Au(cdc)$_2$-containing PMs, with and without FA, were successfully synthesized and labeled with ^{111}In/^{67}Ga. Their significant cytotoxicity towards OC cells, suitable in vitro stability and promising in vivo behavior prompt them to be further explored for theranostic applications.

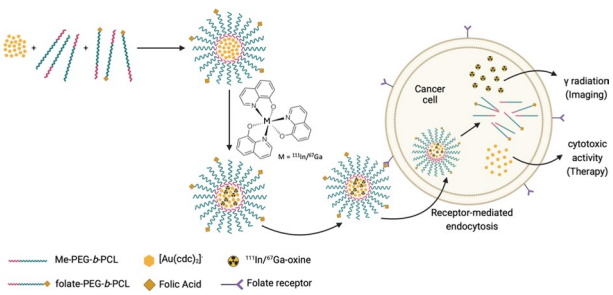

Fig. 1 A schematic representation of the proposed targeted polymeric micelles for image-guided drug delivery.

Acknowledgements
This work was supported by Fundação para a Ciência e Tecnologia, Portugal (projects PTDC/MED-QUI/1554/2020 and UID/

Multi/04349/2019). Joana F. Santos acknowledges the PhD grant PRT/BD/154612/2023.

References

1. Sousa SA, Leitão JH, Silva RAL, Belo D, Santos IC, Guerreiro JF, Martins M, Fontinha D, Prudêncio M, Almeida M, Lorcy D, Marques F. On the path to gold: Monoanionic Au bisdithiolate complexes with antimicrobial and antitumor activities. J Inorg Biochem. 2020; 202:110,904.
2. Sousa A, Santos JF, Silva F, Sousa SA, Leitão JH, Matos AP, Pinheiro T, Silva RAL, Belo D, Almeida M, Marques F, Fernances C. Antitumoral and Antimicrobial Activities of Block Copolymer Micelles Containing Gold Bisdithiolate Complexes. Pharmaceutics. 2023; 15(2):564
3. Hoang B, Reilly RM, Allen C. Block copolymer micelles target Auger electron radiotherapy to the nucleus of HER2-positive breast cancer cells. Biomacromolecules. 2012; 13(2):455–465
4. de la Fuente A, Kramer S, Mohr N, Pektor S, Klasen B, Bausbacher N, Miederer M, Zentel R, Rösch F. ^{68}Ga[Ga]-, ^{111}In[In]-oxine: a novel strategy of in situ radiolabeling of HPMA-based micelles. Am J Nucl Med Mol Imaging. 2019; 9(1):67–83

OP04

Development and characterization of ^{99m}Tc-labeled scFvD2B as a potential theranostic pair for ^{177}Lu-labeled scFvD2B

Emma Nascimbene[1], Laura Meléndez-Alafort[1], Carolina Gobbi[2], Guillermina Ferro-Flores[3], Blanca Ocampo-Garcia[3], Cristina Marzano[4], Barbara Spolaore[4], Giulio Fracasso[5], Antonio Rosato[1,6], Cristina Bolzati[2]
[1]Istituto Oncologico Veneto IOV-IRCCS, Padova, Italia. [2]Institute of Condensed Matter Chemistry and Energy Technologies, (ICMATE-CNR), Padova, Italia. [3]Instituto Nacional de Investigaciones Nucleares, Estado de México, Mexico. [4]Dipartimento di Scienze del Farmaco, Università degli Studi di Padova, Italia. [5]Dipartimento di Scienze Biomediche, Università degli Studi di Padova, Italia. [6]Dipartimento di Scienze Chirurgiche Oncologiche e Gastroenterologiche, Università degli Studi di Padova, Italia.

EJNMMI Radiopharmacy and Chemistry 2024, **9(1)**: OP04

Abstract published here: https://www.mdpi.com/1422-0067/25/1/492

OP05

^{111}In- and ^{161}Tb-labeled conjugates Carrying PSMA and Triphenylphosphonium Derivatives for Auger Therapy of Prostate Cancer

Joana F. Santos[1], Paula Raposinho[1,2], Frederik Cleeren[3], Irwin Cassells[3,4], Simon Leekens[3], Maarten Ooms[4], Michiel Van de Voorde[4], Christopher Cawthorne[5], Filipa Mendes[1,2],Célia Fernandes[1,2], António Paulo[1,2*]

EJNMMI Radiopharmacy and Chemistry 2024, **9(1)**: OP05

Aim: Nuclear DNA is the canonical target for biological damage induced by Auger electrons (AE) but other subcellular components might be also relevant for this purpose, such as the energized mitochondria of tumor cells, as we have proposed recently [1,2]. Having this in mind, we have designed dual-targeted radioconjugates carrying a PSMA inhibitor and a triphenyl phosphonium (TPP) group to promote a selective uptake by prostate cancer (PCa) cells and their accumulation in the mitochondria. For this purpose, we have considered the ^{111}In and ^{161}Tb-radionuclides aiming to compare the radiobiological effect of an AE emitter and a mixed AE and beta emitter, respectively.
Materials and methods: Novel DOTA-based chelators functionalized with PSMA-617 and TPP derivatives were synthesized and used to obtain the respective ^{111}In and ^{161}Tb-labeled complexes. The biological evaluation of the resulting radioconjugates compriese cellular uptake and internalization and PSMA-blocking studies in cell lines expressing different levels of PSMA, subcellular localization experiments, assessment of radiobiological effects in the same cell lines, as well as microSPECT imaging studies in PSMA-positive PCa xenografts.
Results: The dual targeted ^{111}In/^{161}Tb-labeled complexes displayed high cellular uptake and internalization in PSMA-positive PC3 PIP cells. Blocking studies confirmed the specificity of PSMA targeting. The dual-targeted complexes compromised cell survival in a dose-dependent manner, and in some cases to a higher extent than observed for the single targeted M-PSMA (M = ^{111}In, ^{161}Tb) congeners. MicroSPECT imaging studies with the ^{111}In-labeled complexes have shown that the TPP pharmacophore did not interfere with the excellent in vivo tumor uptake of a "golden standard" PSMA-617 derivative although leading to a higher kidney retention.
Conclusion: Dual-targeted ^{111}In/^{161}Tb-labeled complexes, combining the PSMA-617 and TTP moieties, showed a high and specific internalization in PSMA + PCa cells, a significant radiotoxicity in the same cell lines, and a specific and significant tumor uptake in PCa xenografts, emerging as promising tools for Auger therapy of cancer.

References

1. Bavelaar B.M. et al. Subcellular Targeting of Theranostic Radionuclides. Front. Pharmacol 2018; 9:996.
2. Santos J. F. et al. Synthesis and Preclinical Evaluation of PSMA-targeted 111In-Radioconjugates Containing a Mitochondria-Tropic Triphenylphosphonium Carrier. Mol. Pharmaceutics 2024; 21: 216-

Acknowledgements

This work was supported by Fundação para a Ciência e Tecnologia, Portugal (projects UID/Multi/04349/2019 and PTDC /MED-QUI/1554/2020). This project has received funding from the European Union's Horizon 2020 research and innovation programme under grant agreement No 101008571 (PRISMAP – The European medical radionuclides programme).

OP06

Sulfur Symphony: Capturing the Exotic Mercury-197m/g Auger Emitters with Macrocyclic S-Rich Chelators

Marianna Tosato[1,2,3,4*], Parmissa Randhawa[2,3], Shaohuang Chen[2,3], Valery Radchenko[3,5], Valerio Di Marco[1], Mattia Asti[4], Caterina F. Ramogida[2,3]
[1]Department of Chemical Sciences, University of Padova, Padova, Italy. [2]Department of Chemistry, Simon Fraser University, Burnaby, British Columbia, Canada. [3]Life Sciences, TRIUMF, Vancouver, British Columbia, Canada. [4]Radiopharmaceutical Chemistry Section, Nuclear Medicine Unit, AUSL-IRCCS Reggio Emilia, 42122 Reggio Emilia, Italy. [5]Department of Chemistry, University of British Columbia, British Columbia, Canada
[*]**Corresponding author**: marianna.tosato@ausl.re.it

EJNMMI Radiopharmacy and Chemistry 2024, **9(1)**: OP06

Aim: The recent interest in mercury radioisotopes, ^{197m}Hg (t1/2 = 23.8 h) and ^{197g}Hg (t1/2 = 64.14 h), has been sparked by the dual diagnostic and therapeutic nature of their decays. These isotopes emit γ-rays suitable for SPECT imaging and Auger electrons which can be exploited for treating metastatic tumors [1]. However, the clinical utilization of $^{197m/g}$Hg as a theranostic agent is hindered by the lack of chelating agents capable of securely binding them to tumor-seeking vectors. This contribution aims to address this challenge by investigating chemically tailored macrocyclic platforms with sulfur-containing side arms [2,3,4].
Materials and methods: To tackle the challenge, we conducted a comprehensive study encompassing aqueous coordination chemistry investigations through potentiometry, NMR spectroscopy, and DFT calculations, concentration- and temperature-dependent radiolabeling with cyclotron-produced [$^{197m/g}$Hg]Hg^{2+}, and in vitro stability assays.
Results: Our research reveals the crucial role of sulfur atoms in coordinating Hg^{2+}, emphasizing the profound influence of subtle modifications to the pendant arms or polyazamacrocyclic backbone. Among the investigated ligands, chelators based on the cyclen ring exhibited characteristics suitable for nuclear medicine applications. These chelators afforded eightfold coordinated complexes with the highest thermodynamic stability (logK > 32) and displayed the ability to quantitatively incorporate [$^{197m/g}$Hg]Hg^{2+} in mild reaction conditions (radiochemical yield > 99%, 50°C). Moreover, the complexes remained stable in human serum.
Conclusion: Through the identification of viable chelators and the elucidation of the impact of specific structural modifications, our research significantly contributes to addressing the scarcity of suitable chelating agents for $^{197m/g}$Hg. These findings hold immense promise for the potential in vivo application of mercury as a theranostic Auger-emitter radiometal when securely bound to tumor-seeking vectors.

References

1. Randhawa P, Olson AP, Chen S, Gower-Fry KL, Hoehr C, Engle JW, Ramogida C, Radchenko V. Meitner-Auger Electron Emitters for Targeted Radionuclide Therapy: Mercury-197m/g and Antimony-119, Curr. Radiopharm., 2021,14, 394–419.
2. Tosato M, Asti M, Dalla Tiezza M, Orian L, Haussinger D, Vogel R, Koster U, Jensen M, Andrighetto A, Pastore P, Di Marco V. Inorg. Chem., 2020, 59, 10,907–10919.
3. Tosato M, Pelosato M, Franchi S, Isse AA, May NV, Zanoni G, Mancin F, Pastore P, Badocco D, Asti M, Di Marco V. New J. Chem., 2022, 46, 10,012–10025.
4. Tosato M, Franchi S, Isse AA, Del Vecchio A, Zanoni G, Alker A, Asti M, Gyr M, Di Marco V, Mäcke H, Inorg. Chem. 2023, 62, 50, 20,621–20633.

OP07

Synthesis and preclinical evaluation of BOLD-100 labeled with ruthenium-97/103

B. Happl[1,2,3], M. Brandt[1,2,3,4], T. Balber[1,2,4], K. Benčurová[1,2], P. Heffeter[5,6], Z. Talip[7], A. Voegele[8], N. P. van der Meulen[7,8], C. Denk[9,10], J. M. Welch[10], J. H. Sterba[10], U. Köster[11], C. Alliot[12,13], A.-C. Bonraisin[14], F. Haddad[12,14], W. Kandioller[3,6], M. Mitterhauser[1,2,3,4], M. Hacker[2], B. K. Keppler[3,6], T. L. Mindt[1,2,3,4,*]

[1]Ludwig Boltzmann Institute Applied Diagnostics, General Hospital of Vienna, Währinger Gürtel 18-20, 1090 Vienna, Austria. [2]Division of Nuclear Medicine, Department of Biomedical Imaging and Image Guided Therapy, Medical University of Vienna, Währinger Gürtel 18-20, 1090 Vienna, Austria. [3]Institute of Inorganic Chemistry, Faculty of Chemistry, University of Vienna, Josef-Holaubek-Platz 2, 1090 Vienna, Austria. [4]Joint Applied Medicinal Radiochemistry Facility of the University of Vienna and the Medical University of Vienna, Vienna, Austria. [5]Center for Cancer Research and Comprehensive Cancer Center, Medical University of Vienna, Borschkegasse 8A, 1090 Vienna, Austria. [6]Research cluster "Translational Cancer Therapy Research", Währinger Strasse 42, 1090 Vienna, Austria. [7]Center for Radiopharmaceutical Sciences, Paul Scherrer Institute, Forschungsstrasse 111, 5232 Villigen–PSI, Switzerland. [8]Laboratory of Radiochemistry, Paul Scherrer Institute, Forschungsstrasse 111, 5232 Villigen–PSI, Switzerland. [9]Institut of Applied Synthetic Chemistry, Technische Universität (TU) Wien, Getreidemarkt 9, 1060 Vienna, Austria. [10]Center for Labelling and Isotope Production, TRIGA Center Atominstitut, TU Wien, Vienna, Austria. [11]Institut Laue-Langevin, 71 avenue des Martyrs, 38042 Grenoble Cedex 9, France. [13]GIP ARRONAX, 1 rue Aronnax, CS10112, 44817, Saint-Herblain Cedex, France. [14]CRCINA, Inserm/CNRS/Nantes Université, 8 quai Moncousu, 44007, Nantes Cedex 1, France. [15]Laboratoire Subatech, UMR 6457, IMT Nantes Atlantique/CNRS-IN2P3/Nantes Université, 4 Rue A. Kastler, BP 20722, 44307, Nantes Cedex 3, France

[*]**Corresponding author**: thomas.mindt@univie.ac.at

EJNMMI Radiopharmacy and Chemistry 2024, **9(1)**: OP07

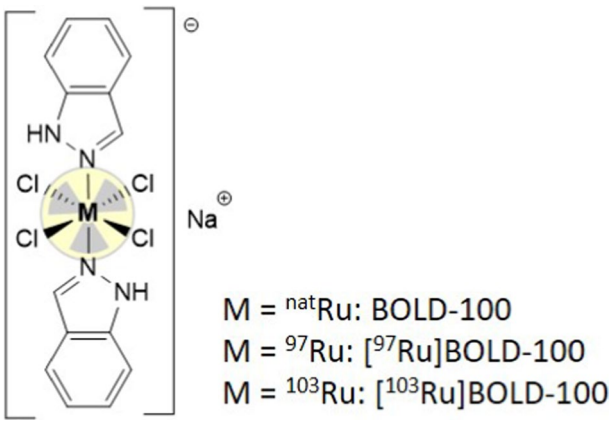

Fig. 1 The anticancer drug candidate BOLD-100 and its radiolabeled versions.

Aim: The first-in-class ruthenium-based chemotherapeutic agent BOLD-100 (Fig. 1) is currently the subject of clinical evaluation for the treatment of gastric, pancreatic, colorectal and bile duct cancer.[1,2] To study the mode of action and the pharmacokinetics of BOLD-100 as well as to enable a stratification of patients by nuclear imaging, a radiolabeled version of the compound could present a helpful diagnostic tool. We report herein a multi-center effort for radionuclide production and the radiosynthesis, quality control and in vitro/in vivo evaluation of isotopically labeled carrier added (c.a.) $^{97/103}$Ru-labeled BOLD-100.[3]

Materials and methods: The β⁻/γ-emitter ruthenium-103 was produced via ^{nat}Ru(n,γ)^{103}Ru and the γ-emitter ruthenium-97 via ^{nat}Mo(α,xn)^{97}Ru nuclear reactions by irradiation of ^{nat}Ru and ^{nat}Mo foil, respectively. Starting from solutions of c.a. [$^{97/103}$Ru]$RuCl_3$, c.a. [$^{97/103}$Ru]BOLD-100 was synthesized in three steps. Intermediates and products were characterized by comparison with the non-radioactive reference compound using HPLC and IR. The antiproliferative activities of [$^{97/103}$Ru]BOLD-100 were determined in human colon carcinoma (HCT116) and murine colon carcinoma (CT26) cell lines using the colorimetric MTT assay with an exposure time of 96 h. Biodistribution of c.a. [^{103}Ru]BOLD-100 in direct comparison with the non-radioactive drug BOLD-100 by ICP-MS were performed at two different doses (3 and 30 mg/kg, 0.76–3.80 MBq/mg, tail vein injection) in female Balb/c mice bearing CT26 allografts over 72 h.

Results: After multi-mg syntheses, c.a. ^{97}Ru- and ^{103}Ru-labeled BOLD-100 were obtained in 13 and 39% chemical yield, 8 and 35% radiochemical yield, > 99% radiochemical purity and at specific activities of 0.05 MBq/µmol and 2.1 MBq/µmol, respectively. The cytotoxicity (IC_{50}) of c.a. [^{103}Ru]BOLD-100 was unchanged in comparison to the non-radioactive drug BOLD-100 in both cell lines (3-digit µM). The biodistribution of c.a. [^{103}Ru]BOLD-100 was also found identical with those of BOLD-100, whereas injection of the lower dose resulted in a relatively higher tumor uptake (13% ID/g) and improved tumor-to-background imaging, in particular at later time points (e.g., tumor/muscle > 10).

Conclusion: ^{97}Ru- and ^{103}Ru-labeled BOLD-100 were successfully synthesized. In comparison to the non-radioactive drug BOLD-100, c.a. [^{103}Ru]BOLD-100 showed identical characteristics in vitro and in vivo, therefore demonstrating the high potential of the ^{97}Ru-analogous compound as a diagnostic tool for the stratification of patients for a therapy with the drug BOLD-100 by SPECT imaging.

References

1. Trondl, R., Heffeter, P., Kowol, C. R., Jakupec, M. A., Berger, W., Keppler, B. K. NKP-1339, the first ruthenium-based anticancer drug on the edge to clinical application. Chem. Sci., 2014, 5: 2925
2. NCT04421820, https://www.clinicaltrials.gov/, (accessed on 05.08.2023)
3. Happl, B., Brandt, M., Balber, T., Bencurová, K., Talip, Z., Voegele, A., Heffeter, P. Kandioller,W., Van der Meulen, N.P., Mitterhauser, M., Hacker M., Keppler B. K., Mindt T. L. Synthesis and Preclinical Evaluation of Radiolabeled [^{103}Ru]BOLD-100. Pharmaceutics 2023, 15: 2626

OP08

Nanobioconjugates of ^{109}Pd/^{109m}Ag in-vivo generators for targeted Auger electron therapy

Nasrin Abbasi Gharibkandi[1], Agnieszka Majkowska-Pilip[1], Rafał Walczak[1], Kamil Wawrowicz[1], Kinga Żelechowska-Matysiak[1], Aleksander Bilewicz[1]

[1]Institute of Nuclear Chemistry and Technology, Dorodna 16, 03-195 Warszawa, Poland

EJNMMI Radiopharmacy and Chemistry 2024, **9(1)**: OP08

Aim: In present work we propose an in-vivo ^{109}Pd/^{109m}Ag generator for combined β- and Auger electron therapy. ^{109}Pd decays by emitting β− particles with a half-life of 13.7 h to ^{109m}Ag (T1/2 = 39.6 s), which emits cascade of conversion and Auger electrons. Thus, ^{109m}Ag combined with ^{109}Pd creates the so-called in-vivo generator emitting more conversion and Auger electrons than well-known ^{161}Tb [1], and it can be easily produced by neutron irradiation of ^{108}Pd.

Materials and methods: ^{109}Pd was used for synthesis of 5 nm pegylated Pd nanoparticles. In the second option ^{109}Pd was immobilized on Au nanoparticles, forming core-shell Au@[^{109}Pd]Pd

nanoparticles. These nanoparticles were further modified with trastuzumab vector. The conjugate was characterized using TEM and DLS methods. Additionally, binding, internalization, and cytotoxicity using the MTS test were investigated.
Results: The HR-TEM images demonstrate a relatively uniform deposition of palladium atoms on the surface of AuNPs. Also in 5 nm nanoparticles most of the atoms are on the surface of the Pd nanoparticles. The formation of a thin layer of ^{109}Pd is crucial due to the extremely limited range of Auger electrons emitted by the ^{109}Pd/^{109m}Ag in-vivo generator. The results of retention experiments reveal that less than 10% of ^{109m}Ag is recoiled from the surface of AuNPs after the nuclear decay of ^{109}Pd. In vitro cell studies indicate specific binding of the ^{109}Pd-labeled trastuzumab bioconjugate to the Her2 receptor on SKOV-3 cells, with 90% internalization. Confocal images illustrate the accumulation of Au@[^{109}Pd]Pd-trastuzumab in the perinuclear area surrounding the cell nucleus. Despite the lack of nuclear localization, which is necessary to achieve an effective cytotoxic effect of Auger electrons, a substantial cytotoxic effect, significantly greater than that of pure β- emitters, was observed. We hypothesize that the cytotoxic effect of the Auger electrons could have also occurred through the damage of the cell nuclear membrane by Auger electrons emitted from nanoparticles accumulated in the perinuclear area.
In the case of 5 nm pegylated ^{109}Pd-labeled nanoparticles, we observed a much greater cytotoxic effect than in the case of ^{125}I immobilized on 5 nm Pd nanoparticles (Auger electron emission) and ^{131}I immobilized (β − emission).
Conclusion: The obtained results show that pegylated ^{109}Pd-labeled nanoparticles and trastuzumab-functionalized ^{109}Pd-labeled nanoparticles can be suitable for the application in combined β- Auger electron targeted radionuclide therapy. The cytotoxic effect is much greater than in similar systems with Auger electron emitters or β − radiation emitters.
Reference

1. Müller C, Umbricht CA, Gracheva N, Tschan VJ, Pellegrini G, Bernhardt P, Zeevaart JR, Köster U, Schibli R, van der Meulen NP. Terbium-161 for PSMA-targeted radionuclide therapy of prostate cancer. Eur J Nucl Med Mol Imaging. 2019;46:1919-1930

OP09

Synthesis, ^{68}Ga-labelling and in vitro evaluation of a PET/PDT agent for prostate cancer theranostics

Laurène Wagner[1]*, Ivan Hawala[1], Veronika Rosecker[1], Stephen M. Stribbling[2], Annah J. Wilson[1], Ross W. Boyle[3], Alexander J. MacRobert[4], Kerstin Sander[2], Graeme J. Stasiuk[1]
[1]Department of Imaging Chemistry & Biology, King's College London, London, United Kingdom. [2]Department of Chemistry, University College London, London, United Kingdom. [3]Department of Chemistry, University of Hull, Hull, United Kingdom. [4]Department of Surgical Biotechnology, University College London, London, United Kingdom
*__Corresponding author__: laurene.wagner@kcl.ac.uk

EJNMMI Radiopharmacy and Chemistry 2024, **9(1)**: OP09
Aim: Theranostic and personalized medicine have proven efficiency by associating diagnosis and treatment to improve patients' healthcare and provide early treatments. Theranostic in nuclear medicine allows the elaboration of an adapted treatment for the patient using dosimetry thanks to the same biodistribution of the diagnostic and therapeutic radiopharmaceuticals. Nevertheless, the therapeutic radiopharmaceutical can be taken up in healthy tissue which can lead to side effects and off-target toxicity.[1] To overcome this eventuality, the combination of a diagnostic modality such as positron emission tomography (PET) with photodynamic therapy (PDT) is a promising alternative.[2,3] The therapeutic effect is triggered by light irradiation after the injection of a photosensitiser (PS) resulting in site-specific cancer treatment and reduction of off-target toxicity. Herein, we propose to study a multimodal PET/PDT agent to diagnose prostate cancer and evaluate tumour uptake for efficiency in PDT (Fig. 1).
Materials and methods: A prostate specific membrane antigen (PSMA) recognition pattern was coupled to an acyclic chelating agent and a porphyrin as PS. This PET/PDT agent was labelled using gallium-68. Stability of the radio-conjugate was evaluated in the formulation solution and in 90% serum. Binding and uptake assays using DU145-PSMA ± cells were performed to determine the affinity of the PET/PDT agent to PSMA.
Results: The PET/PDT agent has been synthetised successfully. The impacts of multiple factors such as pH, buffer, temperature, and concentration of the ligand on the radiochemical conversion (RCC) have been studied. Good stability in formulation solution (94% intact) and serum (76% intact) over 2 h were observed (Fig. 2). DU145-PSMA + cell uptake was observed after 1 h incubation. Specificity to PSMA was confirmed using blockage study. These promising results allowed us to perform further in vitro and in vivo studies.
Conclusion: A PET/PDT theranostic agent has been successfully synthesised and labelled with gallium-68. The radio-conjugate showed good stability over two hours in serum and promising binding affinity to DU145-PSMA + cells. These promising results will be confirmed by PET preclinical trials. The suitability of this agent for PDT will be evaluated further with photophysical characterisation and in vitro/in vivo evaluation.

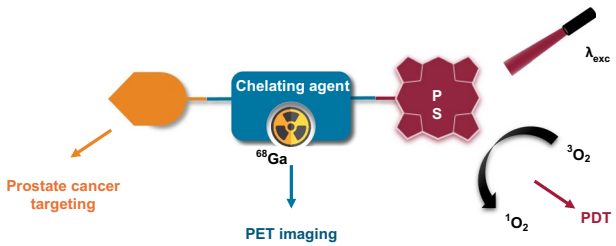

Fig. 1 PET/PDT agent composed of a chelating agent, a PS and a PSMA recognition pattern.

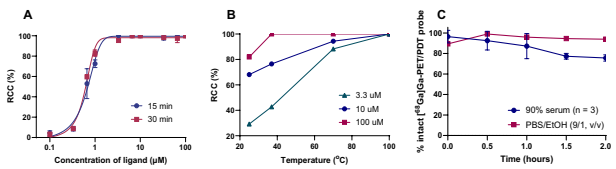

Fig. 2 ^{68}Ga-labelling studies of the PET/PDT agent. **A**. Impact of the ligand concentration of the RCC. **B**. Impact of the temperature of radiolabelling on the RCC. **C**. Stability in formulation solution and in vitro stability in 90% serum of [^{68}Ga]Ga-PET/PDT agent over 2 h.

Acknowledgements
We thank the EPSRC (EP/V027549/1 and EP/T026367/1) for funding this work.

References

1. Parihar AS, Chopra S, Prasad V. Nephrotoxicity after radionuclide therapies. Transl Oncol. 2022; 15(1):101,295.
2. Price TW, Yap SY, Gillet R, Savoie H, Charbonnière LJ, Boyle RW, et al. Evaluation of a Bispidine-Based Chelator for Gallium-68 and of the Porphyrin Conjugate as PET/PDT Theranostic Agent. Chem – Eur J. 2020; 26(34):7602–8.
3. Sandland J, Malatesti N, Boyle R. Porphyrins and related macrocycles: Combining photosensitization with radio- or optical-imaging for next generation theranostic agents. Photodiagnosis Photodyn Ther. 2018; 23:281–94.

OP10

Structure-based design, optimization and development of [^{18}F] F-SK60: A Novel PET radioligand for the imaging of mutated Isocitrate Dehydrogenase

Sarandeep Kaur[1,2*], Sladjana Dukic-Stefanovic[1], Winnie Deuther-Conrad[1], Magali Toussaint[1], Barbara Wenzel[1], Klaus Kopka[1,2], and Rareş-Petru Moldovan[1,2]

[1]Helmholtz-Zentrum Dresden-Rossendorf (HZDR), Institute of Radiopharmaceutical Cancer Research, Department of Neuroradiopharmaceuticals, Research Site Leipzig, 04318 Leipzig, Germany. [2]Faculty of Chemistry and Food Chemistry, School of Science, TU Dresden, 01069 Dresden, Germany

[*]**Corresponding author**: s.kaur@hzdr.de

EJNMMI Radiopharmacy and Chemistry 2024, **9(1)**: OP10

Aim: The mutated isocitrate dehydrogenase (mIDH1)—the most common alteration being the IDH1-R132H mutation—has become an important biomarker in patients with glioma, chondrosarcoma, cholangiocarcinoma and acute myeloid leukemia. Currently, invasive tissue sampling is required to detect mIDH1. The diagnosis, treatment planning, stratification and follow-up of patients would be improved by a noninvasive PET scan method for mIDH1. Until now, there is no PET radiotracer clinically available to target mIDH, therefore, we aimed at the development of a novel mIDH1 PET tracer. In this study, we developed [^{18}F]F-SK60 and are currently evaluating its ability to image mIDH1.

Materials and methods: A structural optimization study was performed on GSK321, a potent mIDH1 inhibitor [1]. This systematic investigation led to the development of SK60 which was radiofluorinated because of its high potency and selectivity towards the IDH1-R132H mutation. To develop [^{18}F]F-SK60, various reaction parameters were investigated, for instance: fluorination agents, solvent, temperature and molar ratios between precursor and copper complex. Internalization of [^{18}F]F-SK60 was determined in vitro using U251 human glioblastoma cells stably transfected with IDH1 and mIDH1-R132H mutation. The in vivo metabolic stability was investigated in female CD-1 mice at 30 min post-injection (p.i) of [^{18}F]F-SK60. The ex vivo biodistribution at 5, 15, 30 and 60 min (n = 3) and dynamic PET scan studies (60 min) were investigated in healthy female CD-1 mice.

Results: The structural optimization and medicinal chemistry on GSK321 resulted in SK60 which has an IC_{50} of 14.5 ± 3.3 nM and 374 ± 59 nM towards IDH1-R132H mutation and IDH1 respectively. Compound [^{18}F]F-SK60 was successfully synthesized by copper-mediated radiofluorination from the respective boronic pinacol ester. In vivo studies conducted in healthy female CD-1 mice, exhibited the excellent metabolic stability of [^{18}F]F-SK60, with parent fractions of 80% and 100% in plasma and brain at 30 min p.i., respectively. The ex vivo biodistribution studies and dynamic PET scan showed a low brain uptake (0.6% ID/g 15 min p.i.) and hepato-biliary excretion of [^{18}F]F-SK60 in healthy mice.

Conclusions: Overall, a novel series of fluorinated IDH1-R132H mutation inhibitors has been developed from this study. Consequently, [^{18}F] F-SK60 was successfully developed and preclinically evaluated in vivo in healthy mice. In general, our results promote the assessment and further modification of [^{18}F]F-SK60 for better brain permeation to enhance the non-invasive detection of glioma and other tumors associated with IDH1-R132H mutation.

Reference

1. Okoye-Okafor UC, Bartholdy B, Cartier J, Gao EN, Pietrak B, Rendina AR, Rominger C, Quinn C, Smallwood A, Wiggall KJ, Reif AJ, Schmidt SJ, Qi H, Zhao H, Joberty G, Faelth-Savitski M, Bantscheff M, Drewes G, Duraiswami C, Brady P, Groy A, Narayanagari SR, Antony-Debre I, Mitchell K, Wang HR, Kao YR, Christopeit M, Carvajal L, Barreyro L, Paietta E, Makishima H, Will B, Concha N, Adams ND, Schwartz B, McCabe MT, Maciejewski J, Verma A, Steidl U. New IDH1 mutant inhibitors for treatment of acute myeloid leukemia. Nat Chem Biol. 2015 Nov;11(11):878-86.

OP11

Molecular Imaging of HER2 Expression in Breast Cancer Using DARPin [^{123}I]I-$(HE)_3$-G3. From mice to Phase I.

Vladimir Tolmachev[1*], Olga Bragina[2,3], Roman Zelchan[2,3], Maria Larkina[3,4], Ruslan Varvashenya[3], Lufti A Hasnowo[3], Anna Orlova[1], Alexey Schulga[3,5], Anzhelika Vorobyeva[1], Elena Konovalova[3,5], Sergey Deyev[3,5], Vladimir Chernov[2,3]

[1]Uppsala University, Uppsala, Sweden. [2]Cancer Research Institute, Tomsk National Research Medical Center, Tomsk, Russia. [3]Research Centrum for Oncotheranostics, Tomsk Polytechnic University, Tomsk, Russia. [4]Siberian State Medical University, Tomsk, Russia. [5]Shemyakin-Ovchinnikov Institute of Bioorganic Chemistry, Russian Academy of Sciences, Moscow, Russia

EJNMMI Radiopharmacy and Chemistry 2024, **9(1)**: OP11

Aim: DARPIns are small (14-18 kDa) robust scaffold proteins suitable for radionuclide molecular imaging. We demonstrated in preclinical experiments, that DARPin G3, which was labelled with [^{99m}Tc]Tc$(CO)_3$ or directly radioiodinated, provides high-contrast specific imaging of HER2-expressing xenografts in mice (1). The use of radioiodination provided much lower accumulation of activity in liver and kidneys. Phase I clinical study has shown that radionuclide imaging using [^{99m}Tc]Tc$(CO)_3$-$(HE)_3$-G3 is safe (2). The aim of this study was a Phase I evaluation of [^{123}I]I-$(HE)_3$-G3.

Materials and methods: This was a prospective Phase I diagnostic study (ClinicalTrials.gov Identifier: NCT05923177). The study was performed in patients with untreated primary breast cancer. At the time of the submission of this report, seven patients were recruited. DARPin $(HE)_3$-G3 was labelled with ^{123}I using Chloramine-T. The injected activity was 222 ± 70 MBq. The mass of the injected protein was adjusted to 3 mg. No blocking of Na/I symporter was performed. Planar scintigraphy was performed 2, 4, 6, 24 and 48 h, after injection. SPECT/CT was done at 2, 4, 6 h. Dosimetry was calculated using OLINDA/EXM 1.1.

Results: The isolated yield of [^{123}I]I-$(HE)_3$-G3 was 90-93%, and the radiochemical purity was 99-100%. No adverse events were registered after injection of [^{123}I]I-$(HE)_3$-G3. The organs with the highest uptake (over 3% of injected activity) were kidney, lungs, mammary glands, stomach wall and liver. The highest absorbed doses were to thyroid, adrenals, ovaries and kidneys (0.79 ± 0.34, 0.17 ± 0.06, 0.11 ± 0.03, and 0.069 ± 0.007, respectively). The effective dose was 0.08 ± 0.02 mSv/MBq. For comparison, the effective dose for [^{99m}Tc]Tc$(CO)_3$-$(HE)_3$-G3 was 0.011 ± 0.004 mSv/MBq. The uptake (SUVmax) in HER2-positive lesions with high (3+) HER2 expression (primary and lymph node metastases) was over 7.5, while for low expression tumors SUVmax was below 3.3. Comparison with the clinical data for [^{99m}Tc]Tc$(CO)_3$-$(HE)_3$-G3 (2) shows that the use of direct radioiodination reduces activity uptake in liver and kidneys, but the extent of such reduction was smaller than in preclinical models.

Conclusion: Injections of [^{123}I]I-$(HE)_3$-G3 are safe. The use of [^{123}I] I-$(HE)_3$-G3 may enable discrimination between breast cancer lesions with high and low HER2 expression.

References

1. Deyev S, Vorobyeva A, Schulga A et al. Comparative Evaluation of Two DARPin Variants: Effect of Affinity, Size, and Label on Tumor Targeting Properties. Mol Pharm. 2019;16: 995–1008
2. Bragina O, Chernov V, Schulga A, et al. Phase I Trial of 99mTc-(HE)3-G3, a DARPin-Based Probe for Imaging of HER2 Expression in Breast Cancer. J Nucl Med. 2022; 63: 528–535.

OP12

Fully automated production of [^{18}F]FB-labeled single-domain antibodies: the immune-checkpoint TIGIT for PET imaging

Herlinde Dierick[1,2], Katty Zeven[1], Laurent Navarro[3], Tony Lahoutte[1,2], Nick Devoogdt[1], Vicky Caveliers[1,2], Jessica Bridoux[1]
[1]Vrije Universiteit Brussel (VUB), Molecular Imaging and Therapy Research Group (MITH), Brussels, Belgium. [2]Vrije Universiteit Brussel (VUB), Universitair Ziekenhuis Brussel (UZ Brussel), Nuclear Medicine Department, Brussels, Belgium.[3]Precirix NV, Brussels, Belgium
EJNMMI Radiopharmacy and Chemistry 2024, **9(1)**: OP12

Aim: Radiofluorination of single-domain antibodies (sdAbs) via *N*-succinimidyl-4-[^{18}F]fluorobenzoate ([^{18}F]SFB) has shown to be a promising strategy for developing PET tracers. Although [^{18}F]SFB automation has been reported, automating protein conjugation proves challenging. Herein we report the fully-automated, cartridge-based production, on a single synthesis module of [^{18}F]FB-anti-human T-cell Ig and ITIM domain receptor (hTIGIT) sdAb. TIGIT is an immune checkpoint (ICP) which exhibits an unfavourable prognostic association with various cancer types. Non-invasive techniques to quantify and monitor TIGIT expression could facilitate patient stratification and play a role in the development of next generation of ICP blockade therapeutics.
Materials and methods: [^{18}F]FB-hTIGIT sdAb was produced on an AllinOne® synthesizer (Trasis). [^{18}F]SFB was produced in a 3-step, 1-pot reaction, purified via HLB cartridge and eluted with ethanol. Next, the ethanolic [^{18}F]SFB was incubated with the anti-hTIGIT sdAb (5,5 mg) for 30 min at room temperature in 0.1M CHES buffer pH = 8,6–9. The radiolabelled sdAb was purified using three disposable desalting Hitraps in series and collected in a final formulation of 5 mg/mL Na-ascorbate in NaCl 0,9%. Radiochemical purity (RCP) of [^{18}F]FB-hTIGIT sdAb was performed by size-exclusion chromatography. The affinity of the tracer towards hTIGIT was assessed via enzyme-linked immuno sorbent assay (ELISA) with recombinant hTIGIT protein and flow cytometry on hTIGIT overexpressing cells. µPET/CT-imaging and tracer biodistribution were performed in immunodeficient mice bearing both negative and hTIGIT-positive TC-1 lung carcinoma tumours.
Results: [^{18}F]FB-hTIGIT sdAb (> 5 GBq) was obtained after fully automated production (1h35min), with a RCP > 95%, apparent molar activity > 15 GBq/µmol and decay-corrected radiochemical yield of 10 ± 3% (n = 4). In vitro assays showed that the radiofluorinated sdAb had nanomolar affinity towards hTIGIT, both on protein and cells (K_D = 2.7nM; K_D = 7.22nM) (Fig. 1). Ex vivo biodistribution at 1h10 after tracer administration (17.369 ± 0.276MBq; 26 ± 2µg; n = 4) indicated three times higher uptake in positive versus negative tumours (Fig. 2) and fast kidney excretion (14.06 ± 1.97%IA/g), as confirmed by PET imaging (Fig. 3).

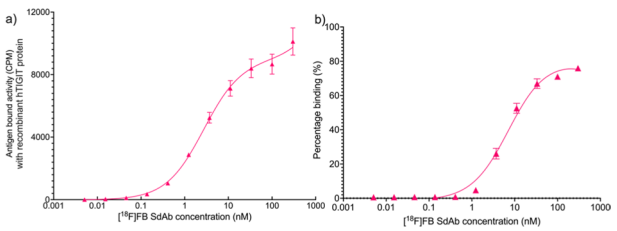

Fig. 1 Binding affinity determined by (**a**) ELISA (K_D = 2.7nM); (**b**) flow cytometry (KD = 7.22nM).

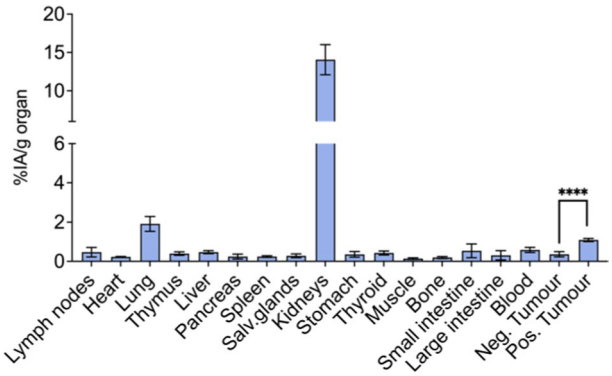

Fig. 2 Ex vivo biodistribution at 1h10 after tracer administration.

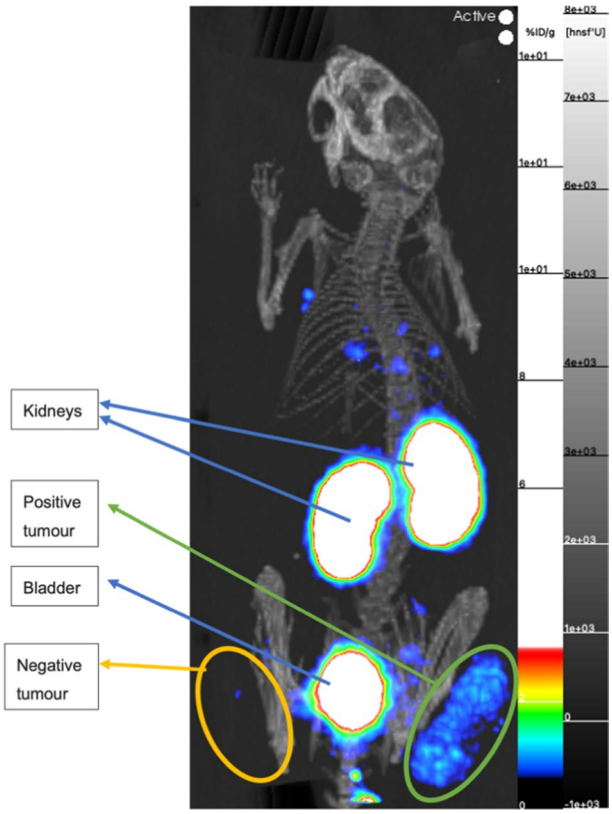

Fig. 3 PET/CT imaging at 1h after tracer administration.
Conclusion: A fully-automated production of radiofluorinated sdAb was developed on a commercially available synthesis module. While we prepared the tracer for preclinical use, this process allows for GMP-production of [^{18}F]FB-sdAbs for clinical translation. [^{18}F]FB-hTIGIT sdAb showed a favourable biodistribution pattern which, together with the nanomolar affinity, makes it a promising PET tracer.

OP13

A novel [^{18}F]AlF-labeled radiotracer for in vivo imaging of CXCR4 using positron emission tomography

Muriel A. Spahn[1], Tom Van Loy[2], Sofie Celen[3], Michel Koole[3], Christopher Cawthorne[3], Christophe M. Deroose[3], Dominique Schols[2], Wim Vanduffel[4], Guy Bormans[1], Frederik Cleeren*[1]
[1]Laboratory for Radiopharmaceutical Research, Department of Pharmaceutical and Pharmacological Sciences, KU Leuven, Leuven, Belgium. [2]Laboratory of Virology and Chemotherapy, Department of Microbiology, Immunology and Transplantation, KU Leuven, Leuven, Belgium. [3]Nuclear Medicine and Molecular Imaging, Department of Imaging and Pathology, KU Leuven, Leuven, Belgium. [4]Laboratory for Neuro- and Psychophysiology, KU Leuven Medical School, Leuven, Belgium
*__Corresponding author__: frederik.cleeren@kuleuven.be

EJNMMI Radiopharmacy and Chemistry 2024, **9(1)**: OP13

Aim: CXCR4 is a chemokine receptor overexpressed in cancer, like multiple myeloma, yet only [^{68}Ga]Ga-PentixaFor is used for clinical PET imaging. Nevertheless, the demand for ^{18}F-labeled CXCR4 radiotracers is growing. Here, we report a novel LY2510924 [1]-based ^{18}F-labeled CXCR4 tracer, [^{18}F]AlF-NOTA-SC (Fig. 1) [2].

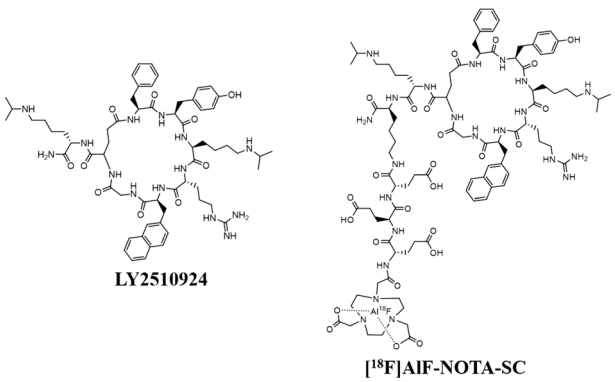

Fig. 1 Schematic structure of LY2510924 (left) and [^{18}F]AlF-NOTA-SC (right).

Materials and methods: The CXCR4 affinity (IC50) was assessed by incubating CXCR4 overexpressing Jurkat cells with the non-radioactive compounds and CXCL12AF647. The NOTA-SC peptide was labeled with [^{18}F]AlF and radioactive cell-binding assays were conducted on MM.1S, U87.MG and U87 cells overexpressing CD4/CD4.CXCR4/CD4.ACKR3 or CD4.CCR5. Receptor specificity was assessed by blocking with non-structurally related competitors such as AMD3100 (CXCR4 antagonist), Maraviroc (CCR5 antagonist), VUF11207 (ACKR3 agonist) or LY2510924 (self-block). The biodistribution was assessed in naïve mice and xenografted mice with U87.CD4 and U87.CD4.CXCR4 (dual subcutaneous) or MM.1S (subcutaneous and systemic) tumors using dynamic µPET/CT (60 min) and ex vivo biodistribution (75 min p.i.). Finally a PET/MRI study was performed in a non-human primate (NHP).

Results: IC50 values of 14.3 ± 2.6nM and 8.6 ± 1.1nM(n = 3) were obtained for [^{nat}F]AlF-NOTA-SC and [^{nat}Ga]Ga-PentixaFor, respectively. [^{18}F]AlF-NOTA-SC was labeled with a RCY of 28.4 ± 6.7%, RCP of 98.6 ± 0.7% and molar activity of 16.4 ± 3.4 GBq/µmol(n = 10). The total-bound fraction on U87.CD4.CXCR4 cells resulted in 7.1 ± 0.5% of administered activity (AMD3100 blocking by 58%) and 2.46 ± 0.13% on MM.1S cells (AMD3100 blocking by 31%). [^{18}F]AlF-NOTA-SC showed a high uptake in U87.CD4.CXCR4 tumors (Standardized Uptake Value (SUV) 3.04 ± 0.65, 75 min p.i.) and in MM.1S tumors (SUV 1.95 ± 0.06), compared to the U87.CD4 tumors (SUV 0.04 ± 0.00) or the AMD3100 blocked MM.1S tumor (SUV 0.06). In the systemic MM.1S model [^{18}F]AlF-NOTA-SC accumulated in multifocal lesions in the femurs, spine and skull (Fig. 2E). In the NHP [^{18}F]AlF-NOTA-SC displayed a moderate uptake in the bone marrow and spleen and a high uptake in kidneys and the left adrenal gland (putative aldosterone-producing adenoma) [3].

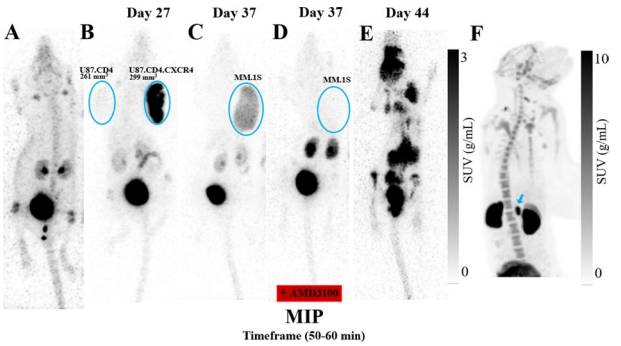

Fig. 2 Whole body maximum intensity projection image (50-60min p.i.) of [^{18}F]AlF-NOTA-SC in naïve mice (A), NHP (F) and mice xenografted with U87.CD4/U87.CD4.CXCR4 (dual subcutaneous model) (B), MM.1S (subcutaneous model) without (C) and with (D) administration of AMD3100 (5mg/kg i.p. 15 min before injection) or MM.1S (systemic model, IV injection) (E).The subcutaneous tumors are circled in blue and time of scanning post tumor cells inoculation is indicated. The blue arrow in the NHP scan indicates a suspected aldosterone-producing adrenal adenoma [3]..

Conclusion: [^{18}F]AlF-NOTA-SC showed in vitro and in vivo CXCR4 specific uptake and is a promising ^{18}F-labeled radiotracer for CXCR4 PET imaging.

References

1. Peng SB, Zhang X, Paul D, et al. Identification of LY2510924, a novel cyclic peptide CXCR4 antagonist that exhibits antitumor activities in solid tumor and breast cancer metastatic models. Mol Cancer Ther. 2015;14(2):480–490.
2. Kwon D, Takata K, Zhang Z, et al. Targeting Refractory Mantle Cell Lymphoma for Imaging and Therapy Using C-X-C Chemokine Receptor Type 4 Radioligands. Clin Cancer Res. 2022;28(8):1628–1639.
3. Zheng Y, Long T, Peng N, et al. The Value of Targeting CXCR4 With ^{68}Ga-Pentixafor PET/CT for Subtyping Primary Aldosteronism. J Clin Endocrinol Metab. 2023;109(1):171–182.

OP14

Radioiodinated closo-dicarbadodecaborane(12)-based cyclooxygenase-2/5-lipoxygenase inhibitors

Jonas Schädlich[1,2], Martin Ullrich[1], Cathleen Haase-Kohn[1], Sebastian Braun[3], Bettina Hofmann[4], Dieter Steinhilber[4], Klaus Kopka[1,2], Evamarie Hey-Hawkins[3], Jens Pietzsch[1,2], Markus Laube[1]
[1]Institute of Radiopharmaceutical Cancer Research, Helmholtz-Zentrum Dresden-Rossendorf (HZDR), Dresden, Germany. [2]Faculty of Chemistry and Food Chemistry, School of Science, Technische Universität Dresden, Dresden, Germany. [3]Faculty of Chemistry and Mineralogy, Universität Leipzig, Leipzig, Germany. [4]Institute of Pharmaceutical Chemistry, Johann Wolfgang Goethe-Universität Frankfurt, Frankfurt, Germany

EJNMMI Radiopharmacy and Chemistry 2024, **9(1)**: OP14

Aim: Cyclooxygenase-2 (COX-2) and 5-lipoxygenase (5-LO) convert arachidonic acid to prostanoids and leukotrienes respectively. Both enzymes are involved in tumorigenesis and show overexpression in cancer which makes them promising targets for radioligands [1,2]. Herein, we present radioiodination of two dual COX-2/5-LO inhibitors featuring a *closo*-dicarbadodecaborane(12) moiety as metabolically stable phenyl mimetic and the results of preliminary *in vitro* and *in vivo* investigations.

Materials and methods: Enzyme inhibition of I-1 and I-2 (Fig. 1) was determined using a fluorescence-based COX assay. 1 and 2 were radioiodinated using chloramine-T and purified by semipreparative HPLC followed by solid-phase extraction. Radiotracer formulations contained ascorbic acid (AA) or gentisic acid (GA). Stability in ethanol, isotonic saline (0.9% NaCl), phosphate-buffered saline pH 7.4 (PBS) and

human plasma was investigated for up to 11 h. Cell uptake studies were performed using U87 glioblastoma, U87 COX-2–knockout, and A2058 melanoma cells. Distribution in U87 tumour-bearing NMRI-nu/nu mice was investigated using single-photon emission computed tomography (SPECT).

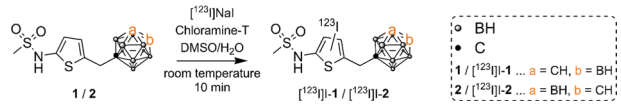

Fig. 1 Radioiodination of 1 and 2.

Results: Radiosynthesis gave high radiochemical yield (41–67%). Radiochemical purity (RCP) depended on addition of antioxidants (none 62–100%, AA > 88%, GA > 97%). Formulations in EtOH were stable for more than 10 h at room temperature. In isotonic saline and PBS, radiodeiodination was decelerated by antioxidants. Radiotracers exhibited stability during incubation with human plasma (RCP > 95% up to 5 h at 37°C with GA). Cell uptake was observed and partially blocked by inhibitors of COX-2 and 5-LO. A SPECT imaging pilot study showed tracer excretion via hepatobiliary and renal routes within 2 h, and thyroid uptake resulting mainly from residual [^{123}I]iodide in the tracer formulation. Furthermore, [^{123}I]I-2 formulated with AA, but not GA, showed uptake in the marginal region of COX-2-positive tumours 24 h after injection (maximum standardised uptake value $SUV_{max} = 9.1$).

Conclusion: Two radioiodinated *closo*-dicarbadodecaborane(12)-based COX-2/5-LO inhibitors were characterised *in vitro* and underwent first explorative SPECT studies *in vivo*. Interestingly, binding of [^{123}I]I-2 at the marginal tumour region was observed in presence of AA but not GA, potentially indicating partial specificity by blocking COX-2 in GA-treated mice. Further investigations, such as an intact cell 5-LO assay and *in vivo* experiments, will allow to validate these initial observations and to assess the applicability of COX-2/5-LO inhibitors as tumour radiotracers.

References

1. Hashemi Goradel N, et al. J Cell Physiol. 2019;234(5):5683–99.
2. Moore GY, et al. Int J Mol Sci. 2017;18(2):236–52.

OP15

Synthesis, stability determination and radiolabeling of new diazabenzene-based azamacrocycles with barium-131, actinium-225, lanthanum-133, and lead-212

Magdalena K Blei [1,3*], Björn Drobot2, Sven Stadlbauer[1], Klaus Kopka[1,3], Jérôme Kretzschmar[2], Constantin Mamat[1,3]
[1]HZDR – Institute of Radiopharmaceutical Cancer Research, Dresden, Saxony, Germany. [2]HZDR – Institute of Resource Ecology, Dresden, Saxony, Germany. [3]TU Dresden – Faculty of Chemistry and Food Chemistry, Dresden, Saxony, Germany
EJNMMI Radiopharmacy and Chemistry 2024, **9(1)**: OP15

Aim: The radium isotopes radium-223/-224 with their diagnostic gamma emitter barium-131 (SPECT) are ideal candidates for targeted alpha therapy. However, in order to use radium as + 2 metal ion in radioconjugates, it must be stably bound. The chelator macropa (mcp) has been found to form the most stable complexes so far, but they are not stable enough for in vivo applications.[1,2] Therefore, novel macrocyclic chelators based on macropa were developed with an additional application for lanthanum, actinium, and lead radionuclides.

Materials and methods: Starting from the diazamacrocycle K2.2, 4 new chelators were prepared in which the picolinic acid side arm was replaced by 3 regioisomeric diazabenzenes with carboxylic acid moiety. All new tendentate chelators and nonradioactive metal complexes were synthesized and characterized by NMR spectroscopy. The stability of the complexes was determined using ITC and radiolabeling was performed with barium-131, lanthanum-133, actinium-225 and lead-212.

Results: The 4 pym chelators were obtained in yields ranging from 19 to 74% including deprotection. Compared to Ba-mcp, a higher stability was found for all Ba-pym complexes. For barium-131, quantitative radiolabeling of all pym chelators was possible down to c = 10 µM, and for actinium-225, lanthanum-133, and lead-212 down to c = 0.1 µM. In competition experiments with the new radiometal complexes using 50 mM EDTA, consistently higher complex stabilities were found in contrast to the respective mcp complexes (barium-131: > 99% intact complex down to 0.1 mM; actinium-225, lanthanum-133 and lead-212: > 99% intact complex down to 0.1 µM).

Conclusion: Four new pym chelators were synthesized, which show a higher stability than macropa due to their modification. They are therefore better suited for complexation with barium-131, as well as for actinium-225, lanthanum-133 and lead-212 and thus also have the potential to form more stable radium-223 complexes.

References

1. Abou DS, Thiele NA, Gutsche NT, Chem. Sci. 2021, 12, 3733–3742.
2. Reissig F, Bauer D, Ullrich M, Pharmaceuticals 2020, 13, 272.

OP16

Evaluation of sydnones-based click chemistry for the labeling with heavy radiohalogens

Ludovic Le Saux[1,2*], Ferid Haddad[2,3], Jean-François Gestin[1], Romain Eychenne[1,2], François Guerard[1]
[1]Nantes Université, Inserm, CNRS, Université d'Angers, CRCI2NA, Nantes, France. [2]Groupement d'Intérêt Public ARRONAX, 1 rue Aronnax, F-44817 Saint-Herblain, France. [3]Laboratoire Subatech, IN2P3-CNRS, IMT Atlantique, Nantes Université, 4 rue Alfred Kastler, F-44307, Nantes, France
EJNMMI Radiopharmacy and Chemistry 2024, **9(1)**: OP16

Aim: Iodine and astatine exhibit several radioisotopes of interest for nuclear medicine whether for imaging or therapy.[1] Bioorthogonal chemistry appears as an interesting alternative to conventional bioconjugation as it is compatible with biological systems and can interact without interfering with natural biochemical processes. Previous work published by our team demonstrated that the use of bioorthogonal systems based on reactions such as CuAAC, SPAAC or IEDDA could significantly improve the radiolabeling of proteins with iodine-125 or astatine-211.[2] The aim of the present study was to further explore the potential of click chemistry for radiohalogenation by assessing sydnone/cyclooctyne couple as potential substrates.[3,4] The objective was to identify the most interesting bioorthogonal systems in terms of radiolabeling efficiency and reaction kinetics.

Materials and methods: Several iodinated reference sydnones (substituted with aryl or alkyl group in N_3 position and/or chlorinated in C_4 position) were prepared in order to evaluate the impact on reaction kinetics with clickable model peptides modified with DBCO (4) or BCN (5) moieties. A kinetic study with non-radioactive sydnones (1a-3a) was performed to determine rate constant of the reaction on cyclooctyne-modified peptides. Reaction kinetics of same bioorthogonal systems were also investigated with radioiodinated sydnones (1b-3b) obtained from the corresponding arylboronic precursors. Comparison of both studies allowed identification of the most reactive systems for a potential application.

Results: All sydnones ^{125}I labeling reactions were quantitative and all ^{125}I-labeled compounds were obtained with > 99% radiochemical purity. Non-radioactive reactions showed similar profiles than radioactive kinetic studies for all systems. As expected, *N*-alkylsydnone (1a, 1b) showed slow kinetic reaction with 0 to 8% radiochemical yields (RCY) after 60 min, as anticipated by non-radioactive experiments with constant rate of 0.04 to 0.10 $M^{-1}.s^{-1}$. *N*-aryl version (2a, 2b) with a hydrogen in C_4 position demonstrated a promising coupling efficiency with DBCO-peptide (RCY > 95% after 60 min) when results were more moderate with BCN-peptide (17%). Once again same tendency was obtained in non-radioactive measurements with values of 5.67 and 0.32 $M^{-1}.s^{-1}$ with DBCO-peptide and BCN-peptide, respectively. Finally, *N*-arylchlorosydnone (3a, 3b) appeared to be more reactive

than all other systems with RCY > 95% after 60 min for both DBCO and BCN systems confirming high constant rates measured (k = 5.69-6.02 $M^{-1}.s^{-1}$).

Conclusion: In this work, results obtained from the non-radioactive kinetic study allowed good prediction of trends obtained for the radiolabeling experiments. Most promising bioorthogonal systems (*N*-arylsydnone/DBCO, *N*-arylchlorosydnone/DBCO and *N*-arylchlorosydnone/BCN) were identified, and are considered for a transposition with astatine-211 and biomolecules radiolabeling.

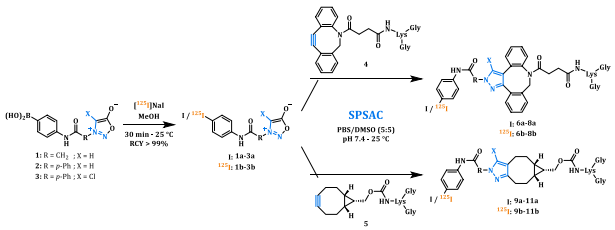

Fig. 1 Structure of sydnones considered in this study for the labeling of clickable model peptides.

References

1. Eychenne R, Chérel M, Haddad F, Guérard F, Gestin JF. Overview of the Most Promising Radionuclides for Targeted Alpha Therapy: The "Hopeful Eight". Pharmaceutics. 2021;13(6):906.
2. Navarro L, Berdal M, Chérel M, Pecorari F, Gestin JF, Guérard F. Prosthetic groups for radioiodination and astatination of peptides and proteins: A comparative study of five potential bioorthogonal labeling strategies. Bioorg Med Chem.2019;27(1):167-74.
3. Plougastel L, Koniev O, Specklin S, Decuypère E, Créminon C, Buisson DA, Wagner A, Kolodych S, Taran F. 4-Halogeno-sydnones for fast strain promoted cycloaddition with bicyclo-[6.1.0]-nonyne.Chem Commun. 2014;50(66):9376-8.
4. Decuypère E, Plougastel L, Audisio D, Taran F. Sydnone–alkyne cycloaddition: applications in synthesis and bioconjugation. Chem Commun. 2017;53(84):11,515-27.

OP17

From Theory to Clinical Application: Understanding Ac-225 radiochemistry through [^{225}Ac]Ac-DOTA-TATE

Eline L. Hooijman[1,2], Jan R. de Jong[1], Alfred Morgenstern[3], Frank Bruchertseifer[3], Erik de Blois[1]*
[1]Erasmus MC, Department of Radiology and Nuclear Medicine, 3015 CN Rotterdam, The Netherlands. [2]Erasmus MC, Department of Hospital Pharmacy, 3015 CN Rotterdam, The Netherlands. [3]Joint Research Centre, European Commission, 76344 Karlsruhe, Germany
***Corresponding author**: r.deblois@erasmusmc.nl

EJNMMI Radiopharmacy and Chemistry 2024, **9(1)**: OP17

Aim: Since interest in treatment with ^{225}Ac-labelled peptides is growing in the field of nuclear medicine, optimal labelling conditions and quality control (QC) of such radiopharmaceuticals is of great importance. Consequently, this research aims to define reaction parameters essential for optimal labelling and robust quality control of ^{225}Ac-labelled radiopharmaceuticals, exemplified by [^{225}Ac]Ac-DOTA-TATE.

Materials and methods: Determination of the quality of different ^{225}Ac sources was performed by evaluating the radionuclidic purity with HP-Ge-detector and quantification of metal-ions (ingrowth) using UPLC-analysis at different time points (1-4 weeks after dissolving). [^{225}Ac]Ac-DOTA-TATE was labelled under standardized conditions (90 kBq/nmol, 35 mM ascorbate, pH = 4) as a reference. Radiochemical yield (RCY) was monitored according to previous work [1]. For radiolabeling the parameters: pH, molar activity, (90kBq/nmol-270kBq/nmol) and labelling volume (100-2000 µL) buffering (0.1-1M TRIS (pH = 9), 0.1-1M Na-Ac (pH = 5)) and quencher (ascorbic acid, cysteine, vanilin and L-methionine) were tested. Radiochemical purity (RCP) is based upon an indirect measurement approach. HPLC-method was optimized and different parameters such as: gradient slopes, recovery/carry and volume per fractions was tested. Other characteristics like microwave heating and storage conditions like dry-ice and -20°C were monitored on HPLC (t0, t4 and t24h).

Results: Three different ^{225}Ac sources were tested and contained different amounts (< 5%) of metal impurities (Fe, Zn, Cu); however, all sources were suitable for radiolabeling, up to 2 weeks after dilution. Standardized radiolabeling of DOTA-TATE with ^{225}Ac was performed successfully, resulting in a RCY > 99% and RCP > 90% up to 24h. 20 min 90°C resulted high incorporation, longer heating times showed no improvement. A positive effect on stability could be observed when buffering with 0.1M TRIS, using ascorbate (35 mM, pH = 5.8) and ethanol (10% v/v). The HPLC-method as published previously [2] showed a good separation profile for [^{225}Ac]Ac-DOTA-TATE, varying the slope and concentration of the mobile phases showed no improvement. It has to be noted that for optimal recovery and carry over, in depth analysis and modifications to the HPLC-system and column, including injection parameters, are required. Furthermore, increased stability was observed when stored on dry-ice and when the molar activity was reduced as well as when the labelling volume was increased.

Conclusion: This research underlines the importance of validating the different radiolabeling conditions for alpha-radionuclides such as ^{225}Ac, as well as the appropriate quality control for implementation towards the clinic.

References

1. Hooijman, E.L., et al., Development of [^{225}Ac]Ac-PSMA-I&T for Targeted Alpha Therapy According to GMP Guidelines for Treatment of mCRPC. Pharmaceutics, 2021. 13(5).
2. de Blois, E., et al., Characteristics of SnO2-based ^{68}Ge/^{68}Ga generator and aspects of radiolabelling DOTA-peptides. Applied Radiation and Isotopes, 2011. 69(2): p. 308–315.

OP18

Radiolabelling of various macrocyclic ligands using ^{155}Tb/^{156}Tb radioisotopes

Mátyás Fodor[1,2], Károly Brezovcsik[2], Balázs Váradi[1,2,3], Gyula Tircsó[3], Zoltán Szűcs[2]
[1]Doctoral School of Chemistry, University of Debrecen, Debrecen, Hungary. [2]Radiochemical Laboratory, Institute for Nuclear Research, Debrecen, Hungary. [3]Department for Physical Chemistry, University of Debrecen, Debrecen, Hungary
***Corresponding author**: fermium@atomki.hu

EJNMMI Radiopharmacy and Chemistry 2024, **9(1)**: OP18

Aim: Horizon Europe is the European Union's research and innovation program, aiming to support research and innovation. Oncology is one of the key fields that Horizon Europe primarily supports, underlining the importance of theranostic agent research. Developing a radiopharmaceutical labelled with ^{155}Tb/^{161}Tb isotope pair would offer a perfect theranostic agent. The aim of our research was to synthesize bifunctional chelators (BFCs) for Tb^{3+} ion complexation based on macrocyclic ligand platforms with good Ln^{3+} ion labelling characteristics. By coupling these BFCs to taxi molecules (peptides, affibodies etc.) our long term goal is the simultaneous targeting and treatment of cancer, the exact type of which depends on the chosen taxi molecule.

Materials and methods: Macrocyclic chelators derived from rigid pyclen macrocycle (see Fig. 1. for the structural formulas, while their full IUPAC name can be found in the Abbreviations section) were synthesized and their Tb^{3+} labelling efficiency was studied as a function of pH, chelator concentration, time and temperature.

Various terbium isotopes were produced via cyclotron, using a proton beam to irradiate [^{nat}Gd]Gd_2O_3 solid target. ^{155}Tb and ^{156}Tb were used in the experiment, as isotopes with shorter half-lives (^{154m}Tb, ^{154g}Tb) decayed during purification steps. Purification was done using strong cation exchange resin (AG 50w-X8) with 2-hydroxyisobutyric acid (α-HIBA) as the eluent following literature References [3].

150 µL solutions were created of pH = 6 buffered Tb^{3+} solution with 2MBq activity of ^{155}Tb/^{156}Tb, and the chelators mixed in 200 µL HPLC vials, and the reaction was followed for up to a day, in most cases 240 min. Complexation was followed by HPLC method using an Agilent 1260 Infinity II system with GINA 12 software. For detection a RayTest Gabi scintillation Radiodetector and multichannel UV/vis detector was utilized.

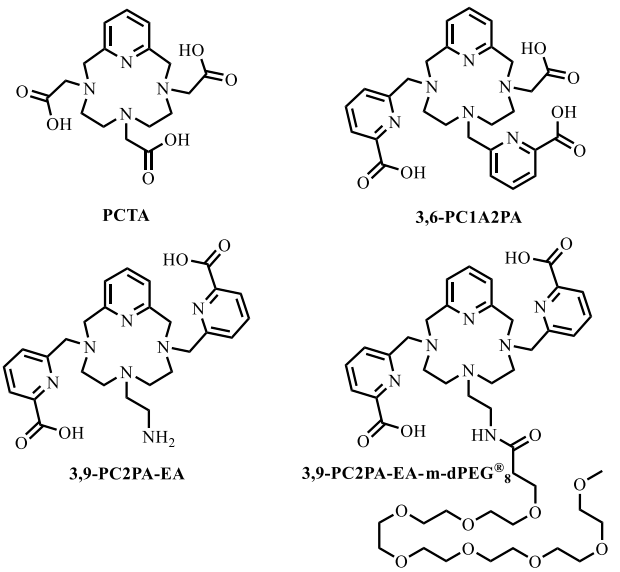

Fig. 1 The investigated macrocyclic chelator molecules.

Results: At 100 µmol/L chelator concentrations, labelling efficacy of 32 ± 4.2% to 95 ± 1.5% was achieved for the various chelator molecules, at pH = 6, 25°C under 240 min. At 10 µmol/L, same experimental conditions the best labelling efficacy achieved was less than 20%. Notably PCTA had the fastest and highest labelling efficacy of the selected molecules. The most promising molecule of the developed PCTA derivatives is 3,6-PCA2PA, with 60 ± 3.5% labelling efficiency achieved in 240 min.

Conclusion: While PCTA might seem more favorable due to a better labelling yield, structural restrictions make 3,6-PCA$_2$PA a better candidate for conjugation with the selected affibody vector molecule. Based on the results the authors are linking 3,6-PCA2PA to an affibody, to obtain the needed molecule for labelling with ^{152}Tb (PET)-^{161}Tb (β^-, Auger e^-) theranostic isotope pair. This will allow animal studies to be carried out, collaborating with colleagues from several European countries.

Reference

1. Cristina Müller et al. A Unique Matched Quadruplet of Terbium Radioisotopes for PET and SPECT and for α- and β^--Radionuclide Therapy: An In Vivo Proof-of-Concept Study with a New Receptor-Targeted Folate Derivative. Journal of Nuclear Medicine 2012; 53:12. 10.2967/jnumed.112.107540.

OP19

^{11}C-carboxylations using Grignard reactions for the preparation of [carbonyl-^{11}C]WAY-100635 and Sodium [1-^{11}C]Acetate

Vanessa A. Tomé[1*], Ângela C. B. Neves[1], Antero J. Abrunhosa[1,2,3]
[1]ICNAS Pharma, Unipessoal, Lda., University of Coimbra, Coimbra, Portugal. [2]Coimbra Institute for Biomedical Imaging and Translational Research (CIBIT), University of Coimbra, Coimbra, Portugal. [3]Institute for Nuclear Sciences Applied to Health (ICNAS), University of Coimbra, Coimbra, Portugal

EJNMMI Radiopharmacy and Chemistry 2024, **9(1)**: OP19

Aim: Cyclotron-produced [^{11}C]carbon dioxide ([^{11}C]CO_2), the most important and versatile primary labeling precursor, can directly be used for the ^{11}C-carboxylation of organic molecules. The direct carboxylation of Grignard reagents with [^{11}C]CO_2 enables the synthesis of ^{11}C-labeled carboxylic acids which have been shown to be useful for the synthesis of functionalised radiopharmaceuticals [1]. In this line, two of the most important Grignard reaction's applications are the preparation of the well known carbon-11 labeled PET-tracers, [carbonyl-^{11}C]WAY-100635 and Sodium [1-^{11}C]Acetate. Nevertheless, the implementation of Grignard reactions is a challenging task. Grignard reagents are very suitable in carbon-11 radiochemistry as they are great nucleophiles for [^{11}C]CO_2. As of consequence, they readily react with atmospheric carbon dioxide, which lowers the molar activity of the final product, being necessary to develop a leak proof, anhydrous, free of air apparatus, constructed with efficient handling and well-controlled flow rates [2,3]. In a general way, such limitations narrow the applicability of these PET-tracers worldwide.

The aim of this work was the development and implementation of reliable synthesis for ^{11}C-carboxylations and subsequent ^{11}C-acylations (only for [carbonyl-^{11}C]WAY-100635) via the modification of commercially available radiosynthesis modules housed in ICNAS Pharma.

Materials and methods: [^{11}C]CO2 was produced by the nuclear reaction ^{14}N(p,α)^{11}C on a IBA Cyclone 18/9 cyclotron. The produced [^{11}C]CO_2 was transferred, through lines, to the Synthra [^{11}C]Choline® commercial module and was delivered by a stream of helium into Synthra reactor containing the Grignard reagent at room temperature. The further reactions and product´s purification were performed on IBA Synthera® Extension and/or Trasis AllinOne automated modules.

Results: In this work, we were able to build a reliable set-up using the commercially available Synthra C11 Choline, IBA Synthera® Extension and Trasis AllinOne automated modules for the routine production of [carbonyl-^{11}C]WAY 100635 and Sodium [1-^{11}C]Acetate. Using this step-up, we achieved the [carbonyl-^{11}C]WAY-100635 with radiochemical yields of 21.6 ± 11% (EOB, d.c.) with a synthesis time of 45 min. [1-^{11}C] Sodium Acetate was obtained with radiochemical yields of 41 ± 8% (n.d.c.) within 35 min. Moreover, the quality of the both PET-tracers was analysed and both PET-tracers passed through all the tests (e.g. appearance, pH, radiochemical purity, chemical purity, radionuclidic purity and residual solvents) assuring its high purity and enabling its use in preclinical and clinical studies.

Conclusion: Modifications and implementation of ^{11}C-carboxylations on commercially available automated modules were successful and straightforward. The set-up´s general applicability was demonstrated using 2 different Grignard compounds in the present work.

References
1. Taddei C, Gee AD. Recent progress in [^{11}C]carbon dioxide ([^{11}C]CO_2) and [^{11}C]carbon monoxide ([^{11}C]CO) chemistry. J Label Compd Radiopharm. 2018; 61:237–251.
2. Rotstein, BH, Liang, SH, Holland, JP, Collier, TL, Hooker, JM, Wilson, AA, Vasdev, N. [^{11}C]CO_2 Fixation: A Renaissance in PET Radiochemistry. Chem. Commun. 2013, 49: 5621–5629.
3. Bongarzone S, Raucci N, Fontana IC, Luzi F, Gee AD. Carbon-11 carboxylation of trialkoxysilane and trimethylsilane derivatives using [^{11}C]CO_2. Chem Commun (Camb). 2020; 56(34):4668–4671.

OP20

Preclinical evaluation of [^{11}C]HSP990 as novel Hsp90 PET brain probe for in vivo visualization of Hsp90 in healthy aging and neurodegeneration

Romy Cools[1], Koen Vermeulen[2], Cassis Varlow[3], Neil Vasdev[3], Guy Bormans[1]
[1]Laboratory for Radiopharmaceutical Research, Department of Pharmacy and Pharmacological Sciences, KU Leuven, Leuven, Belgium. [2]Radiobiology Unit & NURA, Belgian Nuclear Research Centre (SCK CEN), Mol, Belgium. [3]Centre for Addiction and Mental Health (CAMH) & University of Toronto, Canada.

EJNMMI Radiopharmacy and Chemistry 2024, **9(1)**: OP20

Aim: The molecular chaperone Hsp90 plays a crucial role in the protein quality control system, maintaining protein homeostasis under stress conditions[1]. Aberrant Hsp90 function is linked to various neurodegenerative disorders[2]. Hsp90 brain PET with [^{11}C]HSP990 may contribute to clinical investigations and drug development by enabling the study of Hsp90 occupancy, disease monitoring and therapeutic outcomes.
Materials and methods: In vitro saturation binding assays were performed using [^{3}H]HSP990 on homogenate samples of healthy vs. TgP301L mice, healthy vs. TgF344-AD rat and healthy vs. human AD brain tissue. Ex vivo biodistribution of [^{11}C]HSP990 was evaluated in healthy rodents at baseline conditions and after pre-treatment (30 min pre-tracer, ip) with HSP990 (5mg/kg) and SNX-0723 (5mg/kg). In vivo brain uptake was assessed by dynamic PET studies in healthy rats after combined pre-treatment with Onalespib (30mg/kg, 30 min pre-tracer, ip) and HSP990 or SNX-0723 (5mg/kg, 5 min pre- or 30 min post-tracer, iv). Full body dynamic PET scans were performed on APP^{NL-G-F} and healthy age-matched control mice. Dynamic PET brain scans with arterial blood sampling were acquired in a rhesus monkey at baseline blocking (HSP990, 1mg/kg, 5 min pre-tracer, iv) conditions.
Results: Brain homogenate binding assays revealed a B_{max} value of 33 ± 3 pmol/mg protein in healthy human brain tissue, and is notably lower than reported Hsp90 expression values, suggesting that the tracer only binds to a sub-fraction of the Hsp90 pool in brain. Moreover, B_{max} values were significantly lower in AD brain tissue compared to healthy controls, while affinity (K_d) remained unchanged. Biodistribution showed saturable Hsp90 tracer binding in brain, bone marrow and blood cells in healthy rodents and in vivo PET studies demonstrated Hsp90-specific reversible tracer binding in healthy rat brain. Reduced in vivo [^{11}C]HSP990 brain uptake was observed in AD mice compared to age-matched controls (Fig. 1). Finally, high and sustained [^{11}C]HSP990 uptake was observed in cortical brain regions of a rhesus monkey and arterial blood sampling confirmed the presence of a saturable Hsp90 binding pool in the blood cell fraction (Fig. 1).
Conclusion: This study shows that despite the abundant and ubiquitous expression of Hsp90, distinct saturable Hsp90 binding pools are present in blood cells, bone marrow and brain of healthy animals. Moreover, a reduced amount of saturable Hsp90 was observed in AD brain compared to healthy controls, confirming a potential role of Hsp90 in AD. Clinical evaluation of [^{11}C]HSP990 PET is warranted to explore the translatability of these findings to humans.

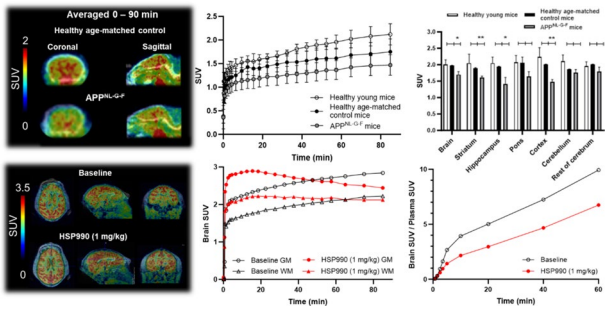

Fig. 1 Dynamic PET brain imaging using [^{11}C]HSP990 in APP^{NL-G-F} versus healthy age-matched control mice and a healthy rhesus monkey.

References
1. Hoter A, El-Sabban ME, Naim HY. The HSP90 family: Structure, regulation, function, and implications in health and disease. Int J Mol Sci. 2018;19.
2. Lackie RE, Maciejewski A, Ostapchenko VG, Marques-Lopes, Jose Choy, Wing-Yiu Duennwald, ML, Prado VF, Marco P. The Hsp70/Hsp90 Chaperone Machinery in Neurodegenerative Diseases. Front Neurosci. 2017;11:254.

OP21

Radiolabeling of M13 bacteriophages for in vivo imaging

Johanna Trommer[1*], Jan Kučka[2], Silvia Vercellino[3,4], Valentina Castagnola[3,4], Alberto Danielli[5], Matteo Calvaresi[6], Luděk Šefc[7], Fabio Benfenati[3,4], Klaus Kopka[1,8], Kristof Zarschler[1]
[1]Institute of Radiopharmaceutical Cancer Research, Helmholtz-Zentrum Dresden-Rossendorf (HZDR), Bautzner Landstrasse 400, 01328 Dresden, Germany. [2]Institute of Macromolecular Chemistry, Academy of Sciences of the Czech Republic, Heyrovského nám. 2, 162 06 Prague 6, Czech Republic. [3]Center for Synaptic Neuroscience and Technology, Istituto Italiano Di Tecnologia, Largo Rosanna Benzi 10, 16132, Genoa, Italy. [4]IRCCS, Ospedale Policlinico San Martino, Largo Rosanna Benzi 10, 16132, Genoa, Italy. [5]Molecular Biotechnology Lab, University of Bologna, Via Selmi 3, 40126, Bologna, Italy. [6]Dipartimento di Chimica "Giacomo Ciamician", Alma Mater Studiorum—Università di Bologna, Via Selmi 2, 40126 Bologna, Italy. [7]Center for Advanced Preclinical Imaging (CAPI), First Faculty of Medicine, Charles University, Salmovska 3, Praha 2, 120 00 Czech Republic. [8]Faculty of Chemistry and Food Chemistry, School of Science, Technische Universität Dresden, Mommsenstraße 4, 01062 Dresden, Germany
[*]**Corresponding author**: j.trommer@hzdr.de

EJNMMI Radiopharmacy and Chemistry 2024, **9(1)**: OP21

Aim: Parkinson's disease is caused by degeneration of nigro-striatal dopaminergic neurons and denervation of the target neurons in the neostriatum. The resulting disruption of dopaminergic modulation produces an imbalance between antagonistic pathways in the basal ganglia leading to rigidity, tremor, and bradykinesia [1]. One state-of-the-art treatment option is the so called deep-brain-stimulation (DBS), whereby an electrode is implanted to re-equilibrate the nervous pathways. Though highly effective, DBS is linked to a complex surgical procedure and can lead to adverse neurological effects [2,3]. The goal of this project is to enable a selective stimulation of striatal dopaminoceptive neurons from outside the brain through polymeric photovoltaic nanoparticles which are transported to the neostriatum using engineered M13 bacteriophage as nanocarrier. To monitor its biodistribution in the organism, the engineered bacteriophages are going to be radiolabeled.

Materials and methods: To allow the radiolabeling with a radiometal, a chelator has to be conjugated to the bacteriophage. Phage conjugates with different chelators were produced, but stability analysis by agarose gel electrophoresis revealed a significantly increased and unexpected aggregation of the radiolabeled conjugates, in comparison to the unconjugated phage, when incubated with 50% human serum. To address this problem and avoid aggregation, a chelator-free radiolabeling approach was chosen instead, by radioiodination of the tyrosine residues using [^{123}I]NaI and Iodogen.
Results: The achieved radiochemical purity was > 96% and the molar activity was 11 MBq/pmol. Stability analysis using agarose gel electrophoresis indeed revealed a low aggregation in serum. C57BL mice were intravenously injected with ~ 30 MBq/mouse of [^{123}I]I-M13 and imaged with SPECT/CT after 20 min, 40 min, 60 min and 18 h. A high amount of activity was observable in the heart of the mice over the whole duration of the experiment, indicating circulation of bacteriophages. In the necropsy after 18 h, a portion of 15% of the activity was still found in the blood. Another accumulation was observed in the lungs, however the signal originated from the blood circulation in the organ, which was confirmed by the necropsy. After 18 h, 5% of the activity was also found in the thyroid, indicating moderate deiodination over time. According to blood samples collected over time the biological half-life was calculated to be ~ 9 h.
Conclusion: In this study, for the first time the successful radioiodination of M13 bacteriophages using [^{123}I]NaI is described. Using the radioiodinated M13, the biodistribution of the phages was studied in vivo and a striking long serum half-life of the [^{123}I]I-M13 was discovered.

References

1. Balestrino R and Schapira A H V. Parkinson Disease. Eur. J. Neurol. 2020; 27: 27–42.
2. Stoker T B et al. Emerging Treatment Approaches for Parkinson's Disease. Front. Neurosci. 2018; 12:693.
3. Krack P et al. Deep Brain Stimulation in Movement Disorders: From Experimental Surgery to Evidence-Based Therapy. Mov. Disord. 2019; 34:12.

OP22

Synthesis, in vitro and in vivo evaluation of novel radioligands for α-synuclein PET

Špela Korat[1,2], Pedro M. Mateus[1,2], Ran Sing Saw[3], Kristina Herfert[3], Wissam Beaino[1,2], Benny Bang-Andersen[4], Iwan J. P. de Esch[5], Danielle J. Vugts[1,2], Albert D. Windhorst[1,2]
[1]Amsterdam UMC location Vrije Universiteit Amsterdam, dept Radiology & Nuclear Medicine, De Boelelaan 1117, 1081HV Amsterdam, The Netherlands;. [2]Amsterdam Neuroscience, Brain imaging, Amsterdam, The Netherlands. [3]Werner Siemens Imaging Center, Department of Preclinical Imaging and Radiopharmacy, Eberhard Karls University Tübingen, Tübingen, Germany. [4]H. Lundbeck A/S, Valby, Denmark. [5]Division of Medicinal Chemistry, Amsterdam Institute for Molecules, Medicines and Systems, VU Amsterdam, De Boelelaan 1108, 1081HV Amsterdam, The Netherlands
EJNMMI Radiopharmacy and Chemistry 2024, **9(1)**: OP22

Aim: Aggregates of α-synuclein are a hallmark of several neurodegenerative diseases, including Parkinson's disease (PD) and multiple system atrophy (MSA).1 Non-invasive quantitative assessment of α-synuclein in vivo using positron emission tomography (PET) could provide valuable insights into the early diagnosis, however a suitable PET tracer does not exist.2 This study aims to design, synthesize and radiolabel new compounds with high affinity and specificity for α-synuclein and evaluate them as potential PET tracers.3
Materials and methods: Based on a pharmacophore model3, a series of potential α-synuclein binding compounds was synthesized and evaluated in vitro using α-synuclein recombinant fibrils. Most potent ligands (Ki < 20 nM) were radiolabeled with tritium using [^{3}H]methyl nosylate. Postmortem human (PD, MSA) brain tissues and α-synuclein fibril-injected mouse brain tissues were used to evaluate specific binding of the radioligands (10nM) by in vitro autoradiography. Specificity was assessed by comparing tracer binding in human brain regions with high ('α-syn + ') versus low/no ('α-syn- ') α-synuclein concentration, as determined by immunohistochemistry with pSer129 α-synuclein antibody. Three compounds were selected, SKP02, SKP05 and SKP08 and radiolabeled with [^{11}C]CH_3I. Brain uptake of the ^{11}C-labelled compounds was evaluated in vivo in wild-type (WT) C57Bl6/J mice with PET.
Results: Initially 11 compounds were designed and synthesized (data not shown). From this series, SKP02, SKP05 and SKP08 showed optimal results in vitro: 1) binding affinity of 7.1 ± 2.3, 18.7 ± 2.4 and 4.5 ± 0.8 nM (mean ± SD;n = 3) on recombinant α-synuclein fibrils respectively, and 2) optimal specificity in autoradiography on post-mortem human brain tissues. Radiolabeling with [^{3}H]methyl nosylate or [^{11}C]CH_3I was achieved from the phenol precursors (Fig. 1A). [^{3}H]SKP02, [^{3}H]SKP05 and [^{3}H]SKP08 were synthesized with radiochemical yields (RCY) of 30–50% (n = 1), a molar activity (AM) of 2.84GBq/μmol and radiochemical purities (RCP) of > 98%. Representative images of in vitro autoradiography demonstrated specific binding to α-synuclein fibril deposits and/or human aggregates (Fig. 1B). The three compounds were radiolabelled with [^{11}C]CH_3I with RCY of 30-32% (d.c.,n = 2), an average AM of 28 GBq/μmol (at EOS) and RCP > 95% (n = 2). PET imaging revealed high brain uptake for [^{11}C]SKP02, [^{11}C]SKP05 and [^{11}C]SKP08, with a peak brain perfusion (1.4-1.9 SUVs) 1-3 min post-injection followed by a washout phase (Fig. 1C). [^{11}C]SKP08 had a longer brain retention time and slower washout compared to [^{11}C]SKP02 and [^{11}C]SKP05 indicating higher non-specific binding.
Conclusion: Based on in vitro fibril binding and autoradiography, three α-synuclein ligands were selected as new leads for PET tracer development. In vitro autoradiography indicated specific binding to α-synuclein in postmortem human tissues and α-synuclein fibril-injected mouse brain. The ^{11}C-labelled analogs showed sufficient brain uptake in WT mice. Further in vivo evaluation, such as ex vivo biodistribution and metabolic stability, is currently underway.
Reference

1. Spillantini,M. et al. Nature 1997, 388, 839–840; 2. Korat,Š. et al. Pharmaceuticals 2021, 14, 847; 3. Korat,Š. et al., NMB 2022, 108-109.

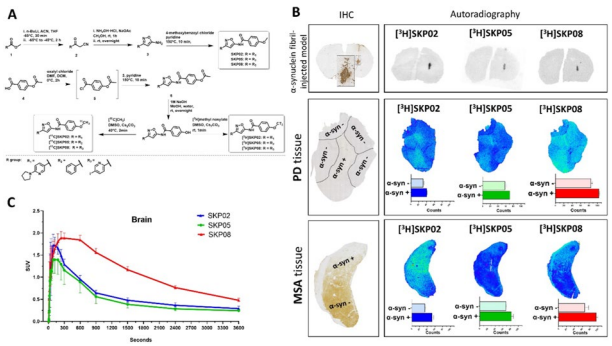

Fig. 1 ABC.OP23 Repurposing a pharmaceutical development for infection theranostics

Martin Kraihammer[1], Milos Petrik[2], Katerina Dvorakova Bendova[2], Isodor Happacher[3], Hubertus Haas[3], Clemens Decristoforo[1], Hristo Varbanov[4]
[1]Department of Nuclear Medicine, Medical University Innsbruck, Innsbruck, Austria. [2]Institute of Molecular and Translational Medicine, Faculty of Medicine and Dentistry and Czech Advanced Technology and Research Institute, Palacky University, Olomouc, Czech Republic. [3]Institute of Molecular Biology, Biocenter, Medical University Innsbruck, Innsbruck, Austria. [4]Department of Pharmaceutical Chemistry, Institute of Pharmacy, University of Innsbruck, Innsbruck, Austria
EJNMMI Radiopharmacy and Chemistry 2024, **9(1)**: OP23

Aim: Recently, multifunctional platinum(IV) complexes, designed as prodrugs for the anticancer drug carboplatin and the iron chelator deferoxamine (DFO) were developed and evaluated as a novel cytotoxic agents however, showing lower cytotoxicity than carboplatin itself (1). As these compounds contain DFO, they hold the potential a) to be labelled with Gallium-68 for molecular imaging and b) to be recognized by microorganisms, which can utilize DFO as a siderophore based iron source being taken up by specific siderophore transporters (SITs). Thereby, conjugation with carboplatin could potentially lead to specific antimicrobial activity of the compounds, particularly against Aspergillus fumigatus (AFU), which causes severe systemic fungal infection and expresses DFO-recognising SITs. Here we present the in vitro and in vivo characterization of two Pt(IV)-DFO-conjugates with a carboplatin core towards application for infection theranostics.
Materials and methods: Two platinum(IV) derivatives of carboplatin featuring a DFO unit and succinic acid or an acetyl group, respectively, incorporated at axial position were radiolabeled with Gallium-68, tested for lipophilicity, protein binding and stability in serum. In vitro uptake assays in AFU and AFU mutants lacking SIT1, which is responsible for ferrioxamine uptake, were performed. natGa complexes were used in MIC assays for antifungal activity in comparison with natGa-DFO. PET/CT imaging of a pulmonary aspergillosis model in rats was performed as well as biodistribution studies, in vivo stability studies in mice are ongoing.
Results: Radiolabeling showed quantitative ^{68}Ga-labeling yields at high molar radioactivities with radiochemical purities exceeding 95%, hydrophilic properties, low protein binding and high stability in serum. Uptake assays revealed high uptake in AFU in iron deplete environment, which was proven to be SIT1 dependent. MIC assays showed moderate antifungal activity, higher than DFO and carboplatin itself, but with limited SIT1 dependence, as some antifungal activity was also observed in mutants lacking SIT1. PET/CT imaging revealed favourable pharmacokinetics with rapid distribution and exclusive renal excretion pattern with high and pronounced accumulation in AFU infected lung tissue.
Conclusion: Overall, this study demonstrated the potential of DFO-carboplatin based conjugates for theranostic applications. DFO conjugation can lead to very selective delivery of antimicrobial active compounds while allowing PET imaging for patient selection and treatment monitoring. Challenges remain in ensuring very high antimicrobial activity and in vivo stability of the compounds. Further work aims to modify the concept to improve antifungal activity and to provide wider application towards antibacterial applications.
Reference

1. Harringer S, Hejl M, Enyedy ÉA, Jakupec MA, Galanski MS, Keppler BK, Dyson PJ, Varbanov HP. Multifunctional Pt(iv) prodrug candidates featuring the carboplatin core and deferoxamine. Dalton Trans. 2021,50(23):8167-8178.

OP24

Synthesis and preclinical evaluation of novel ^{18}F-vancomycin-based tracers for the detection of bacterial infections using positron emission tomography

Gerbren B. Spoelstra[1], Frank F. A. IJpma[2], Youxin Fu[3], Nadja A. Simeth[3], Marleen van Oosten[4], Jan Maarten van Dijl[4], Wiktor Szymanski[5,6], Ben L. Feringa[3], Philip H. Elsinga[1*]
[1]University of Groningen, University Medical Center Groningen, Department of Nuclear Medicine and Molecular Imaging Hanzeplein 1, 9713GZ Groningen, The Netherlands,. [2]University of Groningen, University Medical Center Groningen, Department of Trauma Surgery, Hanzeplein 1, 9713GZ Groningen, The Netherlands,. [3]University of Groningen, Stratingh Institute for Chemistry, Nijenborgh 7, 9747AG Groningen, The Netherlands.. [4]University of Groningen, University Medical Center Groningen, Department of Medical Microbiology and Infection Prevention, Hanzeplein 1, 9713GZ Groningen, The Netherlands,. [5]University of Groningen, University Medical Center Groningen, Department of Radiology, Hanzeplein 1, 9713GZ Groningen, The Netherlands,. [6]University of Groningen, Groningen Research Institute of Pharmacy, Antonius Deusinglaan 1, 9713AV Groningen, The Netherlands
[*]**Corresponding author**: P.H.Elsinga@UMCG.nl

EJNMMI Radiopharmacy and Chemistry 2024, **9(1)**: OP24
Aim: Bacterial infections are a major problem in most medical disciplines[1]. Rapid and accurate detection is essential but can be challenging with the diagnostic tools currently available. Positron Emission Tomography (PET) imaging has the potential to overcome this hurdle if suitable tracers can be developed[2]. Here we report on PET tracers for the imaging of Gram-positive bacteria, employing vancomycin as the targeting molecule. Vancomycin binds peptidoglycan, which is ubiquitously present and accessible in Gram-positive bacteria. This glycopeptide antibiotic is well described in literature and binds specifically to D-Ala-D-Ala moieties present on peptidoglycan[3, 4]. Here, two new vancomycin-based PET tracers, were labelled with ^{18}F and tested, both in vitro and in vivo, in healthy animals, and compared with previous developed [^{18}F]PQ-VE1-vancomycin[5].
Materials and methods: Radiolabeled prosthetic groups [^{18}F]FB-NHS and [^{18}F]BODIPY-FL-NHS were conjugated to vancomycin using an Eckert & Ziegler Modular-Lab PharmTracer synthesis module. The in vitro binding affinity towards Gram-negative and Gram-positive bacteria and minimum inhibitory concentration were investigated and compared to previously reported [^{18}F]PQ-VE1-vancomycin PET tracer. For the first time, the biodistribution of all three tracers was determined in healthy animals to identify potential binding site interference and to evaluate the feasibility of imaging of bacterial infections using vancomycin-based PET tracers.
Results: [^{18}F]FB-vancomycin, [^{18}F]PQ-VE1-vancomycin, and [^{18}F]BODIPY-FL-vancomycin were successfully synthesized with a radiochemical yield of 11.7%, 2.6% and 0.8%, respectively. [^{18}F]FB-vancomycin exhibited poor in vitro and in vivo stability and, as a result, no affinity towards Gram-positive bacteria. In contrast, [^{18}F]BODIPY-FL-vancomycin and [^{18}F]PQ-VE1-vancomycin showed high affinity towards Gram-positive bacteria in vitro. Despite an increased MIC, co-incubation with vancomycin showed binding that matched or even exceeded clinically relevant blood serum levels of vancomycin. For [^{18}F]PQ-VE1-vancomycin, in vitro growth inhibition was not observed, whilst showing slightly higher affinity for the D-Ala-D-Ala targeting moiety, compared to [^{18}F]BODIPY-FL-vancomycin. Biodistribution showed predominantly renal clearance of [^{18}F]PQ-VE1-vancomycin and [^{18}F]BODIPY-FL-vancomycin and, promisingly, low non-specific muscle accumulation.
Conclusion: [^{18}F]BODIPY-FL-vancomycin and [^{18}F]PQ-VE1-vancomycin show great potential for imaging Gram-positive bacteria in vitro and in vivo. This research paves the way for the investigation of vancomycin-based bacterial infection imaging in relevant models of bacterial infection to establish its scope and applicability.

References

1. Suetens C, Latour K, Karki T, Ricchizzi E, Kinross P, Moro ML, et al. Prevalence of healthcare-associated infections, estimated incidence and composite antimicrobial resistance index in acute care hospitals and long-term care facilities: results from two European point prevalence surveys, 2016 to 2017. Euro Surveill. 2018;23(46):1,800,516.
2. Polvoy I, Flavell RR, Rosenberg OS, Ohliger MA, Wilson DM. Nuclear Imaging of Bacterial Infection: The State of the Art and Future Directions. J Nucl Med. 2020;61(12):1708–16.
3. Loll PJ, Axelsen PH. The structural biology of molecular recognition by vancomycin. Annu Rev Biophys Biomol Struct. 2000;29:265–89.
4. Arduino RC, Murray BE. Vancomycin Resistance in Gram-Positive Organisms. Current Opinion in Infectious Diseases. 1993;6(6):715–24.
5. Fu Y, Helbert H, Simeth NA, Crespi S, Spoelstra GB, van Dijl JM, et al. Ultrafast Photoclick Reaction for Selective ^{18}F-Positron Emission Tomography Tracer Synthesis in Flow. J Am Chem Soc. 2021;143(27):10,041–7.

OP25

Artificial biomimetic Siderophores as PET radiopharmaceuticals: Radiolabelling and evaluation for PET imaging of invasive aspergillosis

Milos Petrik[1*], Isabella Hubmann[2], Andrzej Mular[3], Katerina Dvorakova Bendova[1], Barbora Neuzilova[1], Mario Aguiar[4], Patricia Caballero[4], Abraham Shanzer[5], Henryk Kozłowski[2], Hubertus Haas[4], Clemens Decristoforo[2], Elzbieta Gumienna-Kontecka[3]
[1]Institute of Molecular and Translational Medicine, Faculty of Medicine and Dentistry and Czech Advanced Technology and Research Institute, Palacky University, Olomouc, Czech Republic. [2]Department of Nuclear Medicine, Medical University Innsbruck, Innsbruck, Austria. [3]Faculty of Chemistry, University of Wrocław, Wrocław, Poland. [4]Institute of Molecular Biology, Biocenter, Medical University Innsbruck, Innsbruck, Austria. [5]Department of Organic Chemistry, The Weizmann Institute of Science, Rehovot, Israel
[*]**Corresponding author**: milos.petrik@upol.cz

EJNMMI Radiopharmacy and Chemistry 2024, **9(1)**: OP25

Aim: Invasive pulmonary aspergillosis, mainly caused by Aspergillus fumigatus, is a severe and often life-threatening disease in immunocompromised patients, lacking selective and sensitive diagnostic tools. A. fumigatus requires iron for growth and virulence and therefore secretes low molecular weight chelators, called siderophores, to acquire iron from the host. The siderophore ferrioxamine E (synonyms: nocardamine, FOXE, DFO E), produced by Streptomyces sp., can be utilized by A. fumigatus [1]. We report here on the characterization of ^{68}Ga-labelled artificial biomimetic FOXE analogues with respect to recognition by A. fumigatus, targeting properties in vitro and in vivo including PET/CT imaging and selectivity in comparison to bacterial strains.

Materials and methods: Artificial FOXE derivatives, containing a retro-positioned hydroxamate group and variable ring size were synthesized as described previously [2] and labelled with ^{68}Ga. Uptake assays using iron sufficient and depleted A. fumigatus cultures and Staphylococcus aureus cultures were performed, including blocking studies with iron labelled siderophores. Growth promotion assays employing A. fumigatus mutants that grow only in the presence of usable siderophores, possessing or lacking the endogenous ferrioxamine transporter Sit1, complemented recognition analysis of artificial siderophores by A. fumigatus. Furthermore, biodistribution studies in healthy BALB/c mice were performed, as well as PET/CT imaging in a rat model of A. fumigatus and S. aureus infections.

Results: In vitro uptake assays using A. fumigatus wildtype strain showed specific uptake for 68Ga-labelled FOX 2-5 and FOX 2-4, which have a high structural similarity to the original FOXE. Growth assays mostly supported uptake results. Uptake and growth assays indicated Sit1-specific uptake of ^{68}Ga-FOX derivatives. On the contrary, uptake assays in S. aureus suggested higher uptake of [^{68}Ga]Ga-FOX 2-6 and [^{68}Ga]Ga-FOX 3-5. Biodistribution assays showed favourable pharmacokinetic properties with rapid elimination. Dynamic PET/CT imaging of A. fumigatus and S. aureus infected rats revealed rapid accumulation of radiotracer in infected tissues and supported specificity found in vitro.

Conclusion: In vitro and in vivo evaluation indicated superiority of [^{68}Ga]Ga-FOX 2-5 over other ^{68}Ga-FOX derivatives for targeting A. fumigatus. For some compounds, species-specificity in their biological activity was revealed. Pharmacological characterization provided very promising first insights and showed possible applicability of artificial ^{68}Ga-FOX derivatives for selective targeting of pathogenic microorganisms.

Acknowledgements
We gratefully acknowledge the financial support of the project National institute of virology and bacteriology (Programme EXCELES, ID Project No. LX22NPO5103) – Funded by the European Union – Next Generation EU.

References

1. Petrik M, Franssen GM, Haas H, Laverman P, Hörtnagl C, Schrettl M, Helbok A, Lass-Flörl C, Decristoforo C. Preclinical evaluation of two ^{68}Ga-siderophores as potential radiopharmaceuticals for Aspergillus fumigatus infection imaging. Eur J Nucl Med Mol Imaging. 2012; 39:1175–1183.
2. Mular A, Shanzer A, Kozlowski H, Hubmann I, Misslinger M, Krzywik J, Decristoforo C, Gumienna-Kontecka E. Cyclic Analogs of Desferrioxamine E Siderophore for Ga-68 Nuclear Imaging: Coordination Chemistry and Biological Activity in Staphylococcus aureus. Inorg Chem. 2021; 60:17,846–17,857.

OP26

[^{68}Ga]Ga-TEoS-DAZA as PET tracer for liver function determination and diagnosis of liver-bile-related diseases

Julia Greiser[1], Thomas Winkens[1], Christian Kuehnel[1], Steffen Wiegand[1], Robert Drescher[1], Mari Teuter2, Michael Willmann2, Jens P. Bankstahl2, Tobias L. Ross2, Frank M. Bengel2, Martin Freesmeyer[1]
[1]Nuclear Medicine, Jena University Hospital, Jena, Germany. [2]Nuclear Medicine, Hannover Medical School, Hannover, Germany

EJNMMI Radiopharmacy and Chemistry 2024, **9(1)**: OP26

Aim: Liver function determination with nuclear medical imaging methods is usually performed with hepatobiliary scintigraphy (HBS), but limitations regarding the spatiotemporal resolution of the technique prohibit segmental and truly quantitative analysis. In order to allow voxel-based quantification of liver function in high spatial and temporal resolution, [^{68}Ga]Ga-TEoS-DAZA was developed as a hepatocyte-specific tracer for PET imaging.

Materials and methods: TEoS-DAZA was labeled with ^{68}Ga-solution from a ^{68}Ge/^{68}Ga generator, using HEPES buffer (1.5 M, pH 3.6-4.0).1 Labeling must be performed at 25°C (10 min) since elevated temperatures lead to preliminary precursor decomposition.2 [68Ga]Ga-TEoS-DAZA was purified via solid phase extraction (SPE, using C-18 cartridge, 50% ethanol for tracer elution) and diluted with PBS to provide injectable solutions. Preclinical biodistribution studies were performed in embryonated ostrich eggs ($n = 7$) and in C57BL6/N mice ($n = 6$) during different stages of liver fibrosis.2 Blocking studies were performed in embryonated ostrich eggs using cyclosporine A. A toxicity study of the precursor was performed in rodents. Dynamic [^{68}Ga]Ga-TEoS-DAZA PET/CT was performed in three patients with hepatocellular carcinoma (HCC) after giving informed consent.

Results: [^{68}Ga]Ga-TEoS-DAZA exhibits specific liver uptake in ostrich embryos and mice (total organ uptake at peak: 32%IA in ostrich, 39%IA in mice). The hepatic transit was notably faster in mice (time to peak ca. 2 min) as compared to ostriches (approx. 22 min). Mice in prefibrotic-inflammatory phases exhibited decreased biliary excretion rates. Results from blocking studies indicate involvement of OATP1B1 and OATP1B3 transporters in [^{68}Ga]Ga-TEoS-DAZA uptake, similar to other established agents for liver function determination. Batches of [^{68}Ga]Ga-TEoS-DAZA were produced according to guidelines of Good Manufacturing Practice, exhibiting RCP $\geq$ 95% after SPE purification (RCY = 58%).2 The NOAEL of the precursor was determined at 1.4 mg/kg. In patients, the hepatic transit in non-tumorous parenchyma was slower than in healthy mice (time to peak approx. 15 min). HCCs showed early arterial hyperperfusion, followed by a rapid washout of activity > 60 s p.i., after which the activity in HCCs was lower than in surrounding liver tissue, indicating a relation between tracer uptake and hepatocyte function.3 Additionally, the biliary excretion of the tracer allowed for evaluation of bile stent patency.4

Conclusion: [^{68}Ga]Ga-TEoS-DAZA shows high potential as a tracer for liver function quantification by means of determining uptake values and hepatic transit kinetics. Further potential fields of application are liver disease staging, lesion characterization and diagnosis of biliary tree irregularities.

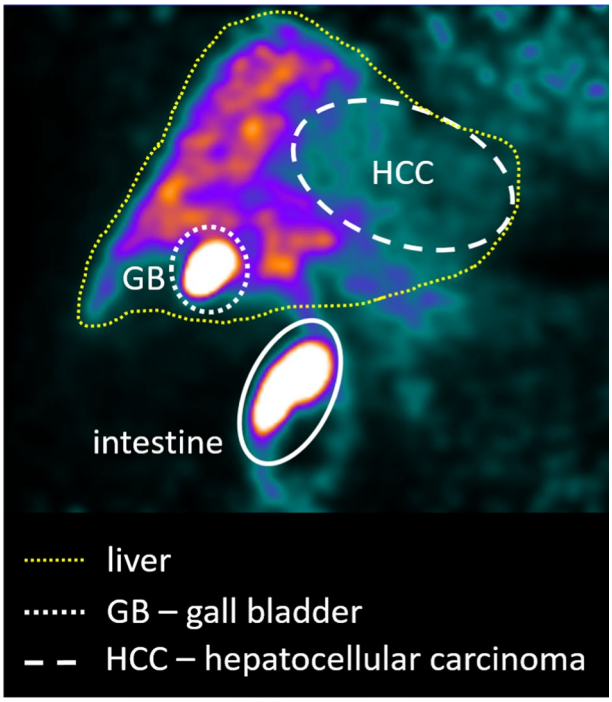

Coronal view of a torso after injection of [^{68}Ga]Ga-TEoS-DAZA with the position of the liver delineated (yellow dotted line). The tracer accumulates in the functional liver parenchyma and subsequently the gall bladder and intestines, while a hepatocellular carcinoma exhibits significantly reduced uptake.

References

1. J. Greiser, C. Kühnel, H. Görls, W. Weigand and M. Freesmeyer, Dalton Transactions, 2018, 47, 9000–9007.
2. J. Greiser, T. Winkens, O. Perkas, C. Kuehnel, W. Weigand and M. Freesmeyer, Pharmaceutics, 2022, 14, 2695.
3. M. Freesmeyer, J. Greiser, T. Winkens, F. Gühne, C. Kühnel, F. Rauchfuß, H.-M. Tautenhahn and R. Drescher, Diagnostics, 2021, 11, 660.
4. M. Freesmeyer, R. Drescher, C. Kühnel, F. Gühne and J. Greiser, Clinical Nuclear Medicine, 2022, 47, 59–60.

OP27

Tumor-targeted alpha therapy using terbium-149 in combination with somatostatin analogues

Cristina Müller[1,2], Ana Katrina Mapanao[1], Sarah D. Busslinger[1], Chiara Favaretto[1,3], Pascal V. Grundler[1], Ulli Köster[4], Karl Johnston[5], Roger Schibli[1,2], Nicholas P. van der Meulen[1,6]
[1]Center for Radiopharmaceutical Sciences ETH-PSI-USZ, Paul Scherrer Institute, Villigen-PSI, Switzerland. [2]Department of Chemistry and Applied Biosciences, ETH Zurich, Zurich, Switzerland,[3]Division of Nuclear Medicine, University Hospital Basel, Basel, Switzerland. [4]Institut Laue-Langevin, Grenoble, France. [5]Physics Department, ISOLDE/CERN, Geneva, Switzerland. [6]Laboratory of Radiochemistry, Paul Scherrer Institute, Villigen-PSI, Switzerland
EJNMMI Radiopharmacy and Chemistry 2024, **9(1)**: OP27

Aim: Terbium-149 was previously proposed as a suitable candidate for targeted α-therapy [1,2]. Combining it with somatostatin analogues appears particularly appealing because of their rapid pharmacokinetics which meet well with the short half-life of terbium-149 ($T_{1/2}$ = 4.12 h). Since the decay chain of terbium-149 does not comprise relevant amounts of α-emitting daughter nuclides, efficient internalization of the radiopharmaceutical may not be a prerequisite and, hence, the use of somatostatin receptor (SSTR) antagonists plausible. The aim of this study was to investigate a SSTR agonist and antagonist, [^{149}Tb]Tb-DOTATATE and [^{149}Tb]Tb-DOTA-LM3, respectively, and compare their therapeutic efficacy and safety in the preclinical setting.
Materials and methods: The labeling of the somatostatin analogues with [^{149}Tb]$TbCl_3$ was performed at pH 4.5 within 15 min at 95 °C, followed by quality control using HPLC. [^{149}Tb]Tb-DOTATATE and [^{149}Tb]Tb-DOTA-LM3 were tested in rat pancreatic AR42J tumor cells. Cell viability (MTT) and survival (colony forming) assays were performed after overnight exposure of AR42J cells to variable activity concentrations of the radiopeptides. Therapy studies were performed in AR42J tumor-bearing mice injected with 1 × 5 MBq or 2 × 5 MBq of the radiopeptides. The tolerability of 20 MBq [^{149}Tb]Tb-DOTATATE or [^{149}Tb]Tb-DOTA-LM3 was assessed in immunocompetent mice without tumors. The body mass of mice was monitored three times a week and blood cell counts were determined on Day 10, 28 and 56. Kidney function was tested using [^{99m}Tc]Tc-DMSA after 10 weeks.
Results: [^{149}Tb]Tb-DOTA-LM3 showed a higher uptake in AR42J tumor cells than [^{149}Tb]Tb-DOTATATE after a 2-h incubation period (63% vs. 41%), with an internalized fraction considerably lower for the SSTR antagonist than for the agonist (5% vs. 42%) (Fig. 1A). Viability of AR42J tumor cells was more effectively reduced with [^{149}Tb]Tb-DOTA-LM3 than with [^{149}Tb]Tb-DOTATATE (EC_{50} = 0.51 vs. 1.24 kBq/mL) (Fig. 1B). In colony forming assays, 6 ± 3% vs. 45 ± 7% of the tumor cells survived after treatment with 1.0 kBq/mL [^{149}Tb]Tb-DOTA-LM3 and [^{149}Tb]Tb-DOTATATE, respectively. In vivo, both radiopeptides showed a comparable efficacy to delay the tumor growth. The median survival of mice injected with 2 × 5 MBq was ~ 30 days as compared to ~ 18 days for mice injected with 1 × 5 MBq and ~ 8 days for untreated controls (Fig. 1C/D). The radiopeptides were well tolerated at 20 MBq/mouse, demonstrated by blood cell counts in the same range for treated mice and untreated controls. No reduction in renal accumulation of [^{99m}Tc]Tc-DMSA was seen in treated mice, indicating unimpaired kidney function.
Conclusion: Both radiopeptides were effectively employed for tumor-targeted α-therapy. An advantage of using a SSTR antagonist was not established, hence, the cell internalizing SSTR agonist, [^{149}Tb]Tb-DOTATATE, may be the preferred radiopeptide in view of future clinical application.

Acknowledgment
The authors thank Colin Hillhouse, Fan Guo-Sozzi and Susan Cohrs for support during the production of the terbium-149 and subsequent preclinical experiments. We are grateful to the ISOLDE technical and RILIS teams as well as for the radiation protection teams at CERN for smooth operation and shipping of the activity. The study was supported by the Ulrich Peter & Hans Rudolf Wirz-Stiftung via Swiss Cancer Research (N° KFS-5624-08-2022), the Swiss National Science Foundation (N° 310030_28897 and 200021_188495) and the European Union's Horizon 2020 research and innovation program under the Marie Skłodowska-Curie grant agreement (N° 884104).

References

1. Beyer GJ, Miederer M, Vranjes-Duric S, Comor JJ, Künzi G, Hartley O, Snekowitsch-Schmidtke R, Soloviev D., Buchegger F. Targeted alpha therapy in vivo: direct evidence for single cancer cell kill using ^{149}Tb-rituximab. Eur J Nucl Med Mol Imaging. 2004; 31:547–54
2. Umbricht C, Köster U, Bernhardt P, Gracheva N, Johnston K, Schibli R, van der Meulen NP, Müller C. Alpha-PET for Prostate Cancer: Preclinical Investigation using ^{149}Tb-PSMA-617. Sci Rep 2019; 9:17,800–17810.

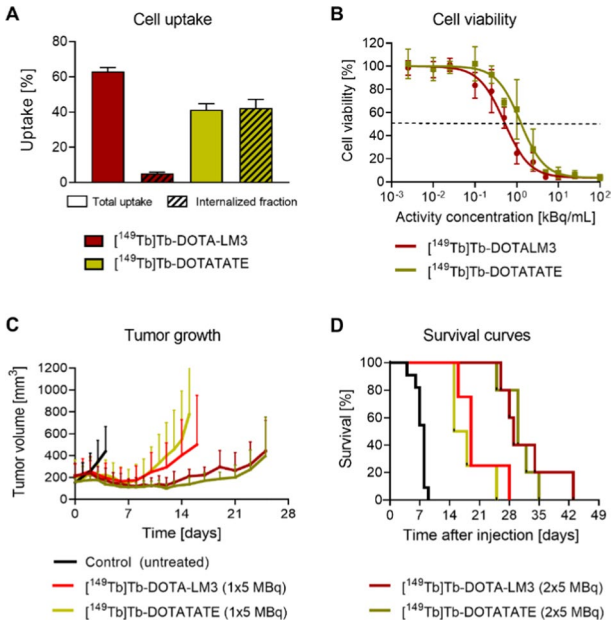

Fig. 1 Data of in vitro and in vivo experiments performed with AR42J tumor cells and respective xenograft mouse models. (**A**) Cell uptake and internalization of [^{149} Tb]Tb-DOTA-LM3 and [^{149} Tb]Tb-DOTATATE; (**B**) Viability of cells exposed to various activity concentrations of [^{149} Tb]Tb-DOTA-LM3 and [^{149} Tb]Tb-DOTATATE; (**C**/**D**) Tumor growth and survival curves of mice injected with 1 × 5 MBq or 2 × 5 MBq [^{149} Tb]Tb-DOTA-LM3 and [^{149} Tb]Tb-DOTATATE.OP28 Synergistic effects of a combination of trastuzumab-emtansine (T-DM1) and β^-- radiation ([^{198}Au]Au-NPs) for targeted HER^{2+} therapy

Kinga Żelechowska-Matysiak[1], Aleksander Bilewicz[1], Agnieszka Majkowska-Pilip[1*]
[1]Institute of Nuclear Chemistry and Technology, Warsaw, Poland
*__Corresponding author__: a.majkowska@ichtj.waw.pl

EJNMMI Radiopharmacy and Chemistry 2024, **9(1)**: OP28

Aim: The future of nanomedicine therapy lies in multifunctional nanoplatforms, which combine therapeutics compounds and targeting vectors – biomolecules, specifically bind to the receptors of cancer cells. Traditional cancer therapies often cause significant damage in normal cells, whereas conjugation of therapeutic agents to vectors improves the selectivity and enhances the cytotoxicity. In particular, the use of gold nanoparticles with unique properties, such as small size, high biocompatibility, and versatility due to the ease of surface functionalization gives a unique opportunity to combine several therapeutic methods in one drug.

This study aimed to synthesize a novel radiobioconjugate containing simultaneously β^- emitter—^{198}Au-labeled NPs ([^{198}Au]Au-NPs), and trastuzumab-emtansine (T-DM1) as Antibody-Drug Conjugate (ADC).

Materials and methods: To synthesize 30 nm of gold nanoparticles, the radioactive precursor of gold-198 (^{198}Au) was applied. The size, zeta potential, and shape of nanoparticles were determined by TEM (Transmission Electron Microscopy) and DLS (Dynamic Light Scattering) techniques. Firstly, T-DM1 was attached to a bifunctional linker OPSS-PEG-NHS (5 kDa) and then conjugated with [^{198}Au]Au-NPs. The stability studies were carried out in saline, and PBS buffer. Biological studies such as binding specificity, receptor internalization, cytotoxicity (MTS and apoptosis assays, spheroids), cell cycle, and confocal microscopy were performed on SKOV-3 (HER2+) and MDA-MB-231 (HER2-) cancer cell lines.

Results: The DLS and TEM measurements confirmed the expected average size of [^{198}Au]Au-NPs (~30 nm) and spherical shape. The zeta potential value showed high stability of 198AuNPs without a tendency to agglomeration. T-DM1 was successfully attached to a bifunctional linker forming a stable peptide bond. Due to the high chemical affinity of sulfur to gold, the 198AuNPs were effectively modified with OPSS-PEG-NH-T-DM1 conjugate. Obtained [^{198}Au]Au-NPs-T-DM1 bioconjugate showed one-week stability in the media tested. In vitro experiments demonstrated a high affinity of the radiobioconjugate to HER2 receptors and cell internalization. Cytotoxicity experiments using the MTS assay showed a significant decrease in the viability of SKOV-3 cells. A synergistic cytotoxic effect due to the simultaneous presence of DM1 at a concentration of 0.031 µg/mL and 198Au at a dose of 20 MBq/mL was revealed after 48 h. Flow cytometry analysis indicated that [^{198}Au]Au-NPs-T-DM1 mainly induced cell cycle arrest in the G2/M phase and late apoptosis. The synergistic effect of the radiobioconjugate was also shown in spheroid models.

Conclusion: The proposed multimodal radiobioconjugate containing in the structure DM1, radionuclide, and trastuzumab shows great potential for the treatment of HER^{2+} cancers by intratumoral or post-resection injection.

Acknowledgments
The research was supported by a grant from the National Center of Science, SONATA 2018/31/D/ST4/01488. The contribution of Ph.D. student Kinga Żelechowska-Matysiak was realized within Project No POWR.03.02.00-00-I009/17-00 (Operational Project Knowledge Education Development 2014-2020 co-financed by European Social Fund).

OP29

Assessment of cell damage produced by somatostatin analog radiopharmaceuticals labelled with lutetium-177 or terbium-161

Laura De Nardo[1,2*], Anna Della Pieta[3], Sara Santi[3], Emma Nascimbene[4], Erika Azorín-Vega[5], Guillermina Ferro-Flores[5], Vito Barbieri[3], Alessandra Zorz[4], Antonio Rosato[3,4], Laura Meléndez-Alafort[4]
[1]Department of Physics and Astronomy, University of Padua Padua, Italy. [2]Istituto Nazionale di Fisica Nucleare (INFN), Padova Division, Padua, Italy. [3]Department of Surgery, Oncology and Gastroenterology, University of Padua, Padua, Italy. [4]Veneto Institute of Oncology IOV-IRCCS, Padua, Italy. [5]Instituto Nacional de Investigaciones Nucleares, Ocoyoacac, Mexico
*__Corresponding author__: laura.denardo@unipd.it

EJNMMI Radiopharmacy and Chemistry 2024, **9(1)**: OP29

Aim: ^{177}Lu-labeled radiopharmaceuticals (RPs), are currently the most widely used for targeted radionuclide therapy (TRT), as they have demonstrated favorable safety and good response rates to treatment [1]. However, worldwide ^{177}Lu availability is limited [2]. To overcome this problem, the use of ^{161}Tb for TRT has been proposed because its decay characteristics are quite similar to those of ^{177}Lu [3]. ^{161}Tb emits low-energy photons (48.9 keV (17%) and 74.6 keV (10%)), useful for SPECT imaging, and relatively low-energy β-particles (Eavg = 154 keV). Unlike ^{177}Lu, ^{161}Tb emits a significant number of internal conversion (IE) and Auger electrons (AE) with energies ≤ 40 keV, which could be advantageous for improving therapeutic efficacy [4]. The aim of this study was to evaluate and compare the biological damage produced by ^{161}Tb-labeled somatostatin (SST) and ^{177}Lu-labeled SST analog RPs localized in different regions within pancreatic tumor AR42J cells [5].

Materials and methods: The biological damage caused to AR42J cell clusters of different sizes by three different SST analog RPs, labeled with ^{161}Tb or ^{177}Lu and located in different regions within the cells, was obtained with the MIRDcell code [6] by evaluating the absorbed dose (AD) to the cell nuclei and the cell survival fraction (Sf). MIRDcell calculated the Sf for each treatment using the linear quadratic model equation and taking into account the AD generated by the radiation emitted within the same cell (self) and the radiation emitted by neighboring cells (cross). The α and β values of AR42J cells were determined experimentally.

Results: Dosimetric evaluations show that most of the β-particles emitted by ^{177}Lu penetrates the membrane and reaches the nucleus to deliver a specific fraction of their energy. Therefore, ^{177}Lu-labeled RPs localization inside the cells only slightly affects the AD and the biological damage generated. In contrast, ^{161}Tb-labeled RPs localization causes differences in AD due to the IE and AE emitted by ^{161}Tb. However, as the cluster size increases, the difference in AD due to RPs

localization is minimal and the Sf depends mainly on the number of labelled cells.

Conclusion: For both ^{177}Lu-labeled RPs and ^{161}Tb-labeled RPs the main factors affecting the biological outcome are the dimensions of the cell cluster and the fraction of labelled cells inside the cluster. For a fixed cluster size and % of labelled cells, the localization of the RP inside the different cell compartments has a minimal influence on the AD to the cell nuclei and cell survival.

References

1. Stokke C, Kvassheim M, Blakkisrud J. Radionuclides for Targeted Therapy: Physical Properties. Molecules. 2022; 27: 5429–48.
2. Chakravarty R, Chakraborty S. A review of advances in the last decade on targeted cancer therapy using Lu-177: focusing on Lu-177 produced by the direct neutron activation route. Am J Nucl Med Molec Imaging. 2021; 11: 443–75.
3. Lehenberger S, Barkhausen C, Cohrs S, et al. The low-energy beta(-) and electron emitter Tb-161 as an alternative to Lu-177 for targeted radionuclide therapy. Nucl Med Biol. 2011; 38: 917–24.
4. Muller C, Reber J, Haller S, et al. Direct in vitro and in vivo comparison of Tb-161 and Lu-177 using a tumour-targeting folate conjugate. Eur J Nucl Med Mol Imaging. 2014; 41: 476–85.
5. Borgna F, Haller S, Rodriguez JMM, Ginj M, Grundler P V., Zeevaart JR, et al. Combination of terbium-161 with somatostatin receptor antagonists—a potential paradigm shift for the treatment of neuroendocrine neoplasms. Eur J Nucl Med Mol Imaging 2022; 49: 1113–26
6. Katugampola S, Wang J, Rosen A, Howell RW. MIRD Pamphlet No. 27: MIRDcell V3, a revised software tool for multicellular dosimetry and bioeffect modeling. J Nucl Med. 2022; 63: 1441–1449

OP30

Preclinical assessment of enhanced blood retention and tumor uptake PSMA-targeting ^{225}Ac-labeled radioconjugates

Zbynek Novy[1], Katarina Hajduova[1], Milos Petrik[1], Katerina Bendova[1], Falco Reissig[2], Kristof Zarschler[2], Klaus Kopka[2], Daniela Kurfurstova[3], Jan Bouchal[3], Constantin Mamat[2], Marian Hajduch[1]

[1]Institute of Molecular and Translational Medicine, Faculty of Medicine and Dentistry, Palacky University in Olomouc, Olomouc, Czech Republic. [2]Helmholtz-Zentrum Dresden-Rossendorf, Institute for Radiopharmaceutical Cancer Research, Dresden, Germany. [3]Institute of Clinical and Molecular Pathology, Faculty of Medicine and Dentistry, Palacky University in Olomouc, Olomouc, Czech Republic.

EJNMMI Radiopharmacy and Chemistry 2024, **9(1)**: OP30

Aim: The prostate-specific membrane antigen (PSMA) is overexpressed in prostate cancer at significantly higher levels compared to healthy tissue. Therefore, PSMA has emerged as very suitable target for molecular imaging as well as targeted radionuclide therapy of metastatic castration-resistant prostate cancer (mCRPC). In this study, we have investigated the in vivo behavior of two novel macropa-based PSMA inhibitors, namely [^{225}Ac]Ac-mcp-D-PSMA and [^{225}Ac]Ac-mcp-M-alb-PSMA modified with albumin binding moiety. The main motivation behind this project was to improve tumor uptake and thus therapeutic efficacy of those novel ^{225}Ac-labeled PSMA inhibitors.

Materials and methods: We have performed in vivo studies involving long-term toxicity study in healthy mice with subsequent immunohistochemical examinations of kidneys and salivary glands. We have also done therapeutic efficacy study in LNCaP-tumor bearing animals employing three different doses (5/15/45 kBq/mouse). Kidneys, livers and tumors were examined using immunohistochemical staining methods to detect PSMA expression, DNA damage (γH2AX), proliferation status (Ki67) and necrosis (H&E).

Results: The toxicity study have not revealed any significant toxic effect in studied parameters. Insignificant DNA damage was observed in the kidney tissue compared to the untreated controls. The therapy study showed no significant effect of two lower doses (5 and 15 kBq/animal) onto tumor volume or survival. The dose of 45 kBq/mouse had significant impact to both mentioned parameters, whereas [^{225}Ac]Ac-mcp-M-alb-PSMA performed better than other two ^{225}Ac-labeled PSMA inhibitors.

Conclusion: In vivo experiments in healthy mice showed very low toxicity of tested PSMA inhibitors. Histological examination of the organs in therapy study confirmed substantial DNA damage in the tumor tissue of mice injected with both studied novel ^{225}Ac-compounds, on the other hand the same parameter revealed only low DNA harm in the kidneys. The therapeutic efficacy of novel compounds was comparable to gold standard [^{225}Ac]Ac-PSMA-617, in case of [^{225}Ac]Ac-mcp-M-alb-PSMA seemed to be even higher.

OP31

Terbium-149 production and separation: the latest development update

Nicholas P. van der Meulen[1,2*], Chiara Favaretto[2,3], Pascal V. Grundler[2], Zeynep Talip[2], Ulli Köster[4], Karl Johnston[5], Roger Schibli[2,6], Robert Eichler[1,7], Cristina Müller[2,6]

[1]Laboratory of Radiochemistry, Paul Scherrer Institute, Villigen-PSI, Switzerland. [2]Center for Radiopharmaceutical Sciences ETH-PSI-USZ, Paul Scherrer Institute, Villigen-PSI, Switzerland. [3]Nuclear Medicine Department, University Hospital Basel, Basel, Switzerland. [4]Institut Laue-Langevin, Grenoble, France. [5]Physics Department, ISOLDE/CERN, Geneva, Switzerland. [6]Department of Chemistry and Applied Biosciences, ETH Zurich, Zurich, Switzerland, [7]Department of Chemistry, Biochemistry and Pharmaceutical Sciences, University of Bern, Bern, Switzerland

EJNMMI Radiopharmacy and Chemistry 2024, **9(1)**: OP31

Aim: Terbium-149 was proposed as an attractive candidate for Targeted Alpha Therapy (TAT) in the late 1990's [1], due to its favourable physical decay properties ($T_{1/2}$ = 4.1 h, E_α = 3.97 MeV, 17%; $E_{\beta+}{}_{mean}$ = 720 keV, 7%) [2]. While preclinical studies continue to demonstrate its therapeutic potential [3-5], it was also shown that it can be used for positron emission tomography [4]. The absence of daughter nuclides emitting relevant quantities of α-particles, an advantage over other radionuclides envisaged for TAT, make it a promising radionuclide, despite its limited development to date.

Materials and methods: Terbium-149 was produced at ISOLDE/CERN via spallation induced in a tantalum target using high-energy (1.4 GeV) protons, followed by effusion, release and ionization of the spallation products, which were mass-separated online. The mass 149 isobars were collected in zinc-coated gold/platinum foils and shipped to Paul Scherrer Institute for processing. Terbium-149 was chemically separated from its isobaric impurities, as well as the collection material, using cation exchange and extraction chromatography, employing an optimized process as compared to the procedure previously reported [5]. The quality of the radionuclide produced was assessed by means of radiolabelling experiments, together with γ-spectrometry and inductively coupled plasma—mass spectrometry measurements.

Results: Up to 1 GBq terbium-149 were collected and transported in two experimental campaigns in 2023, with ~ 450 MBq activity received upon arrival at PSI. The four-hour radiochemical separation process yielded up to 260 MBq final product. The product radiochemical purity, in 1 mL 0.05 HCl, was measured by γ-spectrometry and found to be 99.8%. Quality control was performed using DOTATATE, which was successfully labeled at molar activities up to 50 MBq/nmol with > 99% radiochemical purity [5]. The chemical purity was further proven by ICP-MS measurements, which showed lead, copper, iron and zinc contaminants at ppb levels.

Conclusion: The collection of mass separated-terbium-149 and radiochemical separation process has steadily improved over the years, such that higher activities can be collected and isolated, while the quality of product can ensure more efficient labelling of tumour-targeting small molecules. While only CERN/ISOLDE currently produces this radionuclide with limited available beam time, CERN/MEDICIS is developing efficient methods to do so as well. Despite this, the interest in the radionuclide remains high, with governments in Switzerland and Belgium approving grants to fund facilities (IMPACT and MYRRHA, respectively) to upscale and produce large activities of terbium-149, amongst other interesting radionuclides, towards medical research and potential clinical application.

Acknowledgements
The authors thank CERN and PSI radiation safety and logistics teams, as well as Nicole Pereira da Lima (USP—IPEN/CNEN, Brazil) and Wiktoria Wojtaczka (KU Leuven, Belgium) for assistance in collections.

References

1. Allen. Australasian Radiology 1999, 43:480.
2. Singh & Chen. Nuclear Data Sheets 2022, 185:2
3. Beyer et al. Radiochim Acta 2002, 90:247.
4. Müller et al. EJNMMI Radiopharm Chem 2016, 1:5.
5. Umbricht et al. Sci Rep 2019, 9:17800.
6. Favaretto et al. Sci Rep 2024, under evaluation.

OP32

155Gd-target enrichment for terbium-155 production by low-energy cyclotrons

Francesca Barbaro[1,2], Luciano Canton[2], Nikolay Uzunov[3], Laura De Nardo[1,2], Laura Meléndez-Alafort[4]
[1]Dipartimento di Fisica e Astronomia dell'Università di Padova, Padova, Italia. [2]INFN, Sezione di Padova, Padova, Italia. [3]INFN-Legnaro National Laboratories, Legnaro, Italia. [4]Istituto Oncologico Veneto IOV IRCCS, Padova, Italia

EJNMMI Radiopharmacy and Chemistry 2024, **9(1)**: OP32

Aim: The interest in terbium-155 for SPECT imaging is on the rise thanks to its γ emissions at 87 keV (32%) and 105 keV (25%) and its long half-life that allows to investigate the biodistribution of radiopharmaceuticals over several days. In addition, the possibility to couple it with other Tb radionuclides to produce theranostic pairs increases its appeal for medical purposes [1]. However, an adequate production route for medical applications has not been found yet. In this work the attention is focused on the ^{155}Gd(p,n)^{155}Tb reaction. The co-production of ^{156}Tb has to be limited as much as possible, due to its half-life comparable to the ^{155}Tb one and its high-energy γ emissions that contribute to the dose and compromise the image quality [2].
Materials and methods: The theoretical analysis is crucial to identify the optimal production parameters and irradiation conditions, limiting the co-production of harmful impurities. The theoretical cross sections have been calculated with the TALYS code [3] and compared with the data available in the Literature [4]. Thick-target yields were obtained and dosimetric evaluations were accomplished using the OLINDA software [5], considering an injection of [^{155}Tb]Tb-cm09 [1]. Finally, the dose increase (DI) was determined by combining the yield of all Tb radioisotopes produced with the dosimetric outcomes.
Results: With enriched ^{155}Gd targets, the main issue is represented by the presence of ^{156}Gd as impurity. Different levels of ^{155}Gd enrichment have been compared, namely 93.1%, 98%, 99%, and 100%. For each case the assessment of the radionuclidic purity (RNP) and DI have been performed. The dosimetric assessment shows that a maximum 2% content of ^{156}Gd in the target guarantees a safe clinical application. Even though the RNP of reference for the specific case has yet to be established, a 98% RNP value combined with a DI lower than 10% indicates a promising outcome.
Conclusion: This work proposes a hospital-cyclotron method for high-purity ^{155}Tb production based on an adequate ^{155}Gd-enrichment of the target. The minimum level of enrichment necessary for its use in clinics has been identified. This is alternative to the use of a post-production mass spectrometry purification proposed in the Literature [4].
Acknowledgements
The research is part of the REMIX project, INFN and Legnaro INFN Laboratories.

References

1. Müller C et al.. Future prospects for SPECT imaging using the radiolanthanide terbium-155 production and preclinical evaluation in tumor-bearing mice. Nucl Med Biol. 2014; 41:e58–65.
2. Barbaro F et al.. ^{155}Tb production by cyclotrons: what level of 155Gd enrichment allows clinical applications? ArXiv:fg2309.06250 [physics.med-ph]. 2023.
3. Koning A J, Hilaire S, and Goriely S. TALYS: modeling of nuclear reactions. EPJ A. 2023;59.
4. Dellepiane G et al.. Cross section measurement of terbium radioisotopes for an optimized 155Tb production with an 18 MeV medical PET cyclotron. Appl Radiat Isot. 2022;184:110,175.
5. Stabin M G, Sparks R B, Crowe E. OLINDA/EXM: the second-generation personal computer software for internal dose assessment in nuclear medicine. J. Nucl. Med. 2005;46:1023–1027.

OP33

Development of a new technology for the ^{52}Mn-radiopharmaceuticals cyclotron production

Giorgia Speltri[1*], Francesca Porto[2], Petra Martini[3], Emiliano Cazzola[4], Sara Cisternino[5], Liliana Mou[5], Alessandra Boschi[1], Giancarlo Gorgoni[4], Lorenza Marvelli[1], Licia Uccelli[2], Giovanni di Domenico[6], Gaia Pupillo[5], Juan Esposito[5]
[1]Department of Chemical, Pharmaceutical and Agricultural Sciences, University of Ferrara, Ferrara, Italy. [2]Department of Translational Medicine, University of Ferrara, Ferrara, Italy. [3]Department of Environmental and Prevention Sciences, University of Ferrara, Ferrara, Italy. [4]IRCCS Sacro Cuore Don Calabria Hospital, Negrar di Valpolicella (VR), Italy. [5]Legnaro National Laboratories (LNL-INFN), National Institute of Nuclear Physics, Padua, Italy. [6]Department of Physics and Earth Sciences, University of Ferrara, Ferrara, Italy
[*]**Corresponding author**: giorgia.speltri@unife.it

EJNMMI Radiopharmacy and Chemistry 2024, **9(1)**: OP33
Aim: The main goal of this work is to advance the technology required for cyclotron-driven production of manganese-52 (^{52}Mn), aiming at the preparation of radiopharmaceuticals suitable for positron emission tomography (PET), and for PET/MRI multimodal imaging studies, when they are used in combination with analogous paramagnetic manganese-based compounds. The cyclotron-production of ^{52}Mn implies the use of a natural chromium targets and medium-low energy protons within the range of 10-20 MeV. This process predominantly relies on nuclear reaction pathways, specifically the ^{52}Cr(p,n)^{52}Mn and ^{53}Cr(p,2n)^{52}Mn ones. Alternatively, ^{52}Cr-enriched material can also be employed for this purpose. The developed technology includes: (i) the design and production of chromium metal targets to fit the size of the solid target station of a medical cyclotron; (ii) the development of an automated and efficient procedure for separating ^{52}Mn from the Cr bulk; and (iii) the labeling of specific ligands with ^{52}Mn.
Materials and methods: Both natural chromium and ^{52}Cr enriched targets were produced using the Spark Plasma Sintering (SPS) technique [1]. Irradiation runs were performed with the ACSI TR19/300 cyclotron located at the Sacro Cuore Don Calabria Hospital in Negrar di Valpolicella (Verona, Italy). The separation of the yielded ^{52}Mn from the target was performed, after dissolution with HCl 6M of the target, through the ion exchange chromatography process, with an automatic module. Preliminary labeling experiments were conducted with S-2-(4-Isothiocyanatobenzyl)-1,4,7,10-tetraazacyclododecane tetraacetic acid (DOTA-SCN) at pH 5.5. Radiochemical purity has been determined by TLC chromatography. A preliminary assessment of the imaging quality of ^{52}Mn produced from ^{52}Cr enriched targets has also been carried out on phantom with a microPET tomograph.
Results: Metal pellets of Cr were produced and joined to nobium and gold backing materials using the SPS technique [1]. The targets were irradiated with 16 MeV proton beams at 10 μA for 15 min. The irradiated target was dissolved in concentrated HCl, then diluted to 3% HCl in ethanol and loaded onto a column containing AG1-X8 resin. Chromium was eluted using a solution of 3% HCl in ethanol, while manganese was then eluted with 3 mL of HCl 0.1 M and directly loaded onto an AG50W-X8 resin. After washing with HCl at various concentrations, the purified ^{52}Mn is eluted with HCl 1.5M (recovery yield was determined about 78%). DOTA-SCN has been labeled with the purified [^{52}Mn]$MnCl_2$ with radiochemical yield > 99%.
Conclusion: The developed technology allows to obtain cyclotron-produced ^{52}Mn in high yield and purity. The development of new bimodal probes for manganese-based PET-MRI imaging is currently under investigation.

Acknowledgements
This work was done within the METRICS project founded by CNS5-INFN.

Reference

1. Pupillo G et al. Cyclotron-based production of innovative medical radionuclides at the INFN-LNL: state of the art and perspective. Eur. Phys. J. Plus. 2023; 138:1095.

OP34

An alternative production route for the PET radionuclide copper-61: exploring the ^{62}Ni(p,2n)^{61}Cu nuclear reaction

Santiago A Brühlmann[1,2], Martin Walther[1], Klaus Kopka[1,2,3,4], Martin Kreller[1]
[1]Helmholtz-Zentrum Dresden-Rossendorf, Institute of Radiopharmaceutical Cancer Research, Bautzner Landstraße 400, D-01328 Dresden, Germany. [2]Technische Universität Dresden, School of Science, Faculty of Chemistry and Food Chemistry, D-01062 Dresden, Germany. [3]National Center for Tumor Diseases (NCT) Dresden, University Hospital Carl Gustav Carus, Fetscherstraße 74, 01307 Dresden, Germany. [4]German Cancer Consortium (DKTK), Partner Site Dresden, Fetscherstraße 74, 01307 Dresden, Germany

EJNMMI Radiopharmacy and Chemistry 2024, **9(1)**: OP34

Aim: True theranostic matched pairs of radionuclides are a topic of high interest in the radiopharmaceutical sciences. From the handful of true matched radionuclides, the radiocopper trio copper-61 (^{61}Cu), copper-64 (^{64}Cu) and copper-67 (^{67}Cu), for diagnosis through PET and endoradiotherapy, respectively, stands out due to its simple chemistry and favorable physical properties. Furthermore, the high availability of ^{64}Cu has enabled huge developmental projects of copper-based radiopharmaceuticals [1]. Nevertheless, a shorter-lived PET radionuclide such as ^{61}Cu may as well be beneficial. Currently, ^{61}Cu is being produced either from nickel-61, zinc-64 or natural occuring zinc, however, we present here our results on the production via the ^{62}Ni(p,2n)^{61}Cu nuclear reaction.
Materials and methods: Thick nickel electrodepositions (130-260 mg/cm2) were performed from [^{62}Ni][Ni(NH_3)6]SO_4 solutions (fresh metallic ^{62}Ni ingots or recycled [^{62}Ni]$NiCl_2$, pH 9, I = 26 mA) onto gold backings, similar as already described by our group for ^{64}Ni [2]. These targets were irradiated at our TR-Flex (ACSI) cyclotron, with an incident proton energy of 20-22 MeV (target mass-dependent) and 70 µA current for 1 h. After a 1 h decay to reduce the also occurring ^{62}Cu-activity, radiochemical purification was performed by a one-step separation based on a 2 mL AG-1 × 8 column or a 1 mL TK201 cartridge, respectively. The radiocopper elution was performed with H_2O or 0.01 M HCl, respectively. Aliquots of the nickel, cobalt and copper fractions were analyzed by gamma-spectroscopy means. Apparent molar activities (AMA) of the solution were determined by titration of the [^{61}Cu]$CuCl_2$ fraction with the macrocyclic complexing agent 1,4,8,11-Tetraazacyclotetradecane-1,4,8,11-tetraacetic acid (TETA) in combination with radio-TLC.
Results: Saturation yields of 800-1500 MBq/µA were quantified, representing 25% of the theoretical ones. Copper-61 activities of up to 20 GBq at EOB were quantified, which was translated to up to 8 GBq at end of purification (EOP) contained in 2 mL 1.5 M HCl (which could be dried and re-dissolved in 700 µL H_2O) or in 2 mL 0.01 M HCl, depending on the separation method. Both alternatives lead to comparable results regarding separation yield and product purity. The [^{61}Cu]$CuCl_2$ solution proved radionuclidic purities over 99% and AMA of 260 GBq/µmol with the TETA chelator, EOP corrected.
Conclusion: We present here a comprehensive novel production method for the PET radionuclide ^{61}Cu as alternative to the most popular production routes. Characterization of the [^{61}Cu]$CuCl_2$ product showed both high RNP as well as high AMA up to 9 h after EOP. Furthermore, production scalability could be easily achieved by increasing the irradiation time.

References

1. IAEA. Copper-64 radiopharmaceuticals: Production, quality control and clinical applications. Vienna, Austria: IAEA; 2023.
2. Thieme S, Walther M, Pietzsch H-J, Henniger J, Preusche S, Mäding P, Steinbach J (2012) Module-assisted preparation of ^{64}Cu with high specific activity. Applied Radiation and Isotopes 70:602–608.

PP01

Addressing the side product challenge in copper-mediated radiofluorination

Sarandeep Kaur [1,2], Barbara Wenzel[1], Klaus Kopka [1,2], and Rareş-Petru Moldovan[1]
[1]Helmholtz-Zentrum Dresden-Rossendorf (HZDR), Institute of Radiopharmaceutical Cancer Research, Department of Neuroradiopharmaceuticals, Research Site Leipzig, 04318 Leipzig. [2]Faculty of Chemistry and Food Chemistry, School of Science, TU Dresden, 01069 Dresden, Germany

EJNMMI Radiopharmacy and Chemistry 2024, **9(1)**: PP01

Aim: Copper-Mediated Radiofluorination (CMRF) is one of the most significant developments of the last decade for the production of ^{18}F-aryl-containing radiopharmaceuticals [1]. Despite extensive research and improved radiolabelling conditions, the generation of the H-side product (Fig. 1) continues to be an issue in these CMRF reactions because this impurity is often difficult to separate from the desired radiotracer. In our research, we therefore focused on the identification of the sources and reaction parameters influencing the "H"-side product formation in these CMRF reactions.

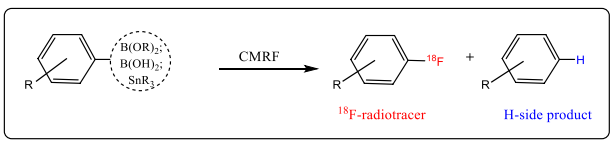

Fig. 1 A general scheme showing the H-side product formation in copper-mediated radiofluorination.
Materials and methods: The CMRF reactions were investigated with two structurally different pinacol boronic ester precursors and optimized by varying the following parameters: solvent (DMA, DMI, *n*-BuOH), reaction time (5—20 min), temperature (110—130 °C), base (K_2CO_3) and molar ratio between precursor and Cu-complex (1:3, 2:3, 1:8). To investigate the source of protons, deuterated reagents (D_2O, *n*-BuOD-d_{10}, $TBADCO_3$, K_2CO_3 in D_2O) were used. The influence of different leaving groups of the precursors (boronic acid, pinacol boronic ester and stannyl group) was also evaluated. The effect of amounts of different eluting phase transfer catalysts (PTCs) ($TBAHCO_3$, $TEHCO_3$, TBAOTf, $DMAPHCO_3$) was also investigated. Moreover, the dependency on the formation of the H-side product from the reaction time (2—30 min) was studied.
Results: The respective radiofluorinated products were achieved with a high radiochemical conversion of about 80-90% using 2 mg of respective pinacol boronic ester, 10 mg of $[Cu(OTf)_2(Py)_4]$ (molar ratio of 1:4) in *n*-BuOH:DMI (1:2, *v/v*) at 110 °C for 5 min. The H-side product was successfully separated from the radiofluorinated product using a semi-preparative HPLC with a pentafluorophenyl-based column. Under deuteration conditions the experiments revealed that quenching the reaction with D_2O had no influence on the H-side product formation, but the use of *n*-BuOD-d_{10} increased its generation by four-fold. The different eluting PTCs (Bu_4NHCO_3, Et_4NHCO_3, Bu_4NOTf, $DMAPHCO_3$) implied no significant influence on the H-side product formation, however, the exclusion of K_2CO_3 not only improved RCC but also decreased the H-side product formation. The use of boronic acid as leaving group led to an increased H-side product formation by several folds as compared to the use of the pinacol boronic ester-bearing precursor. Moreover, the use of a precursor with acidic protons in the molecular structure (e.g. NH) enhance the H-side product formation. In general, the yield of the H-side product formation reached a plateau at 10 min of reaction.

Conclusion: Despite a number of hurdles, the CMRF reactions are currently being widely employed for the production of radiopharmaceuticals embodying a wide variety of ^{18}F-aryl scaffolds. To overcome the purification difficulties of fluorine-18-containing radioligands due to H-side product formation, further improvements and mechanistic studies need to be undertaken.

Reference

1. Wright JS, Kaur T, Preshlock S, et al. *Clin Transl Imaging.* **2020** Jun;8(3):167-206.

PP02

Radionuclidic purity of ^{68}Ga eluted from ^{68}Ge/^{68}Ga generators by Thin Layer Chromatography

Tania P B Tchobnian[1], Joao A Osso Jr[2*]
[1]IPEN-CNEN/SP, Brazil. [2]Retired, independent consultant, Brazil
[*]**Corresponding author**: jaossoj@yahoo.com.br

EJNMMI Radiopharmacy and Chemistry 2024, **9(1)**: PP02

Background: ^{68}Ga is a PET emitter radionuclide with an important role in nuclear medicine diagnosis procedures. The physical half-life of 68 min is compatible with the pharmacokinetics of many biomolecules and low molecular weight substrates. Another important feature is its availability from a generator system, where the parent radionuclide, ^{68}Ge ($t_{1/2} = 270.95$ days) is adsorbed on a column and daughter, ^{68}Ga, is eluted in ionic form $^{68}Ga^{3+}$. The objective of this work was to develop a new method for the determination of the radionuclidic purity [1] of ^{68}Ga, allowing a fast determination of the ^{68}Ge breakthrough in ^{68}Ga eluates.

Materials and methods: The method to evaluate the ^{68}Ge impurity in ^{68}Ga samples recommended by the European Pharmacopeia is to measure the activity of 68Ga eluted from the generator, allow 24 h decay and measure the same sample. All ^{68}Ga activity will come from the decay of ^{68}Ge, so the level of ^{68}Ge is calculated. The proposed methodology was based on the different behaviour of Ge and Ga in thin layer/paper chromatography [2]. Several solvents and strips were tested, as well as different solutions added to the spot point to interact with the species. The detection and quantification limits were calculated for the best system to evaluate the possibility of reaching the maximum level of ^{68}Ge given in the monograph.

Results: The best system was achieved using TLC-SG-IB-F strips, acetone as solvent and a solution of 3 mol L^{-1} HCl added to the spot point of the strip. The retention factors were 0.1 for ^{68}Ge and 0.5-0.6 for ^{68}Ga, allowing to cut the strips into 2 pieces for measuring in the detector. The detection and quantification limits showed that the strip sample could be measured 2 h after the beginning of the quality control procedure, then correcting to the full growth of ^{68}Ge. Samples were measured using the traditional and the proposed method and the values were similar.

Conclusions: The proposed method is simple, fast and allow the evaluation of the ^{68}Ge impurity in samples of ^{68}Ga freshly eluted from the generators.

References

1. IAEA International Atomic Agency Agency. Quality Control in the Production of Radiopharmaceuticals. Vienna: IAEA; 2018
2. Eppard E, Loktionova NS. Rösch F, ^{68}Ge content quality control of Ge/Ga-generator eluates and Ga radiopharmaceuticals – A protocol for determining the Ge content using thin-layer chromatography. Appl Radiat Isot; 2014: vol 91: 92–96

PP03

TECANT Journey: Tracing the Path of ^{99m}Tc-labelled Somatostatin Antagonist from Concept to Clinical Realization

Renata Mikolajczak[1], Irene Virgolini[2], Luka Lezaic[3], Gianpaolo di Santo[2], Clemens Decristoforo[2], Petra Kolenc[3], Marta Opalinska[4], Andrej Studen[5], Piotr Garnuszek[1], Urban Simoncic[5], Malgorzata Trofimiuk-Muldner[4], Christine Rangger[2], Boguslaw Glowa[6], Konrad Skorkiewicz[6], Melpomeni Fani[7], Anna Sowa Staszczak[4], Barbara Janota[1], Marko Kroselj[3], Sebastijan Rep[3], Anton A. Hoermann[2], Alicja Hubalewska-Dydejczyk[4]
[1]National Centre for Nuclear Research Radioisotope Centre POLATOM, Otwock-Swierk, Poland. [2]Department of Nuclear Medicine, Medical University Innsbruck, Innsbruck, Austria, [3]Department of Nuclear Medicine, University Medical Centre Ljubljana, Ljubljana, Slovenia. [4]Chair and Department of Endocrinology, Jagiellonian Medical College, Krakow, Poland. [5]Faculty of Mathematics and Physics, University of Ljubljana, Ljubljana, Slovenia. [6]University Hospital Krakow, Kraków, Poland, 7Universitätsspital Basel, Basel, Switzerland.

EJNMMI Radiopharmacy and Chemistry 2024, **9(1)**: PP03

Aim: Radiolabelled somatostatin analogues targeting tumors overexpressing somatostatin receptors (SST) are powerful tools in managing patients with neuroendocrine neoplasms (NENs). Although SST agonists, labelled with technetium-99m or gallium-68, are currently established diagnostic tools for imaging NENs, there is an extensive ongoing development of radiolabelled SST antagonists. The advantages of ^{68}Ga-labelled SST antagonists have been recently demonstrated (1). Quantitative imaging with single-photon emitting ^{99m}Tc-labelled SST antagonists can be widely available and might represent a significant advancement in the management of NEN patients.

Here we describe the preclinical and pharmaceutical development of the SST antagonist [^{99m}Tc]Tc-TECANT1 and the first results of the feasibility clinical study.

Materials and methods: Two compounds (N4-LM3 and N4-p-Cl-BASS) were successfully radiolabelled with technetium-99m and compared with in vitro and in vivo tests (2). The kit formulation with N4-LM3: p-Cl-Phe-cyclo(D-Cys-Tyr-DAph(Cbm)-Lys-Thr-Cys)-D-Tyr-NH2 (TECANT1) was developed and manufactured in compliance with cGMP requirements (3).

Ten patients with advanced NEN and confirmed SST positivity were enrolled in the phase I multicenter clinical study (EudraCT No: 2019-0033779-20) assessing the safety, tolerability, pharmacokinetics, dosimetry, and NEN targeting properties of [^{99m}Tc]Tc-TECANT1.

Results: Based on extensive preclinical studies the most promising SST antagonist TECANT1 was selected for clinical translation as an investigational medicinal product (IMP). The final composition of the freeze-dried 3-vial kit was established. The kit formulation was successfully adapted for three GMP grade batches that met all predefined specifications, based on several Ph. Eur. monographs and guidelines. These include those for the kit itself and those related to the radiolabelled product.

The subsequent clinical feasibility study confirmed the safety of [^{99m}Tc]Tc-TECANT1. [^{99m}Tc]Tc-TECANT1 showed a rapid distribution with predominant renal excretion and a very high detection rate in all examined patients. In most cases a higher contrast was achieved with [^{99m}Tc]Tc-TECANT1 in comparison to ^{68}Ga-SST agonists, the current gold standard in NENs imaging.

Conclusion: Within the TECANT project (ERA-PER med), the ^{99m}Tc-labelled SST antagonist TECANT1 was selected for clinical translation based on its favorable preclinical data. The 3-vial kit formulation was successfully translated into the clinical setting.

We consider that the [^{99m}Tc]Tc-TECANT1 development may be the key to a reliable assessment of the SST status (primary focus/metastasis) and will be important for improving personalized NEN management. The final results of the clinical study are pending.

References

1. Nicolas G, Schreiter N, Kaul F, Uiters J, Bouterfa H, Kaufmann J, et al. Sensitivity Comparison of ^{68}Ga-OPS202 and ^{68}Ga-DOTATOC PET/CT in Patients with Gastroenteropancreatic Neuroendocrine Tumors: A Prospective Phase II Imaging Study. J Nucl Med 2018; 59:915–921
2. Fani M, Weingaertner V, Kolenc Peitl P, Mansi R, Gaonkar RH, Garnuszek P, et al. Selection of the first ^{99m}Tc-labelled somatostatin receptor subtype 2 antagonist for clinical translation—Preclinical assessment of two optimized candidates. Pharmaceuticals. 2020;14(01):19
3. Novak D, Janota B, Hörmann AA, Sawicka A, Kroselj M, Hubalewska-Dydejczyk A, et al. Development of the ^{99m}Tc-labelled SST2 antagonist

TECANT-1 for a first-in-man multicentre clinical study. Pharmaceutics. 2023;15(3):885.

PP04

The potential use of palladium radionuclides for Targeted Auger electron Therapy (^{103}Pd) and theragnostic applications (^{109}Pd)

Cathryn H.S. Driver[1,2*], Cecile Swanepoel[2], Julie Pineau[3], Nathalie le Bris[3], Thomas Ebenhan[2,4], Raphael Tripier[3], Zoltan Szucs[5], Jan Rijn Zeevaart[1,2]
[1]South African Nuclear Energy Corporation, R104 Pelindaba, North West, 0240, South Africa. [2]Nuclear Medicine Research Infrastructure NPC; Capital Park, Pretoria, 0084, South Africa. [3]UMR-CNRS 6521 CEMCA, University of Brest, Brest, 29200, France. [4]Department of Nuclear Medicine, University of Pretoria, Pretoria, 0084, South Africa. [5]MTA Atomki, Bem Square 18/c, Debrecen, 4026, Hungary

EJNMMI Radiopharmacy and Chemistry 2024, **9(1)**: PP04

Aim: The use of natural palladium for treating disease is well researched, and a number of Pd-complexes exist that are anti-viral, anti-fungal, anti-microbial and anti-cancer [1]. The use of radioactive palladium however, is not widespread except for the use of ^{103}Pd-seeds for brachytherapy treatment of prostate cancer [2] and rare reports of radiolabeled ^{103}Pd- or ^{109}Pd-compounds [3]. The palladium complexation techniques can be adapted to the use of radioactive palladium and therefore great potential exists for the incorporation of this metal into new radiopharmaceuticals.

Palladium-103 ($t_{1/2}$ = 17 d) decays to Rhodium-103m ($t_{1/2}$ = 56 min) to stable Rhodium-103 via electron capture with the releases of low-energy Auger electrons that are suitable for targeted Auger electron therapy [4].Palladium-109 ($t_{1/2}$ = 13.7 h) decays by β-particle emission to Silver-109m ($t_{1/2}$ = 39.6 s) and then to stable silver-109 by emission of gamma-rays with conversion and Auger electrons [5]. The ^{109}Pd-emissions make this radionuclide potentially suitable as a theragnostic agent for Beta and Auger electron therapy, as well as SPECT and Cherenkov luminescence imaging (CLI). The current study aimed to investigate the ^{103}Pd- and ^{109}Pd-labelling of functionalized cyclam macrocycles, as well as evaluating the capacity of ^{109}Pd-radionuclide for CLI and SPECT imaging, both in vitro and in vivo.

Materials and methods: Palladium-103 was obtained through proton irradiation and processing of a rhodium foil target while Palladium-109 was obtained from neutron irradiation of a 94% enriched Pd-108 metal target. ^{103}Pd/^{109}Pd-radiolabelling of functionalized cyclam compounds was done under various time, temperature and pH conditions in NH_4Oac (0.1M) or PBS (0.01 M). In vitro CLI of [^{109}Pd]$PdCl_2$ was done as a 1:2 dilution series in a 24-well plate at half-life appropriate time points. SPECT/CT imaging of [^{109}Pd]$PdCl_2$ phantoms was done according to manufacturer specifications with uniformity and sensitivity analysis. For in vivo CLI and SPECT/CT imaging, [^{109}Pd]$PdCl_2$ was administered to nu/nu mice with imaging for 5 min and 30 min, respectively, at 1, 4 and 24 h.

Results: ^{103}Pd- and ^{109}Pd-complexes were obtained in an 83% and 97% radiochemical yield (> 95% radiochemical purity), respectively at pH 4, 90 °C, 30 min in NH_4Oac and pH 7, 23 °C, 15 min in PBS. [^{109}Pd]$PdCl_2$ exhibited excellent in vitro CLI properties but poor uniformity and low sensitivity on SPECT/CT phantom imaging. However, in vivo studies indicated that ^{109}Pd-radionuclides can be visualized through both CLI and SPECT imaging techniques.

Conclusion: The successful macrocyclic complexation of palladium-103 and -109, and the CLI and SPECT images obtained for [^{109}Pd]$PdCl_2$, indicated that these radionuclides can be incorporated into various ligands for the development on new radiopharmaceuticals for targeted Auger electron therapy or theranostic applications.

References

1. Garoufis, A.; Hadjikakou, S. K.; Hadjiliadis, N. Palladium coordination compounds as anti-viral, anti-fungal, anti-microbial and anti-tumor agents. Coord. Chem. Rev. 2009, 253: 1384–1397.
2. Vicini, F. A.; Kini, V. R.; Edmundson, G.; Gustafson, G. S.; Stromberg, J.; Martinez, A. A comprehensive review of prostate cancer brachytherapy: defining an optimal technique. Int. J. Radiation Oncology Biol. Phys. 1999, 44: 483–491.
3. Le Bris N, Pineau J, Lima L.M.P, Tripier R., Palladium(II) coordination with polyazacycloalkanes. Coordination Chemistry Reviews. 2022, 455: 214,343,
4. Van Rooyen, J.; Szucs, Z.; Zeevaart, J.R. A possible in vivo generator ^{103}Pd/^{103m}Rh—Recoil considerations. Applied Radiation and Isotopes. 2008, 66: 1346–1349.
5. Pineau, J., Lima, L. P., Platas-Inglesias, C., Zeevaart, J. R., Driver, C. H. S., Le Bris, N., Tripier, R. Relevance of Palladium to Radiopharmaceutical Development considering Enhanced Coordination Properties of TE1PA. Chem. Eur. J. 2022, 28: e202200942.

PP05

Fully automated, GMP-compliant, one-pot production of 6-L-[^{18}F]FDOPA using an optimized [^{18}F]fluorodestannylation Approach

Chantal Kwizera[1*], Simon Blok[1], Maria Kominia[1], Rolf Zijlma[1], Hendrikus Boersma[1], Philip Elsinga[1], Erik de Vries[1], Inês Antunes[1], Gert Luurtsema[1]
[1]Department of Nuclear Medicine and Molecular Imaging, University of Groningen, University Medical Center Groningen, Groningen, The Netherlands
[*]**Corresponding author**: c.kwizera@umcg.nl

EJNMMI Radiopharmacy and Chemistry 2024, **9(1)**: PP05

Aim: 6-*L*-[^{18}F]fluoro-3,4-dihydroxyphenylalanine (6-*L*-[^{18}F]FDOPA) is a commonly used PET tracer for the detection and staging of neuroendocrine tumors and for the diagnosis of Parkinson's disease[1]. To satisfy the increasing demand for 6-*L*-[^{18}F]FDOPA in clinical practice, we aimed to develop an automated GMP—compliant method for the synthesis of 6-*L*-[^{18}F]FDOPA in high yields.

Materials and methods: 6-*L*-[^{18}F]FDOPA was prepared via a one-pot Cu-mediated ^{18}F-fluorination on an IBA Synthera® module, followed by acidic removal of the protecting groups (Fig. 1). To improve the radiochemical yield of the radiosynthesis the temperature and time during fluorination were optimized (100-150 °C; 15-30 min). The radiochemical conversion yield(RCC) was assessed by TLC-SG (eluent: ethyl acetate/n-hexane, 1:1, *v/v*). Various HPLC eluents and columns (single and in sequence) were tested for improving the purification of 6-*L*-[^{18}F]FDOPA. The radiochemical purity (RCP) of the final product was assessed by UPLC (column: ACQUITY UPLC® HSS T3, 1.8µm, 3.0mm x 50mm; eluent: 0.05M NaH_2PO_4 pH = 2.5; flow: 0.8 ml/min). For assessing the end product's enantiomeric purity, a chiral column, Chirobotic T 5µm4.6 × 250 mm; eluent: 90% methanol; flow:1.7ml/min) was used.

Results: The Cu-mediated ^{18}F-fluorination was obtained with the highest RCC of 53% at 140 ^{0}C for 30 min. Temperatures higher than 140 ^{0}C did not improve the yield due to the decomposition of the product. Additionally, when heated for 15 min at 110 ^{0}C followed by 15 min at 140 ^{0}C, the RCC increased to 65%. In the purification step of 6-*L*-[^{18}F]FDOPA, when using a single column (Agilent ZorbaxSB or Hamilton PRP-1) the overall radiochemical yield (RCY % n.d.c) was 20%; with a RCP < 92%, and the amount of DMA of 1.35 g/L (n = 5) or 0.93 g/L (n = 5), respectively, which were not within QC release criteria. However, when the purification of 6-*L*-[^{18}F]FDOPA was performed with both HPLC columns in series (Agilent ZorbaxSB – C18, 5 µm, 10 × 250 mm and Hamilton PRP-1, 10 µm, 10 × 250 mm; eluent: 4% ethanol: water containing 0.1% acetic acid) this lead to an overall RCY of 25% with a RCP > 95% containing 0,27 g/L of DMA (Release criteria < 1 g/L) and enantiomeric purity of 99% (n = 5).

Conclusion: We now have an optimized fully automated GMP-compliant synthesis of 6-*L*-[^{18}F]FDOPA in the IBA Synthera module that fulfills all release criteria and is suitable for clinical use.

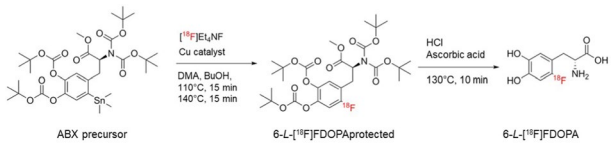

Fig. 1 Schematic representation of one-pot production of 6-*L*-[^{18}F]FDOPA.

Reference

1. Luurtsema G, Boersma HH, Schepers M,et al.. Improved GMP-compliant multi-dose production and quality control of 6-[^{18}F]fluoro-L-DOPA. EJNMMI Radiopharm Chem. 2017;1(1):7. Erratum in: EJNMMI Radiopharm Chem. 2018;3:13.

PP06

Advancing into the realm of innovative theranostic radionuclides: separation of silver-111 from a neutron-irradiated palladium target

Marianna Tosato[1,2], Andrea Gandini[3], Steffen Happel[4], Marine Bas[4], Antonietta Donzella[5,6], Aldo Zenoni[5,6], Andrea Salvini[3], Alberto Andrighetto[7], Valerio Di Marco[2], Mattia Asti[1]
[1]Radiopharmaceutical Chemistry Section, Nuclear Medicine Unit, AUSL—IRCCS Reggio Emilia, 42122 Reggio Emilia, Italy. [2]Department of Chemical Sciences, University of Padova, 35131 Padova, Italy. [3]Laboratory of Applied Nuclear Energy, 27100 Pavia, Italy. [4]TrisKem International SAS, Brittany 35170, France. [5]Department of Mechanical and Industrial Engineering, University of Brescia, 25123 Brescia, Italy. [6]Italian Institute of Nuclear Physics, Pavia Section, 27100 Pavia, Italy. [7]Italian Institute of Nuclear Physics, Legnaro National Laboratories, 35020 Legnaro (Padova), Italy.
EJNMMI Radiopharmacy and Chemistry 2024, **9(1)**: PP06

Aim: Silver-111 ($t_{1/2}$ = 7.47 d) exhibits both medium-energy β − ($E_{β−}$, max = 1.04 MeV) and low-energy γ ($E_γ$ = 245.4 keV, $I_γ$ = 1.24%; $E_γ$ = 342.1 keV, $I_γ$ = 6.7%) emissions with promising potential for targeted radionuclide therapy and associated single photon emission computed tomography imaging. Its decay properties closely recall those of the clinically established lutetium-177, rendering it an alluring candidate for therapeutic applications. Furthermore, the clinical significance of silver-111 is heightened by the presence of a positron-emitting counterpart (silver-103; $t_{1/2}$ = 65.7 min, $E_{β+}$ = 2.4 MeV), thereby endowing this element with true theranostic potential [1]. Such a well-suited pair has the potential to overcome current limitations tied to the compelled use of chemically distinct isotopes as imaging surrogates for lutetium-177. However, the utilization of radiopharmaceuticals labeled with silver isotopes has been hampered by the lack of suitable chelators capable of forming stable complexes, as well as the difficulties associated with their production and the radiochemical separation from target materials [2]. In a noteworthy endeavor to tackle a part of these challenges, this study aims to establish a separation method for the purification of reactor-produced silver-111, affording it in a formulation suitable to the direct radiolabeling of appropriate targeting vectors.
Materials and methods: The adsorption behavior of Ag^+ and Pd^{2+} onto an extraction chromatographic LN Resin was assessed by determining the weight distribution ratios (D_w) over a wide range of HCl concentrations. Then, a separation process involving LN and TK200 resins was first developed for Ag^+ and Pd^{2+} cations in conditions mimicking a real silver-111 production. The effectiveness of the separation was assessed by ICP-OES. Silver-111 (0.6 MBq) was produced via the ^{110}Pd(n,γ)^{111}Pd nuclear reaction on a natural palladium target and the subsequent β − -decay of palladium-111 at TRIGA Mark II nuclear research reactor (LENA, Pavia, Italy) [3]. The separation process developed for the non-radioactive counterpart was translated to the purification of produced silver-111 from the palladium target. The effectiveness of the separations was confirmed by γ-spectrometry.
Results: Silver-111 retrieval was afforded in 10 mL of pure water. Overall recovery was > 90% with a radionuclidic purity > 99% and a separation factor of around $4.21 \cdot 10^{-4}$ from palladium.
Conclusion: The developed separation gave the proof of concept of a method suitable to obtain silver-111 in a ready-to-use water-based formulation. A scale-up production to amounts of silver-111 suitable for pre- and clinical studies is needed to validate the process.

References

1. Tosato M, Asti M. Lights and shadows on the sourcing of silver radioisotopes for targeted imaging and therapy of cancer: production routes and separation methods. Pharmaceuticals. 2023; 16(7): 929
2. Tosato M, Asti M, Dalla Tiezza M, Orian L, Häussinger D, Vogel R, Köster U, Jensen M, Andrighetto A, Pastore P, Di Marco V. Highly stable silver(I) complexes with cyclen-based ligands bearing sulfide arms: a step toward silver-111 labeled radiopharmaceuticals. Inorg. Chem. 2020; 59(15): 10,907–10919.
3. Morselli L, Donzella A, Arzenton A, Asti M, Bortolussi S, Corradetti S, D'Agostino G, Luzio MD, Ferrari M, Gandini A, Lunardon M, Villa V, Salvini A, Zangrando L, Zenoni A, Andrighetto A. Production and characterization of ^{111}Ag radioisotope for medical use in a TRIGA Mark II nuclear research reactor. Appl. Radiat. Isot. 2023; 197: 110,798.

PP07

Modelling ligand depletion for simultaneous affinity and binding site quantification on cells and tissue

Hadis Westin[1], Judith Weber[2], Klara Djurberg[1], Sara Lundsten Salomonsson[1,3], Maria Kamprath[2], Aileen Hoehne[2], Fernanda Vergara[2], Sina Bondza[1,3]
[1]Ridgeview Instruments AB, Uppsala, Sweden. [2]3B Pharmaceuticals GmbH, Berlin, Germany. [3]Department of Immunology, Genetics and Pathology, Uppsala University, Uppsala, Sweden.
EJNMMI Radiopharmacy and Chemistry 2024, **9(1)**: PP07

Abstract published here: https://www.nature.com/articles/s41598-023-37015-1.

PP08

Cationic amino acid-based technetium(I)-99m complexes for cancer imaging

Rúben DM Silva[1]*, Cristina P Matos[1], Catarina IG Pinto[1], Joana F Guerreiro[1], Lurdes Gano[1,2], Filipa Mendes[1,2], João D. G. Correia[1,2]
[1]Centro de Ciências e Tecnologias Nucleares, Universidade de Lisboa, Bobadela LRS, Portugal. [2]Departamento de Engenharia e Ciências Nucleares, IST, Universidade de Lisboa, Bobadela LRS, Portugal
*__Corresponding author__: ruben.silva@ctn.ist.ulisboa.pt

EJNMMI Radiopharmacy and Chemistry 2024, **9(1)**: PP08
Aim: The cellular metabolic reprograming in cancer cells has been seen as an opportunity to develop new radiopharmaceuticals for cancer imaging and therapy [1]. O-(2-[^{18}F]fluoroethyl)-L-tyrosine ([^{18}F]FET) and 2-deoxy-2-[^{18}F]fluoro-glucose ([^{18}F]FDG) are two prime examples of clinically employed radiopharmaceuticals targeting the enhanced metabolism of tumoral cells. [^{18}F]FET has been mostly applied in brain tumors whereas [^{18}F]FDG has a broad field of applications, being the most widely used PET radiopharmaceutical [2]. Many amino acid transporters are overexpressed in cancer cells, and the dysregulation of amino acid uptake impacts the mTOR signaling pathway, initiating a snowball effect and resulting in uncontrolled amino acid consumption and cell growth [3, 4]. Still, very few amino acid radiotracers have been reported and fewer with metallic cores.
Materials and methods: We have previously developed *fac*-[^{99m}Tc][$Tc(CO)_3(k^3$-Pz-L-Arg)]$^+$, a technetium-99m complex based on the amino acid L-Arginine for targeting NO/NOS-related pathways [5]. This complex exhibited moderate levels of time-dependent internalization in three human tumoral cell lines, which seems to be linked to cationic amino acid transporter 1 (CAT1). Furthermore, the radiocomplex is

stable in human plasma and is not cytotoxic in the tested cancer cells. This arginine-containing ^{99m}Tc-labelled organometallic complex paved the way towards the development of a family of complexes based on cationic amino acids with potential for targeting cationic amino acid transporters such as CAT1 and amino acid transporter $B^{0,+}$ ($ATB^{0,+}$).

Results: Herein, we will report on the (radio)synthesis and characterization of new ^{99m}Tc(I)-complexes of the type *fac*-[^{99m}Tc][Tc(CO)$_3$(k^3-Pz-Aa)]$^+$ (Aa = L-Arg, D-Arg, L-Lys, D-Lys, L-His or D-His) complexes, in which the amino acids are presented in both optical isomer forms. Cell uptake and internalization studies of all six complexes in four different cancer cell lines will be presented and compared with a control complex without pendant amino acids. The tested cell lines were selected based on the relative expression of the amino acid transporters CAT1 and $ATB^{0,+}$. All amino acid-containing complexes have shown higher uptake and internalization than the control complex, suggesting an amino acid transporter mediated mechanism. A preliminary biodistribution study in Balb/c nude mice with A549 xenografts of the best performing complex, *fac*-[^{99m}Tc][Tc(CO)$_3$(k^3-L-His)]$^+$, will be also described and discussed.

Conclusion: Overall, L-Histidine-based complexes present better results than other complexes and are promising tools for cancer imaging.

Acknowledgements

The authors would like to thank the Fundação para a Ciência e Tecnologia (FCT), Portugal, for financial support through projects PTDC/QUI-NUC/30147/2017, PTDC/BTM-TEC/29256/2017 UIDP/04349/2020. FCT is also acknowledged for PhD fellowships to RDMS (DFA/BD/4978/2020) and CIGP (DFA/BD/07119/2020).

References

1. Heiden MGV, Cantley LC, Thompson CB. Understanding the warburg effect: The metabolic requirements of cell proliferation. Science. 2009; 324(5930):1029–33.
2. Katsanos AH, Alexiou GA, Fotopoulos AD, Jabbour P, Kyritsis AP, Sioka C. Performance of [^{18}F]FDG, ^{11}C-Methionine, and [^{18}F]FET PET for Glioma Grading. Clin Nucl Med. 2019; 44(11):864–9.

PP09

Fast Screening tools: Unveiling molecular insights through nuclear in vivo imaging and efficient preclinical research

Sofia Lagoumtzi[1*], Maria Georgiou[1], Maritina Rouchota[1], Antonis Gkikas[1], Efthimios Lamprou[1], Eleftherios Fysikopoulos[1], George Loudos[1]
[1]BIOEMTECH, Lefkippos Attica Technology Park—NCSR Demokritos, Athens, Greece

EJNMMI Radiopharmacy and Chemistry 2024, **9(1)**: PP09

Aim: Molecular imaging is widely used for visualizing, characterizing, and measuring various physiological and abnormal biological processes at both molecular and cellular scales in preclinical and clinical levels (1). The assessment, targeting, and therapeutic efficacy of SPECT, PET, and alpha-emitting isotopes through non-invasive, in vivo screening are crucial in laboratory routines. Additionally, alpha and beta emitters demonstrate significant potential as therapeutic agents in clinical settings (2,3). Understanding radiopharmaceutical biokinetics through multimodal, in vivo imaging with short time frames, starting from time-zero post-injection, can open new horizons for various biological applications. Rapid screening of multiple compounds can significantly reduce the time required for conducting a study.

Materials and methods: Experiments were conducted with three dedicated benchtop planar scintigraphic devices. γ-eye™ and γ-eye™ large field of view (LFOV) were used for SPECT and alpha-emitting isotopes detection, while β-eye™ for PET isotope acquisitions.

For in vivo studies, copper-67 and indium-111 were intravenously administered to SKH-1 hairless albino mice with different tumor sizes, and 10 min static acquisition protocols for 7 successive days were used in γ-eye™ and γ-eye™ LFOV, respectively. Lead-212 was administered in an SKH-1 mouse model bearing a tumor, and 10 min static imaging protocol was performed with γ-eye™ using a high energy collimator. Finally, fluorine-18 was administered to a C57BL/6 healthy mouse for a sixty-minute dynamic imaging for zero-time point and a ten-minute static imaging for bone accumulation detection.

Results: In vivo studies have revealed the feasibility of successful different targets detection using diverse modalities across various experimental conditions. Specifically, in mice administered with copper-67 and bearing non-orthotopic tumors, the tumor was detectable at multiple time points, highlighting the effectiveness of the γ-eye™ system in long-term tumor monitoring. Additionally, imaging of four mice with tumors of different sizes, administered with indium-111 and scanned using the γ-eye™ LFOV, proved the ability to simultaneously scan several mice, enabling visual identification and quantification for direct comparison. The study involving tumor model administered with lead-212 suggested that γ-eye™ can reliably spot very low activities of alpha-emitters, serving as a valuable tool for their accurate detection and quantification. Finally, the fluorine-18 study in β-eye™ demonstrated that monitoring the kinetics of an isotope from the initial blood flow to final accumulation can be easily conducted through small-frame dynamic acquisition.

Conclusion: Results indicate that "eyes-series" devices can be used as a valuable tool in preclinical research, enabling the efficient fast screening of newly developed drugs in vivo on several different applications.

References

1. Rowe SP, Pomper MG. Molecular imaging in oncology: Current impact and future directions. CA Cancer J Clin. 2022 Jul;72(4):333–352
2. Lassmann M, Eberlein U. Targeted alpha-particle therapy: imaging, dosimetry, and radiation protection. Ann ICRP. 2018 Oct;47(3–4):187–195
3. Ebrahim S. Delpassand, Izabela Tworowska, Rouzbeh Esfandiari, Julien Torgue, Jason Hurt, Afshin Shafie and Rodolfo Núñez:Targeted α-Emitter Therapy with ^{212}Pb-DOTAMTATE for the Treatment of Metastatic SSTR-Expressing Neuroendocrine Tumors: First-in-Humans Dose-Escalation Clinical Trial, Journal of Nuclear Medicine September 2022, 63 (9) 1326–1333

PP10

Preclinical imaging of therapeutic alpha-emitters

Sofia Lagoumtzi[1*], Maria Georgiou [1*], Eleftherios Fysikopoulos[1], Izabela Tworowska[2], Leo Flores[2], Xuewei Qu[2], Maritina Rouchota[1], Efthimis Lamprou[1], Antonis Gkikas[1], George Loudos[1]
[1]BIOEMTECH, Lefkippos Attica Technology Park—NCSR Demokritos, Athens, Greece, EL. [2]Radiomedix Inc, Houston, Texas, US

EJNMMI Radiopharmacy and Chemistry 2024, **9(1)**: PP10

Aim: Alpha and beta emitters exhibit significant potential as therapeutic agents in clinical settings. (1, 2). Novel radionuclide-based compounds like lead-212 and actinium-225 are undergoing preclinical testing for future radiopharmaceutical development. Quantitative imaging of such compounds is possible via imaging of the gamma rays produced by complex decay schemes. Understanding the alpha and beta emitting radiopharmaceuticals biokinetics, in preclinical studies, is of major importance to evaluate its safety and efficacy (3, 4). Here, we present in vivo and phantom imaging studies of lead-212 and actinium-225.

Materials and methods: In vivo animal studies were performed on a dedicated bench top, mouse-sized, planar scintigraphy system (γ-eyeTM, BIOEMTECH, Greece). The system's ability to quantify activity variations was assessed using phantom experiments. It uses position-sensitive photomultiplier tubes, a CsI(Na) pixelated scintillator, and a high-sensitivity tungsten collimator with hexagonal holes for multiple gamma-emitting isotopes.

To evaluate system's sensitivity to activity variations, three cylindrical phantoms filled with lead-212 and actinium-225 were imaged. A mouse phantom (fillable mouse phantom, BIOEMTECH, Greece) with different isotope activities was used to further assess the system's accuracy.

In vivo lead-212 static scans with 10 min duration were performed at different time points, providing information on the distribution on the same animal. The total administered activity was < 1 MBq. During

imaging, mice were anesthetized using isoflurane, under constant temperature (37° C).
Results: Phantom studies results showed the capability of γ-eye™ to obtain accurate quantitative information of alpha emitting radiopharmaceuticals distribution in preclinical studies.
In vivo studies proved that successful tumor targeting with a ^{212}Pb-labelled compound is feasible in low activity and limited-time scans.
Conclusion: Non-invasive imaging of alpha emitters, by detecting their gammas and positrons, can lead to a derived imaging method. Specialized scintigraphy tools enable long-term tracking, potentially speeding up preclinical research.

References

1. Lassmann M, Eberlein U. Targeted alpha-particle therapy: imaging, dosimetry, and radiation protection. Ann ICRP. 2018 Oct;47(3–4):187–195.
2. Ebrahim S. Delpassand, Izabela Tworowska, Rouzbeh Esfandiari, Julien Torgue, Jason Hurt, Afshin Shafie and Rodolfo Núñez: Targeted α-Emitter Therapy with ^{212}Pb-DOTAMTATE for the Treatment of Metastatic SSTR-Expressing Neuroendocrine Tumors: First-in-Humans Dose-Escalation Clinical Trial, Journal of Nuclear Medicine September 2022, 63 (9) 1326–1333.
3. Seo Y. Quantitative Imaging of Alpha-Emitting Therapeutic Radiopharmaceuticals. Nuclear Medicine and Molecular Imaging. 2019 Jun;53(3):182–188.
4. Poty S, Francesconi LC, McDevitt MR, Morris MJ, Lewis JS. α-Emitters for Radiotherapy: From Basic Radiochemistry to Clinical Studies-Part 1. J Nucl Med. 2018 Jun;59(6):878–884.

PP11

Microwave in PET Radiochemistry

Ângela C.B. Neves[1,2*], Ivanna Hrynchak[1,2], V.H. Alves[1,2], Inês C.F. Fonseca[1,2], Vanessa A. Tomé[1,2], A.J. Abrunhosa[1,2]
[1]ICNAS Pharma Unipessoal, Lda., Ed. ICNAS, Pólo das Ciências da Saúde, University of Coimbra, Coimbra, Portugal. [2]CIBIT/ICNAS—Institute for Nuclear Science Applied to Health—University of Coimbra
[*]**Corresponding author**: angela.neves@uc.pt

EJNMMI Radiopharmacy and Chemistry 2024, **9(1)**: PP11
Aim: Microwave-assisted synthesis has been proven to be a highly effective method for a wide range of chemical transformations that require a heating source [1]. The short half-life of most used radionuclides for Positron Emission Tomography (PET), carbon-11, gallium-68, and fluorine-18, accentuates the crucial need of decrease the reaction times and enhance the yields. Application of this technology in radiopharmaceutical synthesis has been reported and shows higher yields and selectivity than the corresponding conventional heating (CH) source [2-4].
The main goal of this work was to implement the use of microwave heating (MH) in key steps of radiopharmaceuticals synthesis for PET imaging, such as [^{18}F]FDG, [^{18}F]FDOPA, [^{68}Ga]Ga-DOTANOC, [^{68}Ga]Ga-PSMA and [^{11}C]UCB-J.
Materials and methods: No-carrier-added [^{18}F]fluoride and [^{11}C]CO_2 were produced by an IBA Cyclone® 18/9 cyclotron. [^{68}Ga]$GaCl_3$ was obtained from a GalliaPharm® Ge-68/Ga-68 Generator from Eckert & Ziegler Radiopharma. The radiolabeling reactions were performed in a PET-Wave Discover® from CEM [^{11}C]CH_3I was produced at a Synthra® [^{11}C]choline.
Results: Azeotropic drying of K[^{18}F]F- and ^{18}F-fluorination of mannose triflate ([^{18}F]FDG precursor) were performed at a microwave (MW) cavity given a conversion of 78% in 40% of the time, when compared with conventional heating (CH) procedure.
Concerning the production of [^{18}F]FDOPA, one of the most complexes synthesis processes at the moment, fluorination of 6-nitroveratraldehyde was performed with MW heating, with a conversion of 100%, in less 60% of the time. Acid hydrolysis of protected [^{18}F]FDOPA with HCl or HI (37%), was also performed in 4 min, instead of 20 min by CH, which results in a reduction of 84% in the reaction time.
The setup was also tested in the radiolabelling of peptides, such as DOTANOC and PSMA-11 with [^{68}Ga]$GaCl_3$, achieving 100% of labelling yield in 1.5 min, instead the 10 min needed with CH (reduction of 85% in time) [5].
Another challenging process was the radiosynthesis of [^{11}C]UCB-J, performed via Suzuki-Miyaura cross-coupling mediated by a palladium (0) catalyst [6,7,8]. The microwave-assisted reaction was performed in 4.7 min (instead of 10 min by CH). The full synthesis process was implemented at ICNAS-P, yielding [^{11}C]UCB-J, with a global process RCY of 53%, molar activity of 369.7 GBq/μmol and 100% of the (R)-enantiomer.
Conclusion: The use of microwave heating in radiosynthesis gave good radiochemical yields in a significantly shorter reaction times than conventional heating in all tested reaction steps. These results indicate that microwave technology could offer a substantial advantage in the synthesis of radiopharmaceuticals with application in PET.

References

1. Stone-Elander S, Elander N. Microwave application in radiolabelling with short-lived positron-emitting radionuclides. J Label Compd Radiopharm. 2002; 45:715–746.
2. Yadi Y, Shimizu Y, Arimitsu K, Nakamoto Y, Higuchi T, Togashi K, Kimura H. Efficient gallium-68 radiolabelling reaction of DOTA derivatives using a resonant-type microwave reactor. J Label Compd Radiopharm. 2019; 62:132–138.
3. Dahl K, Lindberg A, Vasdev N, Schou M. Reactive Palladium-Ligand complexes for ^{11}C-Carbonylation at Ambient Pressure: A Breakthrough in Carbon-11 Chemistry. Pharmaceuticals. 2023; 16:955–968.
4. Teodoro R, Wenzel B, Oh-Nishi A, Fischer S, Peters D, Suhara T, Deuther-Conrad W, Brust P. A high-yield automated radiosynthesis of the alpha-7 nicotinic receptor radioligand [^{18}F]NS10743. Applied Radiation and Isotopes. 2015; 95:76–84.
5. Alves V, Prata M, Abrunhosa A, Castelo-Branco M. J Radioanal Nucl Chem. GMP production of ^{68}Ga-labelled DOTA-NOC on IBA Synthera. 2015; 305:501–506.
6. Nabulsi, B, Mercier, J, Holden, D, Carr, S, Najafzadeh, S, Vandergeten, C, Lin, F, Deo, A, Price, N, Wood, M, Lara-Jaime, T, Montel, F, Laruelle, M, Carson, E, Hannestad, J, Huang, Y. Synthesis and preclinical evaluation of [^{11}C]UCB-J as a PET tracer for imaging the synaptic vesicle glycoprotein 2A in the brain. J. Nucl. Med. 2016; 57:777–784.
7. Rokka J, Schlein E, Eriksson J. Improved synthesis of SV2A targeting radiotracer [^{11}C]UCB-J. EJNMMI Radiopharm. Chem. 2019; 4:1–10.
8. Sephton S, Miklovicz T, Russell J, Doke A, Li L, Boros I, Aigbirhio I. Automated radiosynthesis of [^{11}C]UCB-J for imaging synaptic density by positron emission tomography. J. Label. Compd. Radiopharm. 2020; 63:151–158.

PP12

Novel concept of a ^{44}Ti/^{44}Sc generator

Đorđe Cvjetinović[1], Patrick Steinegger[1], Dorothea Schumann[1]
[1]Laboratory of Radiochemistry, Paul Scherrer Institut, Villigen, Switzerland
EJNMMI Radiopharmacy and Chemistry 2024, **9(1)**: PP12

Aim: In radiopharmacy, advancements hinge on the accessibility of appropriate radionuclides for use in therapeutic, diagnostic, or dual applications. The potential breakthrough in PET diagnostics lies in the successful establishment of a ^{44}Ti/^{44}Sc generator system. With a half-life of 60 years, titanium-44 decays to scandium-44, a positron emitter with a favorable half-life of 4 h. If such a generator system is developed, it could remain operational for several years, if not decades. This extended operational lifespan would streamline the clinical availability and reduce costs associated with PET diagnostics globally. Despite the promising prospects, the development of a successful prototype has yet to materialize due to challenges such as titanium-44 breakthrough, long-term radiation damage, and low scandium-44 yields. Therefore, due to previous flaws of adsorption-based generator systems we have decided to investigate novel concepts for developing a

^{44}Ti/^{44}Sc generator. One of these concepts includes use of nano-particles enriched with titanium-44 that hasn't been tested before. This approach would potentially allow us to develop a solid state generator system that would have the needed long-term chemical and radiation stability coupled with a high yield of scandium-44.

Materials and methods

Nano-particle synthesis
Gamma spectroscopy
TEM/SEM
EDX

Results: Pending/to be presented

Conclusion: Up to now, various concepts for ^{44}Ti/^{44}Sc generators have been documented. However, due to inherent issues, such as an undesirable chemical form of eluent or the occurrence of titanium-44 breakthrough, none have received approval for medical applications. This situation underscores the need for enhancements and novel approaches in the pursuit of a stable ^{44}Ti/^{44}Sc generator, with potential applications in nuclear medicine. The existing reserve of titanium-44 at PSI arises incidentally from the operation of the institute's extensive research facilities. Consequently, additional quantities can be generated without requiring extra ion beam time. The successful development of a ^{44}Ti/^{44}Sc generator could facilitate uncomplicated access to scandium-44 without additional expenses, transforming it into a sustainable and entirely recyclable product.

References

1. Larenkov AA, Makichyan AG, Iatsenko VN. Separation of scandium-44 from titanium-44 in the Context of A Generator System for Radiopharmaceutical Purposes with the Example of [^{44}Sc] Sc-PSMA-617 and [^{44}Sc] Sc-PSMA-I&T Synthesis. Molecules. 2021 Oct 21;26(21):6371.
2. Singh A, van der Meulen NP, Müller C, Klette I, Kulkarni HR, Türler A, Schibli R, Baum RP. First-in-human PET/CT imaging of metastatic neuroendocrine neoplasms with cyclotron-produced [^{44}Sc]Sc-DOTATOC: a proof-of-concept study. Cancer biotherapy and radiopharmaceuticals. 2017 May 1;32(4):124–32.
3. Filosofov DV, Loktionova NS, Rösch F. A ^{44}Ti/^{44}Sc radionuclide generator for potential application of ^{44}Sc-based PET-radiopharmaceuticals. rca-Radiochimica Acta. 2010 Mar;98(3):149–56.

PP13

Automation of ^{11}C-labelled TSPO-tracer [^{11}C]Me-DPA synthesis with Trasis AllInOne-module

Edla Kerminen[1*], Noora Rajala[1], Simo Salo[1], Sarita Forsback[1,2], Anna K. Kirjavainen[1,2], Thomas Keller[1]
[1]Radiopharmaceutical Chemistry Laboratory, Turku PET Centre, University of Turku and Turku University Central Hospital, Turku, Finland. [2]Department of Chemistry, University of Turku, Turku, Finland
***Corresponding author**: ekkerm@utu.fi

EJNMMI Radiopharmacy and Chemistry 2024, **9(1)**: PP13

Aim: The overexpression of translocator protein (TSPO) is associated with various central nervous system diseases.[1] Me-DPA is a TSPO-ligand with promising binding properties towards radiotracer development such as high affinity and selectivity.[2] Previously, [^{11}C]Me-DPA has been radiolabelled using an in-house built fixed-line device that requires manual steps.[3] Although GMP radiopharmaceutical production is heading towards cassette-based syntheses, carbon-11 labelled tracers are lagging behind in that regard. Our aim was to automate the synthesis of [^{11}C]Me-DPA using the cassette based synthesis module, Trasis AllInOne (AIO).

Materials and methods: The [^{11}C]MeI was produced from [^{11}C]CO_2 using the "wet-method" (Fig. 1).[4] The [^{11}C]Me-DPA was synthesized via the Suzuki-Miyaura coupling reaction.[3] The reaction mixture was purified by semi-preparative HPLC and the final product was analyzed with radio HPLC. The synthesis was performed fully automated.

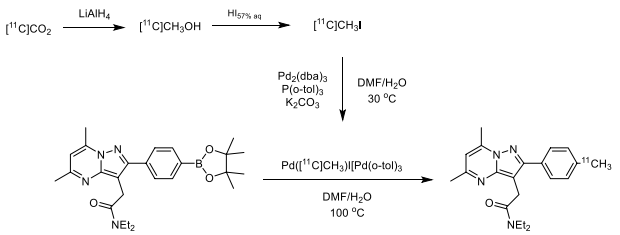

Fig. 1 Synthesis of [^{11}C]Me-DPA [3,4].

Results: The automated sequence developed on AIO was tested with starting activities from 25 to 47 GBq. The [^{11}C]Me-DPA was synthesized in 60 min with a radiochemical yield of 3-5% (calculated from the [^{11}C]CO_2 starting activity and decay corrected to the start of synthesis) and a radiochemical purity of > 99%.

Conclusion: [^{11}C]Me-DPA was successfully synthesized with Trasis AllInOne in a cassette. Although the synthesis was successfully automated, the [^{11}C]MeI production and the HPLC purification require further optimization.

Acknowledgements

The study was funded by the Academy of Finland (grant no. 307924 & 332128)

References

1. Guilarte TR. TSPO in diverse CNS pathologies and psychiatric disease: A critical review and a way forward (review article). Pharmacol Ther 2019;194:44–58
2. Selleri S, Bruni F, Costagli C, Costanzo A, Guerrini G, Ciciani G, et al. 2-Arylpyrazolo[1,5-a]pyrimidin-3-yl acetamides. New potent and selective peripheral benzodiazepine receptor ligands. Bioorg Med Chem 2001;9:2661–71.
3. Keller T, Lopéz-Picón F, Krzyczmonik A, Forsback S, Kirjavainen A, Haaparanta-Solin M, et al. O-36—Synthesis of [^{11}C]Me-DPA and evaluation in transgenic mouse model of Alzheimer's disease. Nucl Med Biol 2022;108–109:S25–6.
4. Långström B, Lundqvist H. The preparation of [^{11}C]methyl iodide and its use in the synthesis of ^{11}C-methyl-L-methionine. Int J Appl Radiat Isot 1976;27:357–63.

PP14

Cytotoxic and Antiproliferative Effects of [^{64}Cu]$CuCl_2$ in Tumor Cells for Radiometabolic Therapy: a Preliminary Study

Francesca Porto[1*], Giorgia Speltri[2], Silvia Pasquini[2], Chiara Contri[1], Martina Cappello[1], Petra Martini[3], Alessandra Boschi[2], Licia Uccelli[1], Katia Varani[1], Giovanni Di Domenico[4], Fabrizio Vincenzi[1]
[1]Department of Translational Medicine, University of Ferrara, Ferrara, Italy. [2]Department of Chemical and Pharmaceutical Sciences, University of Ferrara, Ferrara, Italy. [3]Department of Environmental and Prevention Sciences, University of Ferrara, Ferrara, Italy. [4]Department of Physics and Earth Sciences, University of Ferrara, Ferrara, Italy
***Corresponding author**: francesca.porto@unife.it

EJNMMI Radiopharmacy and Chemistry 2024, **9(1)**: PP14

Aim: Peritoneal carcinomatosis (PC) is a relatively common condition in the advanced stages of many cancers, where malignant tumor cells spread from the organ of origin to the peritoneum. The impact of PC is global, affecting approximately 25,000 individuals in Italy and 1.4 million worldwide every year, with mostly negative outcomes [1]. The aim of this study is to identify a treatment strategy focused on increasing the life expectancy of patients with PC, overcoming the challenge associated with the marked genetic instability of tumor cells, which is incompatible with the receptor-targeted and antigenic therapies

currently proposed [2]. The radionuclide copper-64 was employed in the form of [^{64}Cu]$CuCl_2$ to achieve this objective. It has been shown in recent studies that copper, in its ionic form Cu^{2+}, can accumulate at significantly higher levels in tumor cells than in healthy ones, which makes its cytotoxic effect highly specific. This effect can be achieved by exploiting the nuclear decay characteristics of copper-64 ($t_{1/2}$ 12.7 h; $E_{\beta+mean}$ 278 keV; $E_{\beta-mean}$ 191 keV; Auger emission) [3,4].
Materials and methods: Human tumor cell lines related to the development of peritoneal metastases (MDA-MB-231, human breast adenocarcinoma cell line; NCI-N87, human gastric carcinoma cell line) and a healthy control cell line (HEK293, human embryonic kidney cell line) were utilized in this study. These cell lines were exposed to different activities of [^{64}Cu]$CuCl_2$ (10 µCi/mL; 100 µCi/mL; 250 µCi/mL) to assess their uptake and the antiproliferative and cytotoxic effects. For this purpose, an analysis was conducted to determine the level of ^{64}Cu-incorporation in the nucleus and cytoplasm. Subsequently, in vitro studies on cell viability (XTT assay), apoptosis, and necrosis (Annexin V/SYTOX assay) were conducted after 72 h and 96 h of treatment.
Results: A greater uptake of the [^{64}Cu]$CuCl_2$ was observed in the tumor lines than in the healthy ones and, in particular, a greater localization at the nuclear level. Following exposure to different activities of [^{64}Cu]$CuCl_2$, a greater reduction of the viability in carcinoma lines was observed compared to the healthy control line as well as a significant increase in apoptosis in the MDA-MB-231 and NCI-N87 tumor line.
Conclusion: Our preliminary results confirm the increased uptake of [^{64}Cu]CuCl2 within the nucleus of cancer cells and suggest the ability of the radiopharmaceutical to cause cell death through the induction of apoptosis. Further studies to evaluate the antiproliferative and cytotoxic effects of [^{64}Cu]CuCl2 using higher activities of copper-64 are currently ongoing.

References

1. Klaver YL. Peritoneal carcinomatosis of colorectal origin: Incidence, prognosis and treatment options. World J Gastroenterol. 2012;18(39):5489.
2. Dagogo-Jack I, Shaw AT. Tumour heterogeneity and resistance to cancer therapies. Nat Rev Clin Oncol. febbraio 2018;15(2):81–94.
3. Beaino W, Guo Y, Chang AJ, Anderson CJ. Roles of Atox1 and p53 in the trafficking of copper-64 to tumor cell nuclei: implications for cancer therapy. JBIC J Biol Inorg Chem. marzo 2014;19(3):427–38.
4. Boschi A, Martini P, Janevik-Ivanovska E, Duatti A. The emerging role of copper-64 radiopharmaceuticals as cancer theranostics. Drug Discov Today. agosto 2018;23(8):1489–501.

PP15

PSMA-radioligand therapy: Institutional Experience

Mohammed Al-Qahtani[1*], Riyadh AlSalloum[2], Mohammed AlRowaily[2]
[1]Cyclotron and Radiopharmaceuticals Department, Research and Innovation. [2]Radiology Department, King Faisal Specialist Hospital & Research Center, Riyadh, Saudi Arabia
EJNMMI Radiopharmacy and Chemistry 2024, **9(1)**: PP15

Aim: Theranostics and nuclear medicine have been working together for a long time. The theranostic method has made personalized medicine possible. Molecular imaging with isotopes helps identify patients more likely to benefit from treatment. It also helps determine the best medication dosage for the patient and ensures proper follow-up for therapy. One of the aims is to predict and evaluate the clinical response, such as overall survival and progression-free survival. For instance, Positron Emission Tomography—Computed Tomography (PET/CT) scans with [^{18}F]FDG (fluorodeoxyglucose) help predict the outcome of conventional chemotherapy and targeted therapy.
PSMA-radioligand therapy (PSMA-RLT) is a promising treatment modality for prostate cancer (PC). It involves the administration of the ^{177}Lu-labeled prostate-specific membrane antigen (PSMA) analogue ([^{177}Lu]Lu-PSMA-617)cancer cells specifically. This theranostic approach is practical, and PET/CT using either gallium-68 radiolabeled PSMA analog ([^{68}Ga]Ga-PSMA-11) can confirm the presence of the therapeutic target and tumour uptake. Lutetium-177 is characterized by a therapeutic beta-emission and a gamma-emission that enables post-therapeutic SPECT imaging (single photon emission computed tomography). The practical implementation of the treatments has progressed from clinical research to marketing authorization.
Materials and methods: [^{177}Lu]Lu-PSMA, marketed as a single dose format, may require dose adjustments. Using an automated system reduces the exposure of agents during the highly irradiant stages of dose preparation. The medicinal product administration procedures have also been optimized to minimize the exposure of medical and paramedical workers involved. Diagnostic PET imaging involves the administration of [^{68}Ga]Ga-PSMA-11 analog. Extemporaneous preparations are necessary due to the radionuclide's fast decay. The evolution of clinical research towards nuclear medicine departments has simplified the labeling procedure, initially by industrial good manufacturing practice. These preparations involve high-energy radionuclides, making it necessary to use the most automated techniques for labeling and patient dose preparation.
Results: More than twenty-two patients underwent the [^{177}Lu]Lu-PSMA radioligand therapy with more than eighty treatment cycles during the last six years at our institution.
Conclusion: The treatment resulted in a significant enhancement in patients' quality of life. Our successful results encouraged several other local institutions to plan and use the [^{177}Lu]Lu-PSMA therapy. Nuclear medicine therapy, not only at our institution but also in all of Saudi Arabia, is undergoing a new dynamic. Thus, identifying new molecular targets may enable isotopic theranostic treatment for other cancer types.

PP16

Radiolabelling of [^{68}Ga]Ga-NODAGA-Exendin-4 in sodium acetate buffer

Maïlys Ragot[1*], Alban Revy[1], Sophie Levesque[1], Marion Tempier[1]
[1]Radiopharmacy, Jean Perrin Center, Clermont-Ferrand, France
[*]**Corresponding author**: mailys.ragot@gmail.com

EJNMMI Radiopharmacy and Chemistry 2024, **9(1)**: PP16
Aim: [^{68}Ga]Ga-NODAGA-Exendin-4 is a novel radiopharmaceutical drug for TEP imaging of benign insulinoma. In France, compassionate use of [^{68}Ga]Ga-NODAGA-Exendin-4 is allowed by current regulations. [^{68}Ga]Ga-NODAGA-Exendin-4 synthesis requires submission and expertise of an investigational medical product dossier (IMPD). In this context, we have developed in situ radiolabelling, using acetate buffer instead of HEPES, generally described in publications.
Materials and methods: The radiolabelling is automated on a TRASIS miniAIO® using single-use cassettes. The following steps and parameters were developed and optimized: 68Ga eluate cationic prepurification, pH in the reaction medium and buffer optimum concentration, cooling andfinal HPLC purification using a C18 column. All reagents used were European Ph. Grade. [^{68}Ga]$GaCl_3$ was obtained from a GalliaPharm® E&Z generator. Radiochemical purity of final product was performed using validated radio-HPLC method and must be higher than 95%.
Results: The 10 µg peptide NODAGA-Exendin-4 previously reconstituted in 100 µL wfi is first placed in the reaction vial, prepared with 50 µg of ascorbic acid and 1 mL of sodium acetate buffer 1M. The generator is then eluted with 5 mL of HCl 0.1M. The gallium-68 eluate is purified on a SCX cartridge, eluted with 1.5 mL of NaCl 5 M in HCl (0.1 M). The reaction takes place at 100 °C for 15 min. After labelling, 2 mL of EDTA (50 mM) and /polysorbate 20 (0.15%) solution are added into the reaction vial. After cooling, the solution is then purified on a HLB cartridge. Desorption of [^{68}Ga]Ga-NODAGA-Exendin-4 is achieved by washing with 1,6 mL of ethanol/water 60:40 (v/v). The final product is formulated for intravenous injection with NaCl (0.9%) by passing through a 0.22 µm sterilizing filter.
Three synthesis were realized in those final conditions. The mean final activity was 459 MBq (ranging from 455 to 465 MBq) corresponding to a decay-corrected radioactive synthesis yield of 46.3% (44-48%). The radiochemical purity was always higher than 95%, with a mean of 97%.
Conclusion: These conditions allow radiolabelling of NODAGA-Exendin-4 in sodium acetate buffer with a reliable synthesis process. The final activity and purity are compatible with clinical use. The next

step will be to prepare an IMPD to obtain authorization for clinical use, according to the French compassionate access.

PP17

Clearing Agents based on Poly-L-Lysine scaffolds for improved Pretargeted α-Radioimmunotherapy

Chiara Timperanza[1*], Anna Gustafsson-Lutz[1], Ellinor Hanson[1,2], Erik Leidermark[1], Stig Palm[1], Tom Bäck[1], Damian J. Green[3,4], Sture Lindegren[1*], Emma Aneheim[1,5*]
[1]Department of Medical Radiation Sciences, Institute of Clinical Sciences, Sahlgrenska Academy, University of Gothenburg, Gothenburg, Sweden. [2]Atley Solution AB, SE 41292. [3]Fred Hutchinson Cancer Center, Seattle, WA, USA. [4]University of Washington, Seattle, WA, USA. [5]Region Västra Götaland, Sahlgrenska University Hospital, Department of Oncology, SE 41345, Gothenburg, Sweden
EJNMMI Radiopharmacy and Chemistry 2024, **9(1)**: PP17

Aim: Pretargeted radioimmunotherapy of cancer has the potential to increase tumor-specific uptake of activity when compared with conventional radioimmunotherapy [1, 2]. This is especially true in α-radioimmunotherapy with nuclides that exhibit a relatively short half-life, like astatine-211 ($t_{1/2}$ = 7,2 h) [3, 4]. When administering antibody-based pretargeting molecules systematically, the antibodies often exhibit a relatively slow clearance from the blood [5, 6]. Therefore, the use of a clearing agent is advantageous to remove unbound pretargeting molecules from the circulation, facilitating a reduction in the non-specific radiation exposure to normal tissue while maximizing the dose delivered to the tumors [7].
Materials and methods: In the current study, two types of poly-L-lysine based clearing agents were produced for two different pretargeting systems: (strept)avidin/biotin and tetrazine/transcyclooctene. Poly-lysine is available in multiple sizes for optimization of the clearing abilities and can readily be modified with several functional groups, allowing for different pretargeting strategies to be used..
Results: In vivo evaluation of biotin-functionalized poly-lysine clearing agent (110 repeating units) resulted in a decrease in blood concentration of the iodine-125 labelled pretargeting agent of 50%, circa 23 h after injection, compared to controls. Two sizes of tetrazine-functionalized poly-lysine clearing agents were also evaluated (68 and 143 repeating units), which at 23 h decreased the blood concentration of the iodine-125 labelled pretargeting agent to 58% and 38%, respectively.
Conclusion: The straightforward synthesis of poly-lysine based clearing agents makes kit preparation possible and these agents show good potential for further evaluation, especially within the etrazine/transcyclooctene pretargeting system, where no liver or kidney accumulation was observed.

References

1. Cheal, S.M., et al., Pretargeting: A Path Forward for Radioimmunotherapy. J Nucl Med, 2022. 63(9): p. 1302–1315.
2. Altai, M., et al., Pretargeted Imaging and Therapy. J Nucl Med, 2017. 58(10): p. 1553–1559.
3. Lindegren S., F.S., Pretargeted Radioimmunotherapy with alpha-Particle Emitting Radionuclides. Current Radiopharmaceuticals, 2 011. 4: p. 248–260.
4. Timperanza, C., et al., Pretargeted Alpha Therapy of Disseminated Cancer Combining Click Chemistry and Astatine-211. Pharmaceuticals, 2023. 16(4).
5. Tabrizi, M., G.G. Bornstein, and H. Suria, Biodistribution mechanisms of therapeutic monoclonal antibodies in health and disease. AAPS J, 2010. 12(1): p. 33–43.
6. Ryman, J.T. and B. Meibohm, Pharmacokinetics of Monoclonal Antibodies. CPT Pharmacometrics Syst Pharmacol, 2017. 6(9): p. 576–588.
7. Staudt, M. and M.M. Herth, Clearing and Masking Agents in Pretargeting Strategies. Pharmaceuticals (Basel), 2023. 16(4).

PP18

Radiolabelled antiangiogenic monoclonal antibody ramucirumab as an effective tool for diagnostics and therapy in nuclear medicine

Pavel Barta[1*], Martin Vlk[2], Jana Maixnerova[1], Zbynek Novy[3], Petr Pavek[1], Jan Kozempel[2], Frantisek Trejtnar[1]
[1]Faculty of Pharmacy in Hradec Kralove, Charles University, Czech Republic. [2]Faculty of Nuclear Sciences and Physical Engineering, Czech Technical University in Prague, Czech Republic. [3]Institute of Molecular and Translational Medicine, Faculty of Medicine and Dentistry Palacky University Olomouc, Czech Republic
[*]**Corresponding author**: pavel.barta@faf.cuni.cz

EJNMMI Radiopharmacy and Chemistry 2024, **9(1)**: PP18
Aim: Angiogenesis is a vital process responsible for a nutrition supply in cancer development and invasiveness. One of the key factors determining angiogenesis is vascular endothelial growth factor (VEGF) and its receptors (VEGFRs), particularly VEGFR2. Therefore, angiogenic process is targeted by inhibitory compounds including VEGF blocking molecules or VEGFR2 activity supressing factors like monoclonal antibody ramucirumab (RAM). The fully humanized RAM targets the extracellular receptor binding site and hence prevents interactions with natural VEGF ligands. Besides FDA and EMA approved therapeutic application, RAM has the potential for imaging or improved therapeutic effect of VEGFR2-positive tumours. The presented study summarizes the achieved results in the preparation and in vitro and in vivo characterization of ^{89}Zr- and ^{161}Tb-labelled ramucirumab for PET imaging and therapy targeting of VEGFR2 positive cancer processes.
Materials and methods: Ramucirumab was conjugated with either p-SCN-Bn-deferoxamine (DFO, ^{89}Zr-labelling) or p-SCN-Bn-DOTA (DOTA, ^{161}Tb-labelling). The purified immunoconjugates were further labelled with radionuclides. The binding ability of prepared [^{89}Zr]Zr-DFO-RAM and [^{161}Tb]Tb-DOTA-RAM to the target receptor was tested in vitro on equilibrium dissociation constant (K_d) assessment in human prostate adenocarcinoma (PC-3) and ovary adenocarcinoma (SKOV 3) cell lines. Ex vivo biodistribution and the PET/CT imaging (^{89}Zr-labelled RAM only) experiments followed in BALB/c mice (noncancerous) and SCID (PC-3 or SKOV-3) xenografts in selected timepoints.
Results: Ramucirumab was conjugated with either p-SCN-Bn-deferoxamine (DFO, ^{89}Zr-labelling) or p SCN Bn DOTA (DOTA, ^{161}Tb-labelling). The purified immunoconjugates were further labelled with radionuclides. The binding ability of prepared [^{89}Zr]Zr-DFO-RAM and [^{161}Tb]Tb-DOTA-RAM to the target receptor was tested in vitro on equilibrium dissociation constant (KD) assessment in human prostate adenocarcinoma (PC-3) and ovary adenocarcinoma (SKOV 3) cell lines. Ex vivo biodistribution and the PET/CT imaging (^{89}Zr-labelled RAM only) experiments followed in BALB/c mice (noncancerous) and SCID (PC-3 or SKOV-3) xenografts in selected timepoints.
Radioimmunoconjugates were prepared in the excellent radiochemical purity (> 95%). In vitro experiments found a strong binding affinity for [^{89}Zr]Zr-DFO-RAM (K_d = 65.8 (± 4.2) and 37.6 (± 7.3) nM) and [^{161}Tb]Tb-DOTA-RAM (K_d = 28.1 (± 4.9) and 24.6 (± 7.0) nM) in PC 3 and SKOV 3 cells, respectively. The acquired biodistribution data of [^{89}Zr]Zr-DFO-RAM showed the uptake in PC-3 and SKOV-3 tumours at about 8.7 (± 0.2) and 12.1 (± 1.6) % ID/g respectively. PET/CT images showed high activity accumulation in tumour on the 1st day p.i. The preliminary biodistribution data with [^{161}Tb]Tb-DOTA-RAM demonstrated dominant accumulation in lung, liver and spleen (7.0 (± 1.6), 5.3 (± 0.9) and 3.6 (± 2.0) % ID/g) at 72 h p.i.
Conclusion: According to our findings, [^{89}Zr]Zr-DFO-RAM proved high binding ability to the target receptor both in vitro and in vivo, which makes this radiopharmaceutical a promising tool in PET/CT imaging of VEGFR2-positive tumours. ^{161}Tb-labelled RAM also demonstrated high receptor interaction and standard biodistribution pattern in mice paving the way for its VEGFR2-positive tumour targeting experiments in xenografts.

Acknowledgements
The authors would like to thank for the financial support to Ministry of Health of the Czech Republic, grant nr. 235202 and to Charles University grant program Cooperatio Pharmaceutical Sciences, the Czech Republic.

PP19

Preparation and evaluation of stabilized ^{211}At-labelled aryl compounds

Romain Fouinneteau[1*], Thibault Yssartier[2], Nicolas Galland[2], Cécile Perrio[3], François Guérard[1]
[1]Nantes Université, Inserm, CNRS, Université d'Angers, CRCI[2]NA, Nantes, France. [2]Nantes Université, CNRS, CEISAM UMR 6230, Nantes, France. [3]Normandie Université, UNICAEN, CEA, CNRS, UAR 3408, Cyceron, Caen, France
[*]**Corresponding author**: romain.fouinneteau@univ-nantes.fr

EJNMMI Radiopharmacy and Chemistry 2024, **9(1)**: PP19

Aim: An emerging strategy for treatment of cancers is Targeted α-Therapy. The radiohalogen astatine-211 ($t_{1/2}$ = 7,2h), appears to be amongst the most promising alpha emitters. Despite encouraging initial clinical applications with *N*-[^{211}At]succinimidylastatobenzoate ([^{211}At]SAB) as prosthetic group to label antibodies, in vivo trials have shown that the carbon-astatine bond is weak and leads to release of free astatine into the body which may impair efficacy and patient safety [1,2]. Nevertheless, recent studies have shown that improving the chemical structure carrying astatine-211 could increase its stability in vivo [3,4]. The aim of this project is to develop new prosthetic groups capable of improving the stability of astatoaryl compounds. Novel model structures were designed with hydrogen donor moieties placed in ortho position of At aiming at stabilizing potentially oxidized and subsequently unstable species formed in vivo [5,6]. Hydrogen donors may also reduce selenocysteine mediated dehalogenation [7]. The objective was then to compare their stability with the reference [^{211}At]SAB and validate improved ^{211}At-compounds for further biological studies.

Materials and methods: A series of [^{211}At]astatoaryl compounds bearing one or two hydrogen donors (-OH, -NH) in ortho position were prepared based on aryliodonium salt [8] or boronic ester chemistry [9] (Fig. 1A). After chromatographic purification, products were engaged in biochemical stability assays including previously reported oxidizing/acidic medium, mimicking lysosomal conditions during cell internalization [5] as well as human and rat liver microsomes to simulate cytochrome P-450 degradation metabolism in vivo. The results obtained were compared with a [^{211}At]SAB analogue (1) prepared by the same method (Fig. 1A).

Results: Radiochemical yield (RCY) were respectively 80, 85 and 68% for compounds (1), (2) and (3) from iodonium salts. The boronic ester method led to a RCY of 97% for compound (4). Stability studies showed impressive increase in stability, in particular for (2) with only 2% ^{211}At released after 20 h compared to 100% for SAB reference in oxidizing medium. Similarly, human and rat microsome lead respectively to a reduced deastatination (2-3%) compared to SAB (6-28%) after 20 h (Fig. 1B).

Conclusion: This work has enabled led to identication of promising compounds. In particular, compound (2) exhibits high stability compared with the [^{211}At]SAB reference. Accordingly, a bifunctional analogue allowing for bioconjugation to cancer targeting vector is being developed for further assessment of stability in animal models.

Acknowledgement
This work was supported by the French National Agency for Research, grants ANR-19-CE07-0036 (ExPAt), ANR-11-LABX-18-01 (Labex IRON), ANR-16-IDEX-0007 (ISITE NExT) and INCa-DGOS-INSERM-ITMO Cancer_18011.

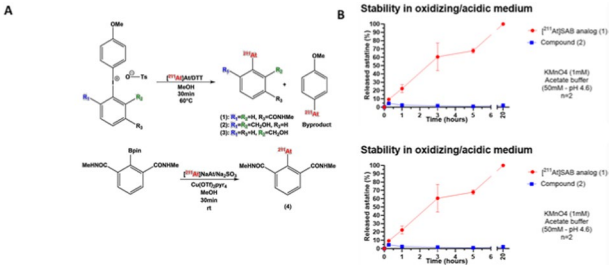

Fig. 1 (**A**) Method for ^{211}At-labeling of [^{211}At]SAB analog (1) and compounds (2), (3) and (4). (**B**) Stability results for compound (2) compared with [211At]SAB analog (1).

References

1. Zalutsky MR, Reardon DA, Akabani G, Coleman RE, Friedman AH, Friedman HS, McLendon RE, Wong TZ, Bigner DD. Clinical Experience with α-Particle–Emitting ^{211} At: Treatment of Recurrent Brain Tumor Patients with ^{211} At-Labeled Chimeric Antitenascin Monoclonal Antibody 81C6. J Nucl Med. 2008; 49(1):30–8.
2. Wilbur DS. [^{211}At]Astatine-Labeled Compound Stability: Issues with Released [^{211}At]Astatide and Development of Labeling Reagents to Increase Stability. Current Radiopharmaceuticals. 2008; 1:144–176.
3. Suzuki H, Kaizuka Y, Tatsuta M, Tanaka H, Washiya N, Shirakami Y, Ooe K, Toyoshima A, Watabe T, Teramoto T, Sasaki I, Watanabe S, Ishioka NS, Hatazawa J, Uehara T, Arano Y. Neopentyl Glycol as a Scaffold to Provide Radiohalogenated Theranostic Pairs of High In Vivo Stability. J Med Chem. 2021; 64(21):15,846–57.
4. Dekempeneer Y, Bäck T, Aneheim E, Jensen H, Puttemans J, Xavier C, Keyaerts M, Palm S, Albertsson P, Lahoutte T, Caveliers V, Lindegren S, D'Huyvetter M. Labeling of Anti-HER2 Nanobodies with Astatine-211: Optimization and the Effect of Different Coupling Reagents on Their in Vivo Behavior. Mol Pharmaceutics. 2019; 16(8):3524–33.
5. Teze D, Sergentu DC, Kalichuk V, Barbet J, Deniaud D, Galland N, Maurice R, Montavon G. Targeted radionuclide therapy with astatine-211: Oxidative dehalogenation of astatobenzoate conjugates. Sci Rep. 2017; 7(1):2579.
6. Li Y, Chyan MK, Hamlin DK, Nguyen H, Corey E, Wilbur DS. Oxidation of p-[^{125}I]Iodobenzoic Acid and p-[^{211}At]Astatobenzoic Acid Derivatives and Evaluation In Vivo. IJMS. 2022; 23(18):10,655.
7. Yssartier T, Liu L, Pardoue S, Le Questel JY, Guérard F, Montavon G, Galland N. In vivo stability of ^{211}At-radiopharmaceuticals: on the impact of halogen bond formation. RSC Med Chem. 2023.
8. Guérard F, Navarro L, Lee YS, Roumesy A, Alliot C, Chérel M, Brechbiel MW, Gestin JF. Bifunctional aryliodonium salts for highly efficient radioiodination and astatination of antibodies. Bioorganic & Medicinal Chemistry. 2017; 25(21):5975–80.
9. Reilly SW, Makvandi M, Xu K, Mach RH. Rapid Cu-Catalyzed [^{211} At]Astatination and [^{125}I]Iodination of Boronic Esters at Room Temperature. Org Lett. 2018; 20(7):1752–5.

PP20

Synthesis and characterization of Rhenium and Technetium-99m nitrido complexes with tridentate thiosemicarbazones ligands

Nicola Salvarese[1], Davide Lucchini[2], Carolina Gobbi[1], Marco Baron[2], Alessandro Dolmella[3], Alessio Zavaroni[4], Dominga Rogolino[4], Mauro Carcelli[4], Cristina Bolzati[1]
[1]Institute of Condensed Matter Chemistry and Energy Technologies, (ICMATE-CNR), Padova, Italy. [2]Department of Chemical Science,

University of Padua, Padova, Italy. [3]Department of Pharmaceutical and Pharmacological Sciences, University of Padua, Padova, Italy. [4]Department of Chemistry, Life Sciences, Environmental Sustainability, University of Parma, Parma, Italy
EJNMMI Radiopharmacy and Chemistry 2024, **9(1)**: PP20

Aim: The coordination chemistry of technetium and rhenium is intrinsically connected due to their position in the periodic table of elements and remains under current interest.
Despite the increased general emphasis on PET technology, SPECT is the first-line imaging modality in nuclear medicine. This is because SPECT imaging predominantly relies on technetium-99m, which, due to its ideal physical-chemical properties and convenient availability, remains the most used radionuclide in clinical practice. To emphasize the importance of this radionuclide, is the existence of radioactive rhenium congeners (Re-186/Re-188) that for their nuclear features have been shown to be very attractive candidates for endoradiotherapy. [1] This makes ^{99m}Tc and ^{186}Re/^{188}Re ideal for the development of a matching theranostic pair that combines diagnosis and therapy.
Thiosemicarbazones (TSC) represent an interesting class of ligands that form stable complexes with Re and Tc. Most of our research activity is based on the study of M(N) core (M = Tc, Re).[2,3] Believing in the potential for developing new radiopharmaceuticals based on the M(N) core with TSC, here we describe the reactivity of two tridentate TSC (3-methoxysalicylaldehyde thiosemicarbazone, H2AC01; 3-methoxysalicylaldehyde N,N-dimethyl-thiosemicarbazone, H2SD8) with the M(N) core where M is Re and Tc-99m.
Materials and methods: Reactions were performed by reacting 2.5 eq of H2AC01 and H2SD8 with the prereduced $[ReVNCl_2(PPh3)_2]$ complex in the presence of Et_3N, in CH_2Cl_2/MeOH mixture at reflux for 30 min. Alternatively the $[NBu4ReVNCl_4]$ precursor can be used. Complexes were fully characterized by spectroscopic and spectrometric techniques and single-crystal XRD analysis.
Radiosynthesis were also performed using a two-step procedure. In solution stability of the 99mTc-complexes were evaluated.
Results: Reactions of thiosemicarbazone ligands, H2AC01 and H2SD8, with pre-reduced Re precursors led to the formation of pentacoordinate rhenium(V) complexes of general composition $[ReN(TSC)(PPh3)_2]$ in good yield. XRD analysis of $[ReN(AC01)(PPh3)_2]$ shows a square pyramidal geometry.
$[^{99m}Tc][TcN(TSC)(PPh3)_2]$ were efficiently prepared at tracer level and carrier added conditions, and characterized by HPLC comparison with the corresponding Re complexes. Stability studies revealed that they are adequately stable in solution (PBS, HS). Both compounds have a high interaction with serum proteins.
Conclusion: Within the scope of synthesizing complexes aiming at medical applications, the basic coordination chemistry of the MN core (M = Re, ^{99m}Tc) toward tridentate TSCs was evaluated. Stable compounds were efficiently prepared as prototype with potential to be used in radiopharmaceuticals development. This study deserves further investigation.
Acknowledgment
The authors thank Associazione Italiana per la Ricerca sul Cancro (AIRC, IG 2020 ID 24528)

References
1. Wuillemin, M. A.; Reber, M. J.; Fox, T.; Spingler, B.; Brühwiler, D.; Alberto, R.; Braband, H. Towards ^{99m}Tc- and Re-Based Multifunctional Silica Platforms for Theranostic Applications. Inorganics 2019, 7, 134.
2. Bolzati, C.; Dolmella, A. Nitrido Technetium-99 m Core in Radiopharmaceutical Applications: Four Decades of Research. Inorganics 2020, 8, 3.
3. Salvarese, N.; Spolaore, B.; Marangoni, S.; Pasin, A.; Galenda, A.; Tamburini, S.; Cicoria, G.; Refosco, F.; Bolzati, C. Transglutaminase-Mediated Conjugation and Nitride-Technetium-99m Labelling of a Bis(Thiosemicarbazone) Bifunctional Chelator. J. Inorg. Biochem. 2018, 183, 18.

PP21

^{67}Cu produced at a biomedical cyclotron for preclinical in vivo studies

Ursula Søndergaard[1,2,3*], Thomas K Ekaney[1], Mathias Kranz[1,2], Rune Sundset[1,2], Kristina S Pedersen[3], Angel Moldes-Anaya[1,2], Mikael Jensen[3] [1]The PET Imaging Center, University Hospital of North Norway, Tromsø, Norway. [2]Department of Clinical Medicine, UiT The Arctic University of Norway, Tromsø, Norway. [3]Hevesy Laboratory, DTU Health Technology, Technical University of Denmark, Risø, Denmark
[*]**Corresponding author**: ursula.sondergaard@unn.no

EJNMMI Radiopharmacy and Chemistry 2024, **9(1)**: PP21
Aim: The demand for ^{67}Cu is high due to recent developments in radioendotherapy and theranostics. With 100% β^--emission, a half-life of 61.83 h and a dose point kernel similar to that of the clinically established ^{177}Lu [1], ^{67}Cu is ideal for radionuclide therapy. In addition, with positron-emitter ^{64}Cu having a half-life allowing tumour-dosimetry and excellent imaging properties, precision medicine theranostics is enabled, a constellation rarely present. In this study, we aimed to establish ^{67}Cu production at a biomedical cyclotron via the ^{70}Zn(p,α)^{67}Cu nuclear reaction, suitable for in vivo animal experimentation.
Materials and methods: Bombardments were performed at 16.5 MeV nominal incoming proton energy (GE PETTrace 860). Target electrodeposition was based on a method by Engle et al. [2]. Scaling up from test runs, enriched ^{70}Zn (97.5%) was electrodeposited to a target thickness of 50 mg/cm^2, and bombarded for either 4 or 12 h at respectively 60 and 40 µA. On the next day, the target was dissolved in 6 M HCl, evaporated to dryness and reconstituted in metal-free water. Solid phase extraction (SPE) was applied for final purification using two commercially available resins in series, TK200 and CU-resin (Triskem). Activity measurements and assessment of radionuclidic purity were done via γ-ray spectrometry. Non-radioactive metal content in the final product was assessed by ICP-OES. Radiolabelling was performed by adding PSMA-617 (70µL, 20nmol) in metal-free H_2O to 300µL $^{67}Cu^{2+}$ reconstituted in NaOAc buffer (pH 4.6) in a glass vial, mixing thoroughly and incubating at 90°C for 10 min. The final product was formulated in isotonic saline after purification by C18 SPE (Waters), i.v. injected (5.1 MBq) into a healthy C57BL6 mouse (12 weeks, 21.5 g) and subsequently SPECT imaged (40s/ projection,50 ROR, Trifoil SPECT CT) 1h, 24h, 48 and 72h.
Results: Maximum produced EOB activity reached to date was 120 MBq, of which 94% was recovered for radiolabelling and in vivo testing. Radionuclidic purity at start of synthesis was > 99.4%. Specific activity of purified ^{67}Cu end product varied from 144-573 MBq/ug in scale-up experiments. The radiochemical yield of ^{67}Cu-PSMA-617 was 94% after final evaporation and reconstitution in saline. Biodistribution (Fig. 1) with SPECT revealed high uptake in kidneys and liver followed by a washout phase.
Conclusion: We have established production of ^{67}Cu. The product quality is suitable for preclinical investigations, showing that the capabilities of biomedical cyclotrons can be explored for producing radiometals of therapeutic interest.

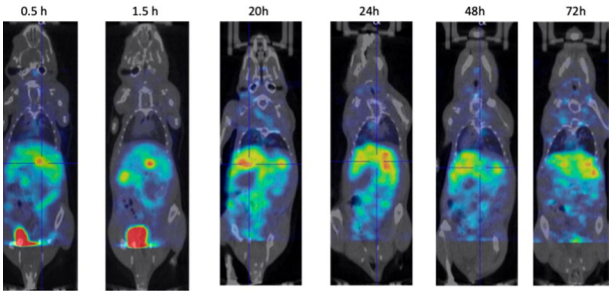

Fig. 1 Kinetic micro-SPECT/CT/MR of a healthy mouse injected with ^{67}Cu-PSMA-617.

Acknowledgements
Dr. Samuel Kuttner is gratefully acknowledged for assisting with the SPECT calibrations to ^{67}Cu. This work has in parts received funding from the European Union's Horizon 2020 research and innovation programme under grant agreement No 101008571 (PRISMAP—https://www.prismap.eu/about/project/) and in part from HelseNord (https://www.helse-nord.no/forskning-og-innovasjon/)

References

1. Graves SA, Lopez-Rodriguez V, Gaspar-Carcamo RE, Valdovinos HF, Valle-Gonzalez M, Trejo-Ballado F, Severin GW, Barnhart TE, Nickles RJ, Avila-Rodriguez et al. Dose point kernels for 2,174 radionuclides. Med Phys 2019; 46:5284–5293.
2. Engle JW, Lopez-Rodriguez V, Gaspar-Carcamo RE, Valdovinos HF, Valle-Gonzalez M, Trejo-Ballado F, Severin GW, Barnhart TE, Nickles RJ, Avila-Rodriguez MA. Very high specific activity ^{66}/^{68}Ga from zinc targets for PET. Appl Radiat Isot. 2012; 70:1792–1796

PP22

Production of research radionuclides for Targeted Auger Electron Therapy (TAET) at TRIUMF

Valery Radchenko[1,2], Shaohuang Chen[1,3], Parmissa Randhawa[1,3], Patrick Davey[1,3], Neil Weatherall[1], Aivija Grundmane[1,3], Behrad Saeedi[1,2], Marianna Tosato[1,3,4], Paul Schaffer[1,3,5], Cornelia Hoehr[1], Hua Yang[1,3], Raymond Reilly[6,7], Caterina Ramogida[1,3]
[1]Life Sciences Division, TRIUMF, Vancouver, BC, Canada. [2]Department of Chemistry, University of British Columbia, BC, Canada. [3]Department of Chemistry, Simon Fraser University, Burnaby, BC, Canada. [4]Department of Chemical Sciences, University of Padova, Padova, Italy. [5]Department of Radiology, University of British Columbia, BC, Canada*f*. [6]Department of Pharmaceutical Sciences, Leslie Dan Faculty of Pharmacy, University of Toronto, Toronto, ON, Canada. [7]Princess Margaret Cancer Centre, University Health Network, Toronto, ON, Canada
EJNMMI Radiopharmacy and Chemistry 2024, **9(1)**: PP22

Aim: Targeted Auger Electron Therapy (TAET) has a great potential to be the most selective and precise therapy for cancer due to the low energy (eV-keV) (compared with beta and alpha emitters) and high Linear Energy Transfer (LET) of Auger electrons. This allows the design of the therapeutic agents at the cellular level and minimizes unwanted damage to surrounding healthy tissues. To design the most effective TAET radiopharmaceuticals, it is crucial to identify suitable radionuclides and develop their regular production to enable further studies with various suitable delivery systems [1].
One of the advantages of Auger electron emitters over other radionuclides for therapy is that many suitable candidates can be produced with low and medium-energy medical cyclotrons (10-20 MeV), which can allow easy access and clinical-scale production at many medical centers around the world [2].
Materials and methods: The Life Sciences Division at TRIUMF is actively exploring the production of research candidates for TAET with its TR-13 (13 MeV) cyclotron. In addition to radionuclide production, the TRIUMF group is also exploring novel radiochemical separation techniques and developing suitable chelators for the targeted delivery of candidate radioisotopes using a range of targeting vectors.
Results: Production of pre-clinical quantities of several promising candidates previously identified in [2] was established. $^{197m+g}$Hg ($t_{1/2}$ 23.8 h(m)/64.1 h(g)), ^{119}Sb ($t_{1/2}$ 38.2 h), and ^{165}Er ($t_{1/2}$ 10.36 h) were produced using p, n reaction at TRIUMF's 13 MeV cyclotron using solid targets. Radiochemical purification of proposed radionuclides from the target material was performed using ion exchange, solid phase, and liquid extraction. A series of commercially available and novel chelators were tested to determine the ideal radioisotope-chelate complexation conditions. Several complexes were transferred to the University of Toronto for testing their therapeutic potential in vitro and in vivo.

References

1. Bolcaen J., et al. Marshalling the Potential of Auger Electron Radiopharmaceutical Therapy J. Nuc. Med. 2023 64(9), 1344–1351.
2. Filosofov D, et al. Potent candidates for Targeted Auger Therapy: Production and radiochemical considerations. Nucl Med Biol. 2021 94–95:1–19.

PP23

The development of lyophilised kit preparations: Gateway to larger clinical uptake of Ga-68 radiopharmaceuticals

Jan Rijn Zeevaart[1,2], Biljana Marjanovic-Painter[1], Thomas Ebenhan[1,2,3] and Janine Suthiram[1]
[1]Radiochemistry, The South African Nuclear Energy Corporation, Pelindaba, South Africa. [2]Nuclear Medicine Research Infrastructure NPC, Pretoria, South Africa. [3]Department of Nuclear Medicine, University of Pretoria, Pretoria, South Africa
EJNMMI Radiopharmacy and Chemistry 2024, **9(1)**: PP23

Aim: In recent years, there has been a considerable increase in studies aimed at the development of lyophilised (cold kit) formulations as an alternative to automated synthesis methods for the preparation of ^{68}Ga-radiopharmaceuticals [1]. Kit based radiopharmaceutical preparation is not only user friendly, robust and cost-effective but also offers the convenience of in-house preparation using generator produced radioactivity. It is these advantages that have contributed to the extensive use and success of ^{99m}Tc-based SPECT radiopharmaceuticals. A similar approach that involves simple and efficient radiolabelling methods and minimal equipment is necessary to improve the technical and economical feasibility of ^{68}Ga based PET radiopharmaceuticals. Commercially available kit based ^{68}Ga-radiopharmaceuticals coupled with market authorized ^{68}Ge/^{68}Ga generator systems have already demonstrated the feasibility of such an approach (cyclotron produced ^{68}Ga can also be used).
Materials and methods: Achieving a lyophilised kit of acceptable quality requires consideration of all aspects of the design and manufacture process [2, 3]. The targeting vectors e.g. DOTATATE are considered as API's and will have to conform to all requirements of an API before use in the kit [3]. Process validation evaluates the data that has been gathered over the product lifecycle to confirm that the process is able to reliably generate a product to a determined quality standard. Sterile filtration, aseptic dispensing and freeze drying are the main steps in kit production that must be validated. Herein we report our experiences in the process validation of the GMP manufacture of a lyophilised kit for PET imaging. Several batches of kits were produced over a period of months by different operators and analysed using the validated quality control methods for visual inspection, pH (cold and radiolabelled), loss on drying, mass of kit pellet, concentration and radiochemical purity and yield.
Results: Following visual inspection, the average yield of kits was ~ 80% with the number of minor, major and critical defects within acceptable limits. Temperature and vacuum pressure settings together with time of pre-freezing and freeze drying had an influence on the visual appearance of the kit pellet and moisture in the kit. These factors must be taken into consideration for translation to routine manufacture especially where buffer solutions that have complex freeze-drying profiles are used.
Conclusion: The gold standard "shake-and-shoot" type kit production facilitating a one-step "instant" radiolabelling is expected to also

accelerate the uptake of ^{68}Ga radiopharmaceuticals as already demonstrated by commercially available kits paving the way for more kit-based ^{68}Ga radiopharmaceuticals to be developed.

References

1. Nicolas Lepareur, Cold Kit Labeling: The Future of 68Ga Radiopharmaceuticals? Front. Med., 10 February 2022, https://doi.org/10.3389/fmed.2022.812050.
2. Gillings, N., Hjelstuen, O., Ballinger, J. et al. Guideline on current good radiopharmacy practice (cGRPP) for the small-scale preparation of radiopharmaceuticals. EJNMMI radiopharm. chem. 6, 8 (2021). https://doi.org/10.1186/s41181-021-00123-2
3. Korde A, Patt M, Selivanova SV, Scott AM, Hesselmann R, Kiss O, Ramamoorthy N, Todde S, Rubow SM, Gwaza L, Lyashchenko S, Andersson J, Hockley B, Kaslival R and Decristoforo C. Position paper to facilitate patient access to radiopharmaceuticals: considerations for a suitable pharmaceutical regulatory framework. EJNMMI Radiopharmacy and Chemistry (2024) 9:2

PP24

Challenges in IMP preparation for a clinical trial – on the example of DuoNen, personalized PRRT with mixed doses of [^{177}Lu]Lu-DOTA-TATE and [^{90}Y]Y-DOTA-TATE in neuroendocrine neoplasm treatment

Renata Mikolajczak[1*], Izabela Cieszykowska[1], Marta Opalinska[2], Grzegorz Kamiński[3], Marek Dedecjus[4], Aldona Kowalska[5], Maciej Kolodziej[3], Marek Saracyn[3], Piotr Garnuszek[1], Wioletta Lenda-Tracz[6], Danuta Gąsior-Perczak[5], Anna Borkowska[6], Joanna Januszkiewicz-Caulier[4], Joanna Długosińska[4], Anna Sowa Staszczak[2], Anna Budzyńska[7], Agata Kubik[7], Patrycja Pastusiak[7], Krzysztof Kacperski[7], Wioletta Chalewska[4], Paulina Cegła[4], Alicja Hubalewska-Dydejczyk[2]

[1]National Centre for Nuclear Research, Radioisotope Center POLATOM, Otwock-Swierk, Poland. [2]Jagiellonian University Medical College, Chair and Department of Endocrinology, Krakow, Poland. [3]Military Institute of Medicine—National Research Institute, Department of Endocrinology and Isotope Therapy, Warsaw, Poland. [4]National Institute of Oncology, National Institute of Oncology, Warsaw, Poland. [5]Jan Kochanowski University in Kielce, Collegium Medicum, Kielce, Poland. [6]Jagiellonian University Medical College, Faculty of Health Sciences, Kraków, Poland, [7]Military Institute of Medicine—National Research Institute, Department of Nuclear Medicine, Warsaw, Poland

EJNMMI Radiopharmacy and Chemistry 2024, **9(1)**: PP24

Aim: The protocol of DuoNEN clinical trial, a phase III, multicenter, non-commercial clinical study (EudraCT No. 2020-006068-99) was designed to develop the optimal algorithm of Peptide Receptor Radionuclide Therapy (PRRT) for patients with disseminated NET based on personalized dosimetry and to evaluate the safety and effectiveness of personalized therapy with mixed doses of [^{177}Lu]Lu-DOTA-TATE and [^{90}Y]Y-DOTA-TATE compared to [^{177}Lu]Lu-DOTATATE in standard doses. Despite the long experience with tandem therapy in Poland [1], defining a mixed [^{177}Lu]Lu-DOTA-TATE and [^{90}Y]Y-DOTA-TATE dose meeting the investigational medicinal product (IMP) requirements is a challenge.

Materials and methods: DuoNEN's IMP consists of two components with varying radioactivities: [^{177}Lu]Lu-DOTA-TATE from 930 to 7400 MBq and [^{90}Y]Y-DOTA-TATE from 0 to 1850 MBq. Each patient dose is prepared individually, under GMP conditions, to obtain a 1.0 GBq/mL radioactive concentration.

Adult patients with advanced, unresectable well-differentiated (G1 and G2) NETs, progressing on long-acting somatostatin analogs are randomized into four arms:

A—treated with [^{177}Lu]Lu -DOTA-TATE with constant radioactivity of 7400MBq per cycle

B—treated with mixed [^{177}Lu]Lu-DOTA-TATE and [^{90}Y]Y-DOTA-TATE, initially at ratio of

3700:1850MBq/MBq. The [^{177}Lu]Lu-DOTATATE radioactivity remains constant in all cycles and the [^{90}Y]Y-DOTA-TATE radioactivity is adjusted in the next cycles to the highest radiation dose in the tumor tissue

C—analogous to arm B, except that here the radioactivity of [^{90}Y]Y-DOTA-TATE remains constant and the radioactivity of [^{177}Lu]Lu-DOTA-TATE is adjusted

D – first dose analogous to arm A and individualized in the next cycles.

The treatment efficacy is evaluated by morphological imaging (CT or MR) according to RECIST 1.1 criteria. The safety of PRRT is assessed by the kidney and bone marrow biochemical function.

Results: Up to date 52 batches of DuoNEN have been released and 94 cycles of PRRT were administered, with no deviation from approved protocols. These included 57 fixed doses (first doses or arm A), and 37 doses adjusted based on personalized dosimetry. The first eight patients were evaluated post-PRRT according to RECIST 1.1 criteria, achieving stable disease in 3 cases and partial and complete response in 4 and 1, respectively.

Conclusion: Our ongoing study showed that personalized renal and bone marrow dosimetry affects individual PRRT doses in each subsequent treatment cycle. The final results of the clinical study are pending.

The Medical Research Agency in Poland financed the study (Project number 2019/ABM/01/00077-00).

Reference

1. Kunikowska J., Zemczak A., Kołodziej M. et al. Tandem peptide receptor radionuclide therapy using ^{90}Y/^{177}Lu-DOTATATE for neuroendocrine tumors efficacy and side-effects—polish multicenter experience. Eur. J. Nucl. Med. Mol. Imaging. 2020; 47:922-933.

PP25

3D cancer models for the theranostic evaluation of $^{64}CuCl_2$

Catarina I. G. Pinto[1], André Dargen de Matos Branco[2], Alexandra Fonseca[3], Laura Ordas[4] Antero J. Abrunhosa[3], Cláudia L. da Silva[2], Joana F. Guerreiro[1], Sophie Poty[4], Jean-Pierre Pouget[4], Filipa Mendes [1,5,*]

[1]C2TN – Centro de Ciências e Tecnologias Nucleares, Instituto Superior Técnico, Universidade de Lisboa, Loures, Portugal. [2]Departamento de Bioengenharia, iBB – Institute dor Bioengineering and Biosciences, Instituto Superior Técnico, Universidade de Lisboa, Lisbon, Portugal. [3]CIBIT/ICNAS – Instituto de Ciências Nucleares Aplicadas à Saúde, Universidade de Coimbra, Coimbra, Portugal. [4]Institut de Recherche en Cancérologie de Montpellier (IRCM), Institut National de la Santé et de la Recherche Médicale (INSERM) Unité 1194, Université de Montpellier, Institut Régional du Cancer de Montpellier (ICM), Montpellier, France. [5]DECN – Departamento de Engenharia e Ciências Nucleares, Instituto Superior Técnico, Universidade de Lisboa, Lisbon, Portugal. Current address + CIISA—Centro de Investigação Interdisciplinar em Sanidade Animal, Faculdade de Medicina Veterinária, Universidade de Lisboa, Lisboa, Portugal and Laboratório Associado para Ciência Animal e Veterinária (AL4AnimalS)

[*]**Corresponding author**: fmendes@ctn.tecnico.ulisboa.pt

EJNMMI Radiopharmacy and Chemistry 2024, **9(1)**: PP25

Aim: Conventionally, monolayer culture systems are used in preclinical studies of new radiopharmaceuticals. However, due to the unnatural growth conformation cells are forced to adapt, failing to simulate important in vivo features of tumors, such as cell-to-cell, and cell-to-extracellular matrix interactions. These adaptations that monolayer cultured cells go through might produce misleading results in drug screening studies due to differences in drug penetration and resistance mechanisms. Considering this and aiming at improving the clinical translatability of preclinical studies, there has been an increased awareness of the need for more advanced culture models, such as 3D cultures, that can better mimic the complexity and heterogeneity of in vivo tumors. [1] Among the more advanced culture models,

there are multicellular tumor spheroids that can recreate some of the tumoral environmental clues and phenotypes absent in monolayer cultures, such as gradients of oxygen, nutrients, and metabolites; and preservation of tumor's heterogeneity, for instance through the conservation of a population of stem-like cells, that contribute for tumor recurrence and increased drug resistance. [2] Hence, the use of these types of models would bring great profit to estimate the clinical translational potential of new radiopharmaceuticals.
Here, we explored the theranostic potential of the simple radiopharmaceutical, $^{64}CuCl_2$, in prostate cancer and glioblastoma spheroids, considering that previous studies had already shown that it can target these two types of malignant tumors [3, 4].
Materials and methods: After establishing and characterizing spheroids derived from prostate cancer (22RV1, DU145, LNCaP) and glioblastoma (T98G, U87, U373), we exposed them to $^{64}CuCl_2$ and evaluated its effects on the spheroids' growth, viability, and the proliferative capacity of spheroid-derived cells. Additionally, the uptake of ^{64}Cu was evaluated, in intact spheroids and spheroids' slices through autoradiography. Preliminary studies concerning the production of ROS after exposure to ^{64}Cu and the presence of a population of cancer stem-like cells were performed.
Results: The results obtained revealed that $^{64}CuCl_2$ can significantly reduce spheroids' growth, viability, and proliferation capacity of both types of tumors, which could be related to its uptake and uniform distribution inside spheroids. Furthermore, a relation between the detection of a larger population of cancer stem-like cells and an increased resistance to radiation was noticed. In glioblastoma, increased ROS production was correlated with increased susceptibility to $^{64}CuCl_2$.
Conclusion: Overall, the results obtained in this study further highlighted the large potential of $^{64}CuCl_2$ as a theranostic agent for both, prostate cancer and glioblastoma.

References

1. Engrácia DM, Pinto ClG, Mendes F. Cancer 3D models for metallodrug preclinical testing. Int J Mol Sci. 2023; 24(15):11,915.
2. Pinto ClG, Bucar S, Alves V, Fonseca A, Abrunhosa AJ, da Silva CL, et al. Copper-64 chloride exhibits therapeutic potential in three-dimensional cellular models of prostate cancer. Front Mol Biosci. 2020; 7:609,172.
3. Piccardo A, Paparo F, Puntoni M, Righi S, Bottoni G, Bacigalupo L, et al. $^{64}CuCl_2$ PET/CT in prostate cancer relapse. J Nuclear Med. 2018; 59:444–451
4. Pérès EA, Toutain J, Paty LP, Divoux D, Ibazizène M, Guillouet S, et al.^{64}Cu-ATSM/64Cu-Cl2 and their relationship to hypoxia in glioblastoma: a preclinical study. EJNMMI Res. 2019; 9(1):114

Acknowledgments

This work was supported by Fundação para a Ciência e Tecnologia (FCT), Portugal, through the grant UID/Multi/04349/2019 to C2TN, the PhD Fellowship 2020.07119.BD to ClGPinto. FCT and Campus France are also acknowledged for Program PESSOA grant 2021.09137.CBM to FMendes and 47890XB to JPPouget.. iBB also acknowledges FCT for the funding received through the grant UIDB/04565/2020 and Lisboa2020, through the Project N. 007317.

PP26

The Potential of Terbium-161 labeled Compounds for Clinical Implementation

C.M. Ntihabose[1,2], L. van Dalen[1], H. Ma[1], M. Handula[1], G. Tamborino[1], M. Konijnenberg[1], Y. Seimbille[1,3], E. de Blois[1]
[1]Erasmus Medical Centre, Department of Radiology and Nuclear Medicine, 3015 CN Rotterdam, The Netherland. [2]Erasmus Medical Centre, Department of Pharmacy, 3015 CN Rotterdam, The Netherland. [3]Division of Life sciences, TRIUMF, Vancouver, BC V6T 2A3, Canada
EJNMMI Radiopharmacy and Chemistry 2024, **9(1)**: PP26

Aim: Terbium is nearly identical radionuclide and showed a similar pattern in the first (pre)clinical studies to Lu-177 [1]. Next to Tb-161 near-identical characteristics, it has additional auger and conversion electrons that have a higher linear energy transfer (LET) compared to β^-, which could potentially improve the efficacy of TRT.
In this study, the fundamentals of Tb-161 labeled compounds (such as DOTA-TATE, PSMA-I&T, FAP2286, and JR11) were be studied, and investigated if they have the potential to be clinical applied for TRT.
Materials and methods: Labeling conditions of DOTA-TATE, PSMA-I&T, FAP-2286 and JR11, including kinetics of Tb-161 labeling, were investigated and compared to Lu-177 under different molar activities (40- 110 MBq/nmol). The presence of other metal ions such as; Fe, Zn, and Cu, in the Tb-161 stock solution were determined and quantified by UPLC, including Gd_{target} and Dy_{decay} [2]. Different labeling conditions were investigated including the effect of temperature, pH, incubation time and added quenchers. The radiochemical yield (RCY) and radiochemical purity (RCP) were determined for all conditions, by iTLC and radio-HPLC, respectively. Stability of [^{161}Tb]Tb-PSMA-I&T, was studied in formulation solution. Whereas the stability of [^{161}Tb]Tb-DOTA-TATE and[^{161}Tb]Tb-FAP2286, [^{161}Tb]Tb-JR11 were studied in phosphate-buffer saline (PBS) and mouse serum (MS) at 37°C at 2 and 24 h as well.
Results: The all compounds were successfully labeled at a molar activity up to 160 MBq/nmol. The presents of Gd_{target} and Dy_{decay} and other impurities cause a decreased molar activity of < 160 MBq/nmol which was obtained up to 2 weeks after production in comparison to maximum achievable molar activity (165 MBq/nmol). The presence of the impurities causes a 7 time less than the theoretical molar activity of 700 MBq/nmol at day of production. DOTA-TATE and FAP-2286 were labeled with 5 mM gentisic acid and ascorbic acid resulting in > 90% RCP up to > 48 h in labeling formulation and PBS. PSMA-I&T showed > 90% RCP up to > 24h when labeled with gentisic acid, ascorbic acid and L-methionine. Optimal labeling conditions for all radiopharmaceuticals were at 90°C for 20 min at a pH of 4-5.
Conclusion: This study demonstrates that the presence of Gd_{target} and Dy_{decay} and other trace metals have influence on molar activity of the compounds labeled with Tb-161, however < 160 MBq/nmol can still be reached 2 weeks after production. All compounds showed to be stable in labeling formulation (> 90% RCP up to 24 h), indicating promising radiopharmaceuticals in the treatment of patients.

References

1. 1 Müller, C., van der Meulen, N.P. & Schibli, R. Opportunities and potential challenges of using terbium-161 for targeted radionuclide therapy in clinics. *Eur J Nucl Med Mol Imaging* 50, 3181–3184 (2023). https://doi.org/10.1007/s00259-023-06316-y
2. 2 Breeman, Wap & Chan, Ho Sze & Blois, Erik. (2014). Determination of peptide content and purity of DOTA-peptides by metal ion titration and UPLC: An alternative method to monitor quality of DOTA-peptides. Journal of Radioanalytical and Nuclear Chemistry. 302. 825–830. 10.1007/s10967-014–3248-1.

PP27

Implementing Ac-225 Labelled Radiopharmaceuticals: Practical Considerations and (Pre-)Clinical Perspectives

Eline L. Hooijman[1,2*], Valery Radchenko[3,4], Sui Wai Ling[1], Mark Konijnenberg[1], Tessa Brabander[1], Stijn L.W. Koolen[1,2,5],Erik de Blois[1]
[1]Erasmus MC, Department of Radiology and Nuclear Medicine, 3015 CN Rotterdam, The Netherlands. [2]Erasmus MC, Department of Hospital Pharmacy, 3015 CN Rotterdam, The Netherlands. [3]Life Sciences Division, TRIUMF, Vancouver, BC V6T 2A3, Canada. [4]Chemistry Department, University of British Columbia, Vancouver, BC Canada V6T 1Z1. [5]Department of Medical Oncology, Erasmus MC Cancer Institute, 3015 CN Rotterdam, The Netherlands
[*]**Corresponding author**: Eline Hooijman, e.hooijman@erasmusmc.nl, Erasmus MC, Rotterdam, The Netherlands

EJNMMI Radiopharmacy and Chemistry 2024, **9(1)**: PP27
Abstract published here: https://www.ncbi.nlm.nih.gov/pmc/articles/PMC10847084/

PP28

Development and primary evaluation of [^{99m}Tc] Tc(CO)$_3$-NOTA-Erlotinib as a potential radiopharmaceutical for molecular imaging in triple negative breast cancer

Valentina Lembo[1], Paula Decuadra[1], Ma. Emilia Tejería[1], Ana Rey[1*].
[1]Área Radioquímica, Facultad de Química, Universidad de la República (UdelaR), Montevideo, Uruguay.

EJNMMI Radiopharmacy and Chemistry 2024, **9(1)**: PP28

Aim: Triple negative breast cancer is a global public health problem since it occurs at an early age and has a high recurrence and mortality rate. In 60% of the cases there is an overexpression of the epidermal growth factor receptor (EGFR). Consequently, we have prepared and evaluated a ^{99m}Tc labelled derivative of Erlotinib, a reversible inhibitor of EGFR with the objective of developing a potential molecular imaging agent for this disease.

Materials and methods: Erlotinib (0.25 mmoles, 100 mg) and 1,4,7-Triazacyclononane-1,4-bis (acetic acid)-7-(3-azidopropylacetamide) (NOTA) (0.25 mmoles, 123.7mg) were reacted in a mixture of tert-butanol:H_2O (3:2, v,v) using copper acetate (0.4 eq.) and ascorbic acid (0.2 eq) as catalysts to yield the desired ligand (L). L was labeled in 2 steps: preparation of the tricarbonyl precursor fac-[[^{99m}Tc]Tc(I)$(CO)_3(H_2O)_3$] + (1110-1850 MBq) and substitution by adding L (1mg) for 30 min at 105°C (111-222 MBq). Radiochemical purity (RCP) was evaluated by high efficiency liquid chromatography (HPLC). Stability was evaluated by HPLC up to 4 h post labelling, lipophilicity was determined through partition coefficient between octanol and phosphate buffer 0.1M, pH = 7.4 and protein binding was measured by molecular exclusion at 30 and 60 min.

Results: The labeling strategy used was the formation of a [^{99m}Tc]Tc tricarbonyl complex with a derivative of Erlotinib containing NOTA as tridentate chelator. The Erlotinib derivative (L) was successfully obtained through a Cu(I)-catalyzed Huisgen cycloaddition 3 + 2 reaction between the triple bond of Erlotinib and an azide group of NOTA. The structure was confirmed by spectroscopic techniques.

Labeling was achieved through formation of a Tc(I) tricarbonyl complex. HPLC analysis showed a main species with retention time of 22.2 min, which was purified by HPLC and remained stable for at least 4 h (RCP ≥ 95%). Lipophilicity expressed as log P was 0.8 ± 0.4. The average protein binding was 12 ± 1%.

Conclusion: A [^{99m}Tc]Tc tricarbonyl-NOTA complex bearing a EGFR binding moiety was obtained with high RCP after purification. The complex showed high stability. Lipophilicity was adequate to ensure penetration through biological membranes and protein binding was low. Biological evaluation including in vitro studies in MDA-MB-231 cells will be performed to evaluate the specific binding to the receptor and the internalization.

Acknowledgements
Centro de Medicina Nuclear, Hospital de Clínicas, Pedeciba-Química.

Reference

1. Makris G, Bandari RP, Kuchuk M, Jurisson SS, Smith CJ, Hennkens HM.Development and Preclinical Evaluation of ^{99m}Tc- and ^{186}Re-Labeled NOTA and NODAGA Bioconjugates Demonstrating Matched Pair Targeting of GRPR-Expressing Tumors. Mol Imaging Biol. 2021;23(1):52-61.

PP29

A novel capsule design results in efficient production of ^{89}Zr

Johan Svedjehed[1,2], Martin Pärnaste[1], Per Sondén[1], Roger Lundqvist[1], Katherine Gagnon[1]
[1]GE HealthCare. [2]Uppsala University, Uppsala, Sweden

EJNMMI Radiopharmacy and Chemistry 2024, **9(1)**: PP29

Aim: When selecting a radionuclide for theranostic purposes, it is generally desirable to match the half-life of the radionuclide with the biological half-life of the tracer of interest. For this purpose, ^{89}Zr with its 78.4-h half-life offers characteristics suitable for biomolecules with longer kinetics, e.g. antibodies. For this reason, a new capsule design for ^{89}Zr production was developed for use with an existing solid target platform [1].

Materials and methods: To assess the functionality of the capsule design, four capsules were tested for a total of > 7500 µAh accumulated (proton) beam at 13 MeV. The main functionality of the design was achieved by utilizing a tantalum washer to secure an yttrium foil to a silver backing to enhance heat transfer.

For each production, a fresh foil was clamped into the capsule before placing it on the GE HealthCare solid target platform for automated transfer and irradiation. Post irradiation, the capsules were assayed in a dose calibrator. For select productions, the irradiated foil was dissolved and processed into zirconium oxalate.

Results: Four different capsules were used for a total of 21 runs and 153 h of beam. All capsules maintained performance and integrity through the studies with results summarized in Table 1. For nearly all runs, to determine the integrity of the design and foil, a picture of the capsule was taken post irradiation; an example of this is shown in Figure.

Table 1 Summary of runs performed

	µA	A	B	C	D
Runs	40	1 × 4 h 1 × 8 h			1 × 4 h 3 × 8 h
	50	1 × 7.5 h 8 × 8 h	1 × 8 h	1 × 5.5 h 2 × 8 h	
	60		1 × 8 h		
Totals	N	11	2	3	5
	h	83.5	16	21.5	32
	µAh	4055	880	1075	1520
	$Y_{Cumulative}$ (GBq)	82*	19	22	25*
	Y_{Sat} (GBq/µA)	2.47 ± 0.11*	2.54 ± 0.13	2.43 ± 0.17	2.43 ± 0.17*

*Excludes the 4-h-runs as not assayed in dose calibrator pre-purification (N = 3)

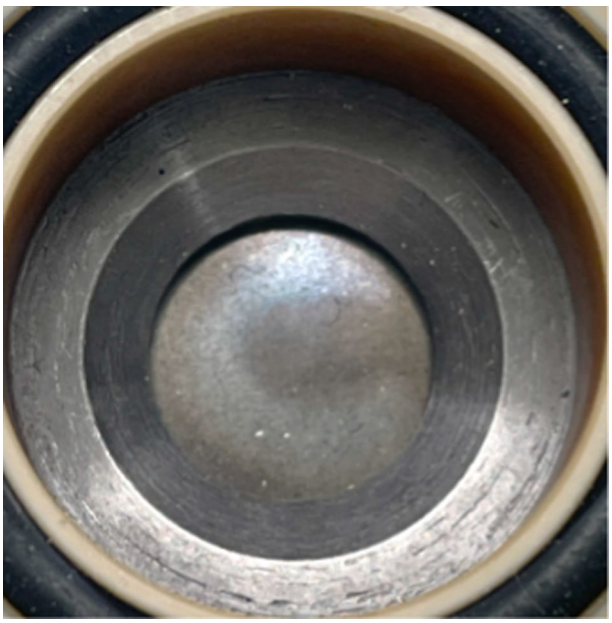

Fig. 1 Picture of foil taken ~ 1 week post irradiation (8h, 50μA, 13MeV).

Focusing on Capsule A, a total of 82 GBq (EOB) of ^{89}Zr was produced over 11 runs, with saturation yields of ~ 2.4 GBq/μA. Of these 11 runs, several automated dissolution and purifications into zirconium oxalate were performed, with the last triplicate runs yielding 84 ± 2% RCY and a dissolution efficiency of 98.3 ± 0.4%.

Conclusion: The new capsule design was proven to be capable of sustaining significant accumulated beam time (> 4000 μAh on a single capsule) without degrading its functionality, resulting in approximately 150 GBq total of ^{89}Zr produced through 21 test runs with saturation yields ~ 2.4 GBq/μA.

Reference

1. J. Svedjehed, M. Pärnaste, K. Gagnon. Demystifying solid targets: Simple and rapid distribution-scale production of [^{68}Ga]$GaCl_3$ and [^{68}Ga]Ga-PSMA-11. Nucl. Med. Biol. 2022, 104–105, 1–10.

PP30

A novel dual-modality imaging agents targeting FAP based on fusarinine C scaffold

Giacomo Gariglio[1*], Thomas Hasenöhrl[2], Christine Rangger[1], Barbara Matuszczak[2], Clemens Decristoforo[1]
[1]Department of Nuclear Medicine, Medical University of Innsbruck, Innsbruck, Austria. [2]Department of Pharmaceutical Chemistry, Institute of Pharmacy, University of Innsbruck, Innsbruck, Austria
[*]**Corresponding author**: giacomo.gariglio@student.i-med.ac.at

EJNMMI Radiopharmacy and Chemistry 2024, **9(1)**: PP30

Aim: The complete resection of solid tumours remains challenging and end of surgery positive surgical margins are common especially for ovarian and prostate cancer [1]. Dual-modality probes, combining PET with fluorescence imaging (FI) capabilities in the same molecule, can be used for both preoperative imaging and intraoperative real-time guidance and therefore can improve surgery outcomes [2].

We herein present a PET/FI agent targeting the fibroblast activation protein (FAP): [^{68}Ga]Ga-ZW800FFAPI. In this probe, the ZW800 fluorophore and two units of a FAPI-04 derivative were individually coupled to the siderophore Fusarinine C acting as core scaffold. An analogue compound without fluorophore, [^{68}Ga]Ga-AcFFAPI, was prepared in order to investigate the influence of the dye on the overall properties.

Materials and methods: The alkyne bearing FAPI-04 was synthesised by a modified procedure following Toms et al. [3].

The iron complex of Fusarinine C was first derivatised with an amino-PEG2 and two azido-PEG4 linkers. The selected fluorophore and two units of FAPI-04, respectively, were then introduced on the modified siderophore by amide coupling and click reaction. Eventually, the coordinated metal was removed by transchelation. Analogously, an acetylated ligand lacking the fluorophore was prepared as control.

^{68}Ga-labelling of the precursors (5 nmol) was accomplished within 10 min at pH 4.4 and RT. Radiochemical purity was analysed by radio-analytical RP-HPLC. In vitro characterisation included the evaluation of lipophilicity ($LogD_{7.4}$), protein binding and stability in human serum. Internalisation assays were performed by using tumour cells transfected with the human FAP gene. Biodistribution experiments in healthy BALB/c mice were performed to evaluate pharmacokinetics up to 2h p.i. In vivo tumour targeting properties will further be assessed by biodistribution, PET and fluorescence imaging studies.

Results: ^{68}Ga-labelling resulted in > 94% radiochemical purity for both precursors. Hydrophilic properties ($LogD_{7.4}$: -2.4 and -2.5), moderate protein binding (27.7 and 20.9%) and elevated stability in human serum were observed over 4 h respectively for [^{68}Ga]Ga-ZW800FFAPI and [^{68}Ga]Ga-AcFFAPI.

Preliminary cell uptake studies showed comparable high and specific receptor-mediated internalization (> 22% after 1h incubation at 37°C) for both radiotracers. Biodistribution data (2h p.i.) for [^{68}Ga]Ga-ZW800FFAPI indicated slow clearance from blood pool (2.1% ID/g) and low kidney and liver uptake (< 6.5% ID/g).

Conclusion: In this study we successfully used the multifunctional chelator FSC to prepare a novel PET/FI agent targeting FAP. Our preliminary results showed promising in vitro properties and their comparison with the control indicated that these are minimally modified by the introduction of the ZW800 dye.

References

1. Orosco RK, Tapia VJ, Califano JA, Clary B, Cohen EE, Kane C, et al. Positive Surgical Margins in the 10 Most Common Solid Cancers. Sci Rep. 2018; 8(1): 5686.
2. Kubeil M, Martínez II, Bachmann M, Kopka K, Tuck KL, Stephan H. Dual-labelling strategies for nuclear and fluorescence molecular imaging: current status and future perspectives. Pharmaceuticals. 2022;15(4):432
3. Toms J, Kogler J, Maschauer S, Daniel C, Schmidkonz C, Kuwert T, Prante O. Targeting Fibroblast Activation Protein: Radiosynthesis and Preclinical Evaluation of an 18F-Labeled FAP Inhibitor. J Nucl Med. 2020; 61(12): 1806–1813.

PP31

Optimization and Automation of Copper-mediated one-step [^{18}F] SFB synthesis starting from the boronic acid pinacol ester

Markus Laube[1], Reik Löser[1], Klaus Kopka[1,2], Jens Pietzsch[1,2]
[1]Institute of Radiopharmaceutical Cancer Research, Helmholtz-Zentrum Dresden-Rossendorf,Dresden,Germany. [2]Faculty of Chemistry and Food Chemistry, Technische Universität Dresden, Dresden, Germany.

EJNMMI Radiopharmacy and Chemistry 2024, **9(1)**: PP31

Aim: *N*-Succinimidyl-4-[^{18}F]fluorobenzoate [^{18}F]SFB is a commonly used active ester suitable for the labeling of peptides and proteins. Radiosynthesis of [^{18}F]SFB has been described by various methods, most often multi-step radiofluorination syntheses. Recently, the copper-mediated radiofluorination starting from boronic acid pinacol ester 1 [1] (Fig. 1) or the tributyl stannyl analog [2] in manual and

automated radiosyntheses, respectively, were reported as one-step access to [^{18}F]SFB. To substitute our automated three-step method starting from *tert*-butyl protected *N,N,N*-trimethylammoniobenzoic acid ester triflate, we attempted both approaches and detail results of optimization and automation starting from 1 herein.

Materials and methods: Organic syntheses comprised the synthesis of the stannyl-based precursor as described [2] as well as that of 1 starting from commercial 4-carboxy-phenyl boronic acid pinacol ester and *N*-hydroxysuccinimide using DCC as coupling reagent. Radiosyntheses were optimized regarding base ($KHCO_3$/K_3PO_4) for QMA conditioning, pre-mix time (0-60 min), concentration (2.5-10 mM precursor and 10-40 mM [$Cu(OTf)_2(py)_4$]), reaction temperature (90, 110, 130°C), and solvent (DMF, DMA, DMI) using our recently described microliter-scale radiofluorination approach in HPLC vials [3]. Optimized reaction conditions were transferred to an automated radiosynthesizer (TracerlabFx2N) and purification was performed by semi-preparative HPLC and SPE to obtain [^{18}F]SFB in high chemical and radiochemical purity for further conjugation chemistry.

Results: As a starting point, we envisaged the synthesis of the tributyl stannyl analog as precursor but failed to reproduce the reported synthesis starting from *N*-succinimidyl 4-iodobenzoate [2]. In comparison, the boronic acid pinacol ester was readily accessable from commercial starting materials in 84-89% yield. The optimized radiosynthesis sequence included elution of [^{18}F]fluoride from a K_3PO_4-conditioned QMA cartridge with KOTf/K_2CO_3 in MeCN/H_2O, evaporation at 130°C followed by radiofluorination using 10 mM of 1 and 40 mM of [$Cu(OTf)_2(py)_4$] in DMI at 90°C for 15 min. Automation furnished [^{18}F]SFB in 13-20% isolated radiochemical yield after 68-83 min (n = 3).

Conclusion: Radiosynthesis of [^{18}F]SFB starting from 1 was successfully optimized and transferred to an automated radiosynthesizer. The method provides the synthon in slightly lower RCY compared to our three-step method but preparation and the reaction sequence is considerable easier, allowing also to use the second reaction vessel of the module for conjugation chemistry which was not possible in the three-step two-pot approach applied before.

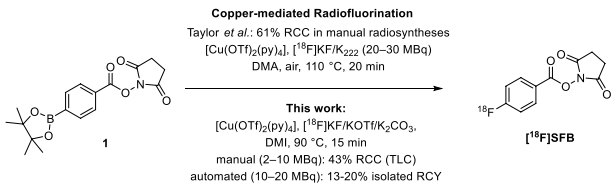

Fig. 1 Radiosynthesis of [^{18}F]SFB.

References

1. Taylor et al., JACS, 2017, 139: 8267.
2. Nagachinta et al. *Sci Rep,* 2022, 12: 18,655.
3. Laube et al. Nucl Med Biol, 2021, 96–97:S61

PP32

Implementation of Design of Experiments methodology for optimization of ^{18}F-PSMA-11 radiolabeling with {Al^{18}F}$^{2+}$ on AIO (Trasis®)

Laurene Wagner[1,2], Julia Budzinski[3], Samir Acherar[1], Thierry Bastogne[3,4], Charlotte Collet-Defossez[2,5]
[1]Université de Lorraine, CNRS, LCPM, F-54000 Nancy, France. [2]Nancyclotep, Plateforme d'imagerie moléculaire, F-54511 Vandœuvre-lès-Nancy, France. [3]Cybernano, F-54000, Nancy, France. [4]Université de Lorraine, CNRS, CRAN, F-54000 Nancy, France. [5]Université de Lorraine, Inserm, IADI, F-54000 Nancy, France

EJNMMI Radiopharmacy and Chemistry 2024, **9(1)**: PP32

Aim: In 2009, the Al^{18}F-labeling technique was described for the first time by McBride et al. and is now largely used as a fast and high-yield radiofluorination strategy.[1] Nowadays, several Al^{18}F-radioconjugates are under clinical trials such as [^{18}F]Alfatide II, [^{18}F]AlF-PSMA-11. As this strategy is quite recent, the development of a robust and high-yield radiosynthesis of Al^{18}F-conjugates is still ongoing and numerous factors can affect the radiochemical yield.[2] We therefore propose to use the Quality by Design, ICHQ8 (R2) [3] with Design of Experiments (DoE) methodology to develop robust and efficient [^{18}F]AlF-PSMA-11 radiopharmaceuticals production.[4]

Materials and methods: The radiolabeling step corresponding to complexation of {Al^{18}F}$^{2+}$ with PSMA-11 was evaluated by determination of radiochemical conversion (RCC) rate determined using radio-UHPLC and radio-TLC scanner. Firstly, manual experiments were carried out to identify the critical process parameters and determine a Design Space. Then, home-made labelling sequences were developed on AllInOne® (Trasis) module.

Results: To give access to optimized [^{18}F]AlF-PSMA-11 product, five sprint studies were implemented in the roadmap of Quality by design. Firstly, critical material attributes and process parameters were identified in a first study cycle. Secondly, operating ranges leading to optimal RCC were estimated in manual synthesis for the temperature of radiolabeling, PSMA-11 amount, $AlCl_3$ equivalent and ethanol rate. A validation study was performed in a third step and confirmed a successful RCC > 80%. After this proof of concept, a fourth QbD sequence was applied to address the automatic synthesis and to identify the new design space related to this manufacturing mode. Finally, we have successfully validated a normal operating region able to meet the initial specification: RCC > 80%. It allows us to produce [^{18}F]AlF-PSMA-11 including a purification step with a radiosynthesis yield of 53 ± 1% dc and a radiochemical purity of 97 ± 2%.

Conclusion: The power of DoE to optimize the automated [^{18}F]AlF -labeling of PSMA-11 has been illustrated, as a low number of tests was necessary to optimize the RCC and to validate the model for each radiolabeling modes. In this application study, we estimate the Quality by Design approach allowed us to reduce the duration of the product development by approximately 50%.

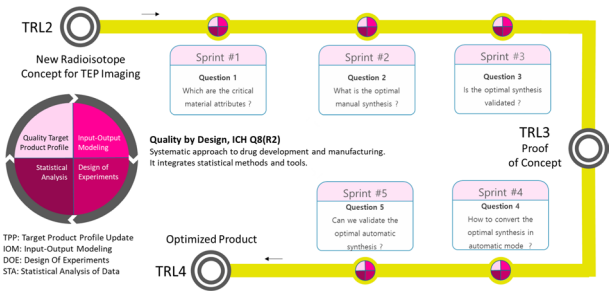

References

1. McBride, W. J., et al., A Novel Method of ^{18}F-Radiolabeling for PET. J. Nucl. Med., 2009, 50 (6), 991–998.
2. Schmitt, S.; Moreau, E. Radiochemistry with {Al^{18}F}2 + : Current Status and Optimization Perspectives for Efficient Radiofluorination by Complexation. Coord. Chem. Rev., 2023, 480, 215,028.
3. Bastogne, T. Quality-by-design of nanopharmaceuticals – A state of the art. Nanomedicine: Nanotechnology, Biology and Medicine, vol. 13, no. 7, pp. 2151–2157, 2017.
4. Bowden, G. D., et al., DoE Optimization Empowers the Automated Preparation of Enantiomerically Pure [^{18}F]Talazoparib and Its In Vivo Evaluation as a PARP Radiotracer. J. Med. Chem., 2021, 64 (21), 15,690–15701.

PP33

Fully-automated production of [^{18}F]Amylovis on the trasis AllinOne module

Fernando Trejo-Ballado[1*], Efrain Zamora-Romo[1], Hector M. Gama-Romero[1], Monica J. Mendoza-Figueroa[1], Gregorio R.

Tecuapetla-Chantes[1], Ulises Rabadan-Dominguez[1], Gabriela Contreras-Castañon[1], Edgar A. Aguilar-Ortiz[1], Adolfo Zarate-Morales[1], Armando Flores-Moreno[1], Miguel A. Avila-Rodriguez[1]
[1]Unidad Radiofarmacia-Ciclotrón, Facultad de Medicina, Universidad Nacional Autónoma de México, CDMX, México
*__Corresponding author__: fernandotrejob@hotmail.com

EJNMMI Radiopharmacy and Chemistry 2024, **9(1)**: PP33
Aim: PET imaging with [^{11}C]Pittsburgh compound-B has proven effectiveness and efficacy to visualize and quantify beta-amyloid plaques in the brain, a hallmark of Alzheimer's disease; however, the 20 min half-life of C-11 limits its widespread applicability. The PET imaging agent [^{18}F]Amylovis has exhibited promising results in silico, in vitro, and in vivo, proving efficacy in detecting the presence of A senile plaques in transgenic mice [1]. Our goal was to implement the fully automated production of [^{18}F]Amylovis on a cassette-based synthesizer.
Materials and methods: Synthesis was performed via nucleophilic substitution using the chemical precursor 2-(3-fluoropropyl)-6-methoxynaphthalene, using a commercial methylation cassette with minor changes. Briefly, [^{18}F]Fluoride ion was trapped in a QMA cartridge and eluted with 1.5 mL solution of K.2.2.2. (5.3 mg/mL)/ K2CO3 (1.4 mg/mL) in MeCN/H_2O (95/5). After drying of the azeotropic mixture, 1.0 mg of the precursor dissolved in 1.0 mL MeCN/0.3 mL DMSO were added to the reaction vessel and heated at 100°C for 10 min under intermittent purging with nitrogen.
The reaction mixture was diluted with 4 mL of the HPLC eluent (MeCN:H_2O (70:30)) and the solution was then loaded onto the HPLC-loop for purification in a semi-preparative C18 reverse phase column (250 × 10 mm, Nucleosil 100-7 C18, Macherey-Nagel). Purification was performed under isocratic elution at 4 mL/min flow rate. The collected product-fraction was diluted with water (1:5) and loaded onto a preconditioned C18 cartridge. After rinsing with 12 mL of water, [^{18}F]Amylovis was eluted with 1 mL EtOH, diluted with 12 mL 0.9% NaCl, 1000 µL Na_2HPO_4 (0.1 mmol/L, pH 8.5) and 700 µL Tween 80 (0.11 mmol/L in 0.9% NaCl), and sterilized by filtration (0.22 µm Sartorius Minisart).
Results: Using an initial activity of 37 ± 3 GBq of [^{18}F]fluoride, [^{18}F]Amylovis synthesis was satisfactorily accomplished yielding the final product with a decay corrected radiochemical yield of 14 ± 2% (n = 3) after a synthesis time of 50 min, with a radiochemical purity > 98% determined by analytical HPLC.
Conclusion: A convenient and reliable synthesis of [^{18}F]Amylovis was successfully implemented in an automated module by using a commercially available cassette with minor adaptations. The final product showed no radioactive or non-radioactive impurities obtaining [^{18}F]Amylovis in enough quantity and quality for preclinical applications.
Project supported by UNAM-DGAPA PAPIIT-IT201623 and CONACYT-PRONACES 322512.

Reference

1. Rivera-Marrero S, et. al. [^{18}F]Amylovis as a Potential PET Probe for β-Amyloid Plaque: Synthesis, In Silico, In vitro and In vivo Evaluations. Curr Radiopharm. 2019; 12:58-71.

PP34

[^{89}Zr]Zr-DFO-Atezolizumab for PD-L1 Imaging of Glioblastoma: Clinical Experience

[1]Department of Radiopharmacy and Preclinical PET Imaging, Maria Sklodowska-Curie National Research Institute of Oncology, Gliwice, Poland. [2]Department of Nuclear Medicine and Endocrine Oncology, Maria Sklodowska-Curie National Research Institute of Oncology, Gliwice, Poland. [3]Department of Neurosurgery, Medical University of Silesia, Katowice, Poland. [4]Department of Radiotherapy and Imaging, Institute of Cancer Research, London, United Kingdom. [5]Department of Tumour Pathology, Maria Sklodowska-Curie National Research Institute of Oncology, Gliwice, Poland. [6]Department of Radiology and Imaging Diagnostic, Maria Sklodowska-Curie National Research Institute of Oncology, Gliwice, Poland
*__Corresponding author__: gabriela.kramer-marek@gliwice.nio.gov.pl

EJNMMI Radiopharmacy and Chemistry 2024, **9(1)**: PP34
Aim: High expression of programmed death ligand 1 (PD-L1) is correlated with the immunosuppressive and aggressive properties of glioblastoma (GBM). Although blocking immune checkpoints to restore anti-tumour immunity and treat a variety of cancers has been demonstrated, an effective therapy for GBM has not yet been developed. Currently, there is no standardized evaluation of PD-L1 expression levels to aid in predicting the response to immune checkpoint inhibitors. Therefore, we investigated the utility of 89Zr-labelled Atezolizumab to measure PD-L1 expression in clinical settings.
Materials and methods: [^{89}Zr]Zr-DFO-Atezolizumab was prepared from commercially available Atezolizumab (Tecentriq, 1200 mg/20 mL, Roche) according to Good Manufacturing Practice (GMP) guidelines and under metal-free conditions. The chelate number per antibody was determined by matrix-assisted laser desorption/ionisation time-of-flight mass spectrometry (MALDI Ultraflex TOF/TOF mass spectrometer, Bruker). An average of 1.09 ± 0.52 chelators per protein was estimated. GMP compliant ^{89}Zr in 1 M oxalic acid was supplied by BV CyclotronVU (The Netherlands). Quality control tests included iTLC to determine the RCP, size-exclusion HPLC analysis for the antibody integrity and assessment of the presence of aggregates, UV spectrophotometry for protein concentration. Additionally, the immunoreactivity, binding affinity, and specificity of [^{89}Zr]Zr-DFO-Atezolizumab were assessed in vitro using GBM cell lines with different PD-L1 expression.
Prior to surgery, all patients were administered intravenously with the radio-conjugate, and PET/CT scans performed 48 h and 72 h p.i. Radioconjugate uptake was quantified (SUVmax) in the tumour and normal tissues. Post-surgery, tumour samples were collected for IHC (PD-L1 staining).
Results: The [^{89}Zr]Zr-DFO-Atezolizumab radio-conjugate was produced with a radiochemical purity (RCP) > 99%, radiochemical yield (RCY) of 73.34 -98% and 21.73 – 43.86 MBq/mg apparent specific activity. When used in a rapid bead-based radioimmunoassay, the radioconjugate showed a target binding fraction of 96.91%, indicating a good retention of the target recognition properties. The [^{89}Zr]Zr-DFO-Atezolizumab specificity binding studies showed a correlation between the cell-associated radioactivity and level of PD-L1 expression in human and murine GBM cells as seen by flow cytometry.
Patients (n = 3) experienced no [^{89}Zr]Zr-DFO-Atezolizumab-related side effects. High radioconjugate accumulation was observed in the vital part of the tumours 48 h post-administration. In normal tissues, uptake was seen in the spleen, liver, and intestines. The radioconjugate tumour targeting was associated with PD-L1 expression assessed by IHC and was consistent with an increased T-cell infiltration.
Conclusion: [^{89}Zr]Zr-DFO-Atezolizumab has demonstrated high specificity in detecting PD-L1 in patients with newly diagnosed GBM. The imaging data also complemented the information obtained from IHC data.

PP35

Investigation into the metabolic stability of ^{18}F-labeled PSMA inhibitor derivatives bearing aryl-fluorosulfates for PET tracer development applications

Guillermo Luque Consuegra[1], Austin Craig[1], Jürgen Kogler[1,2], Martin Ullrich[1], Cornelius K. Donat[1], Klaus Kopka[1,2], Sven Stadlbauer[1,2*]
[1]Institute of Radiopharmaceutical Cancer Research; Helmholtz-Zentrum Dresden-Rossendorf, D-01328 Dresden, Germany. [2]Faculty of Chemistry and Food Chemistry, School of Science, Technische Universität Dresden, D-01062 Dresden, Germany
EJNMMI Radiopharmacy and Chemistry 2024, **9(1)**: PP35

Aim: Radiolabeled PSMA inhibitors are clinically employed for the identification and treatment of prostate cancer [1]. The sulfur-[^{18}F]fluoride exchange ([^{18}F]SuFEx) radiolabeling approach has been

demonstrated to prepare ^{18}F-labeled radiotracers with high radiochemical yield (RCY) and radiochemical purity (RCP) [2]. However, the in vivo stability of radiolabeled aryl-fluorosulfates has been shown to limit this promising radiofluorination method [3]. This work is aiming at assessing the metabolic stability of two ^{18}F-labeled PSMA inhibitor derivatives bearing aryl-fluorosulfates to establish whether electron deficient aryl-fluorosulfates may influence in vivo defluorination.

Materials and methods: The manual radiosynthetic method began with [^{18}F]fluoride loading onto a QMA-cartridge which was subsequently eluted with dry 0.7 mL MeOH containing 3.0 mg (9.6 µmol) $BnEt_3NCl$. Thereafter, the evaporation of the solvent was carried out under reduced pressure at 70 °C for 5 min (Fig. 1 A). The radiolabeling precursor 0.1 mg (0.145 µmol) 3 in 0.5 mL MeCN was added to the reaction vial, and the [^{18}F]SuFEx reaction proceeded without stirring for 5 min at 23 °C. The reaction was quenched by (10 mL) water dilution followed by SPE-based purification using a HLB cartridge. HLB elution with 2 mL EtOH was used to isolate ^{18}F-labeled 2, and the ethanolic solvent was removed under vacuum for 10 min at 70 °C. Deprotection of the radiolabeled intermediate compound was performed using 0.5 mL (6 M) HCl, which was added to the reaction vial and further stirred for 15 min which furnished ^{18}F-labeled product 2 following SPE purification using a HLB cartridge as mentioned previously. The activity yield (AY) of ^{18}F-labeled product 2 was determined, and RCP was confirmed by UHPLC and HPLC. The future preparation of ^{18}F-labeled product 4 (Fig. 1 B) will be carried out according to the aforementioned protocol.

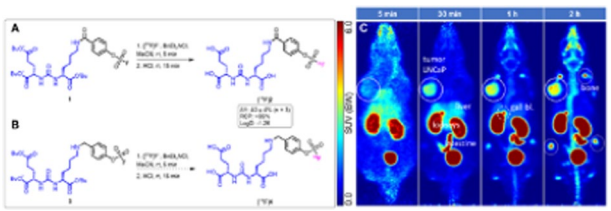

Fig. 1 A: Preparation of ^{18}F-labeled product 2 via [^{18}F]SuFEx radiofluorination protocol; B: Proposed preparation of ^{18}F-labeled product 4; C: PET imaging experiments of ^{18}F-labeled product 2 in nude mice at 5, 30, 60 and 120 min.

Results: A radiolabeled PSMA inhibitor (^{18}F-labeled product 2) was prepared via the [^{18}F]SuFEx reaction (Fig. 1 A) according to recently described optimized radiolabeling protocols, in high AY and RCP [3]. PET imaging experiments show tumor uptake of ^{18}F-labeled product 2 30 min post-injection, as well as increasing activity in the bones and joints (Fig. 1 C).

Conclusion: Evidence of ^{18}F-defluorination of ^{18}F-labeled product 2 was visible after 30 min p.i. as indicated by the increasing activity uptake in the bones and joints over time in the corresponding PET images (Fig. 1 C). The future preparation and biological evaluation of ^{18}F-labeled product 4 may provide key insights into the effect of the electron deficient aryl-fluorosulfates on overall metabolic stability of radioligands accessed via the [^{18}F]SuFEx radiolabeling approach (Fig. 1 B).

References

1. Capasso G, Stefanucci A, Tolomeo A. A systematic review on the current status of PSMA-targeted imaging and radioligand therapy. Eur J Med Chem. 2024 Jan;263:115,966.
2. Walter N, Bertram J, Drewes B, Bahutski V, Timmer M, Schütz MB, Krämer F, Neumaier F, Endepols H, Neumaier B, Zlatopolskiy B, Convenient PET-tracer production via SuFEx ^{18}F-fluorination of nanomolar precursor amounts. Eur J Med Chem. 2022 Jul;237:114,383.
3. Craig A, Kogler J, Krutzek F, Brandt F, Laube M, Ullrich M, Donat C, Wodtke R, Kopka K, Stadlbauer S. Sulfur [^{18}F]Fluoride Exchange Reaction Enables Rapid Access to ^{18}F-Labeled PET Tracers. Med Sci Forum. 2022;14(1):127.

PP36

Biodistribution of orally administered nano-particle polymers

Steen Jakobsen[1*], Malgorzata M Pakula[2], Mette I Simonsen[1], Mikkel H Vendelbo[1], Klaus Gregorius[3], Amanda Andresen[3], Nicolas Krogh[3]
[1]Nuclearmedicine and PET Center, Aarhus University Hospital, Aarhus, Denmark. [2]Dept of Biomedicine, Aarhus University, Aarhus, Denmark. [3]MipSalus Aps, Hørsholm, Denmark

EJNMMI Radiopharmacy and Chemistry 2024, **9(1)**: PP36

Aim: Labeling of polymeric nano-particles and subsequent determination of biodistribution.

Materials and methods: Co-polymers (COP) of methacrylic acid and nitrogen-containing monomer were subjected to three different radioactive labeling strategies including carbon-11, fluorine-18 and copper-64.

15 mg COP (size 50—200 nm) dissolved in aqueous/organic solvent mixtures with auxillary base present was reacted with [^{11}C]methyl iodide, to convert residual acid functionality to the corresponding ester, followed by size-exclusion chromatography for product purification.

[^{18}F]Aluminum-fluoride or [^{64}Cu]Cu chloride was mixed with 15 mg COP in aqueous sodium acetate buffer at varying pH. Either PD10 G25 MidiTrap columns, Nanosep 3K spinfilter or ultracentrifugation was used for product purification and/or determination of product radiochemical purity.

Mice were administered 2 – 25 MBq [^{18}F]-AlF-COP or 0.2 – 5 MBq ^{64}Cu-labeled COP by oral gavage and subsequently prepared for microPET/MR scanning. At scan termination, mice were sacrificed and organs excised and counted for radioactivity.

Results:^{64}Cu-labeled COP may be obtained in > 98% radiochemical purity and 50% radiochemical yield, at pH 5.5—6.0.

Optimum conditions for ^{18}F-labeling were pH 4.5 yet radiochemical yield was only 5-10% and > 90% purity.

Attempts to label COP with carbon-11 proved elusive.

MicroPET imaging (Fig. 1) and biodistribution (Fig. 2) showed primarily distribution of radioactivity to GI tract and intestines, although bones were clearly visible with the ^{18}F-labeled tracer.

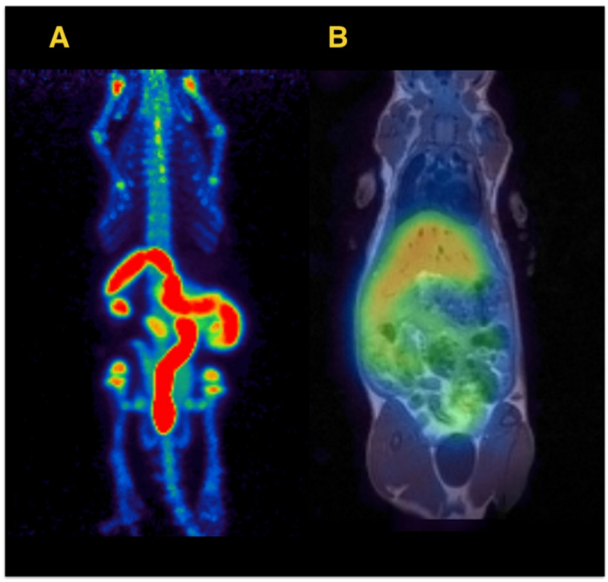

Fig. 1 Static MicroPET image of [^{18}F]-AlF-COP (A) and [^{64}Cu]Cu-COP (B) 2 h post administration.

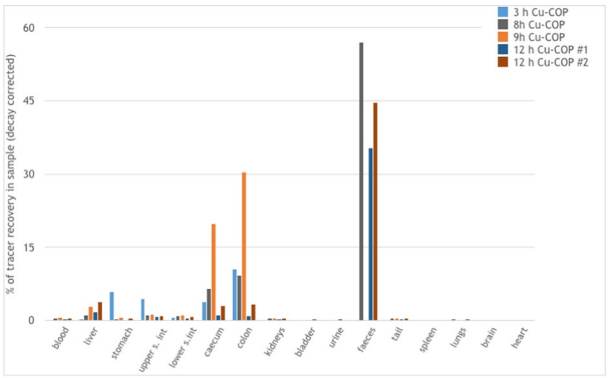

Fig. 2 Biodistribution of [^{64}Cu]Cu-COP at different times post oral gavage.

Conclusion: Nano-particle sized polymers can succesfully be labeled with copper-64/fluorine-18 and imaged for up to 18 h in mice. [^{64}Cu]Cu-COP is preferable to [^{18}F]AlF-COP as the latter shows some deflurination.

PP37

Titanium-45: Production, Extraction, and Trans-chelation with DOTA

Chubina P. Kumarananthan[1], Unni A. Kvitastein[1], Tamal Roy[2], Camillo Bruhn[1], Erwan Le Roux[2], Tom C. H. Adamsen[1,2]
[1]Department of Radiology, Haukeland University Hospital, Bergen, Norway. [2]Department of Chemistry, University of Bergen, Bergen, Norway
EJNMMI Radiopharmacy and Chemistry 2024, **9(1)**: PP37

Introduction: Titanium-45 ($t_{1/2}$ = 3.08 h) is PET-nuclide that can be utilized to study slower physiological processes. This is due to its favorable decay characteristics (β^+: 85%, E_{max} = 1040.1 keV) and intermediate half-life of 3 hours[1]. The challenging chemistry of titanium has led to a slow advancement in the radiotracer development of titanium-45, primarily due to its hydrolytic instability and highly oxophilic nature[2]. One approach to stabilize the radionuclide involves the use of chelators to form stable complexes. This study focuses on complexing titanium-45 with a widely used chelator in radiochemistry, 1,4,7,10-tetraazacyclododecane-1,4,7,10-tetraacetic acid (DOTA), a task previously deemed impossible[3]. The objectives of this study are (1) to produce high activities of titanium-45 using a liquid target in a medical cyclotron, (2) to extract titanium-45 by solid phase extraction (SPE) or liquid-liquid extraction (LLE), and (3) to complex titanium-45 with DOTA.

Materials and Methods: Different solutions of scandium nitrate (0.5 – 2.5 M) in nitric acid (0.05 – 0.3 M) were irradiated with 14.3 MeV protons to follow the ^{nat}Sc(p,n)^{45}Ti reaction. The irradiations were carried out in a medical cyclotron using varying irradiation times (1 – 4 h) and beam currents (15 – 35 µA). The first extraction method was an automated SPE utilizing a hydroxamate resin (ZR-resin) and different eluents. The eluates were either directly used for complexation with DOTA, or further purified on a quaternary ammonium anion-exchange (QMA) resin before complexation[4]. The second method was a manual LLE using a mixture of guaiacol and anisole (9/1) (*v/v*) as the organic phase and the cyclotron product as the aqueous phase[5]. The phases were mixed by shaking and separated using a centrifuge. Following this, the organic phase was used for complexation. The extracted titanium-45 from both methods was mixed with the DOTA-solution (in DMSO w/ pyridine) for 20 min at 90°C.

Results: The irradiations (n = 70) resulted in an activity of titanium-45 ranging from 0.2 to 4 GBq (EOB, RNP: 94.7 – 99.8%). Gamma-ray spectrometry analysis of all fractions from both extraction methods indicated that scandium species and radionuclidic impurities were removed. Most of the radioactivity was present in the organic phase for many of the LLEs. In these cases, analysis of the crude reaction mixture in a radio-HPLC indicated that [^{45}Ti]Ti-DOTA was formed (n = 3, radiochemical conversion: 96.8 – 99.5%) as the retention times coincides with that of the Ti-DOTA reference. However, some of the LLEs had an incomplete phase separation, which hindered complexation. The incomplete separation was probably caused by higher nitric acid concentrations in the cyclotron products. For the SPE-method, eluents such as oxalic acid, ascorbic acid, and citrate eluted titanium-45 in various amounts, but the trans-chelation with DOTA was not evident in the radio-HPLC.

Conclusion: The liquid target productions resulted in high enough activities of titanium-45 to study separation and complexation with DOTA. Both separation methods extracted titanium in various amounts, and the LLE-method facilitated to the formation of [^{45}Ti]Ti-DOTA. Further purification and optimization of separation methods are required for [^{45}Ti]Ti-DOTA to be used for animal studies.

References

1. Kuhn, S.; Spahn, I.; Scholten, B.; Coenen, H. H. Positron and γ-ray intensities in the decay of ^{45}Ti. Radiochimica Acta 2015, 103 (6), 403–409. https://doi.org/10.1515/ract-2014- 0006.*
2. Giesen, K.; Spahn, I.; Neumaier, B. Thermochromatographic separation of 45Ti and subsequent radiosynthesis of [^{45}Ti]salan. Journal of Radioanalytical and Nuclear Chemistry 2020, 326 (2), 1281–1287. https://doi.org/10.1007/s10967-020-07376-2.
3. Pedersen, K. S.; Baun, C.; Nielsen, K. M.; Thisgaard, H.; Jensen, A. I.; Zhuravlev, F. Design, Synthesis, Computational, and Preclinical Evaluation of ^{nat}Ti/^{45}Ti-Labeled Urea-Based Glutamate PSMA Ligand. Molecules 2020, 25(5), 1104. https://doi.org/10.3390/molecules25051104
4. Holland, J. P.; Sheh, Y.; Lewis J. S. Standardized methods for the production of high specific-activity zirconium-89. Nuclear medicine and biology 2009, 36(7), 729–739, https://doi.org/10.1016/j.nucmedbio.2009.05.007
5. Pedersen, K. S.; Imbrogno, J.; Fonslet, J.; Lusardi, M.; Jensen, K. F.; Zhuravlev, F. Liquid–liquid extraction in flow of the radioisotope titanium-45 for positron emission tomography applications. Reaction Chemistry & Engineering 2018, 3 (6), 898–904. https://doi.org/10.1039/c8re00175h.

PP38

Synthesis and Quality Control of [^{68}Ga]Ga-PSMA-11 Cold Kits Produced Using Two Different Generator Models Simultaneously

Sarah Benkhoris[1*], Daniele Alizé[1], Johanne Vanney[2],Cyril Fersing[2], Pierre Olivier Kotzki[1,2]
[1]Médicine nucléaire, ICG, Nîmes, France. [2]Médecine nucléaire, ICM, Montpellier, France
EJNMMI Radiopharmacy and Chemistry 2024, **9(1)**: PP38

Aim: [^{68}Ga]Ga-PSMA-11 PET scans is steadily increasing, particularly with the broader indications of the corresponding single vial cold kit (Locametz®, Novartis). The final activities obtained for [^{68}Ga]Ga-PSMA-11 preparations significantly decrease over time as the ^{68}Ga-generator decays, resulting in a lower number of examinations per preparation. Given the robustness of the radiopharmaceutical preparation kits and the possibility of replacing a generator several months before its expiry date, alternative solutions are conceivable to maintain sufficient end-of-synthesis (EoS) activities, ensuring a consistent response to the patients flow. Furthermore, when a new call for tenders is issued, selecting a new supplier may be necessary, prompting the exploration of production methods using two generators from different suppliers.The aim of this study is to validate a preparation protocol for [^{68}Ga]Ga-PSMA-11 formulated in a single vial cold kit using two GMP generators from different suppliers.

Materials and methods: Two generators, GALLIAD® (IRE, calibrated on 30/12/2022) and GALLIAPHARM® (Curium, calibrated on 14/11/2023), were employed. Three preparations of Locametz® radiolabeled with gallium -68 were carried out using an original automated method configured on a GAIA® module (Elysia-Raytest) for reproducible sequential elution of the two generators. After preparation, EoS activities were measured, and various quality controls were conducted. These included organoleptic characteristics, pH, radiochemical purity (RCP) and identification (by TLC and HPLC), sterility tests, bacterial endotoxin tests, and radionuclidic purity. All controls

were performed immediately after EoS (H0), and radiochemical purity was additionally measured every hour for 4 h (H1 to H4).
Results: EoS activities for the three [^{68}Ga]Ga-PSMA-11 preparations were 1540 MBq, 1265 MBq, and 1510 MBq. Automation enhanced radiation protection for operators, yielding excellent results in a serial elution configuration. Decay-corrected radiochemical yield remained high (96.9%, 94.6%, and 94.8%), allowing up to 10 patients per preparation, compared to 6 with a single generator configuration. Therefore, the average cost per patient is reduced by 20%, despite the use of a synthesis module tubing set. Quality controls indicated an average RCP of 99.72% in both TLC and HPLC. The product demonstrated stability (RCP > 99.41%) between H0 and H4. Endotoxin detection and sterility tests yielded negative results.
Conclusion: Automated production of [^{68}Ga]Ga-PSMA-11 using two different generators was successful with quality control results meeting European Pharmacopoeia requirements. Sequential elution automation ensured radiation protection while being reproducible and reliable. Double-generator radiolabeling of the PSMA-11 cold kit emerges as an efficient alternative, extending the lifespan of generators. Additionally, this strategy reduces the cost per patient for this preparation.

References

1. Rodnick M.E., Sollert C., Stark D. and al. Synthesis of ^{68}Ga-radiopharmaceuticals using both generator-derived and cyclotron-produced ^{68}Ga as exemplified by [68Ga]Ga-PSMA-11 for prostate cancer PET imaging. Nat Protocols. 2022; 17: 980–1003.
2. Nelson B.J.B., Andersson J.D., Wuest F. and al. Good practices for ^{68}Ga radiopharmaceutical production. EJNMMI radiopharm. chem. 2022; 7:1–27.

PP40

A fast and automated method for the production of [^{13}N]AMMO

Ole H Kvernenes[1], Tom CH Adamsen[1,2]
[1]Centre for Nuclear Medicine, Department of Radiology, Haukeland University Hospital, Bergen, Norway. [2]Department of Chemistry, University of Bergen, Bergen, Norway
EJNMMI Radiopharmacy and Chemistry 2024, **9(1)**: PP40

Aim: To establish a simple and automated ammonia production platform for the production of multiple doses of ammonia.
Materials and methods: The production of [^{13}N]ammonia is performed by bombarding a 5 mM EtOH in H_2O (PhEur, WFI) in a dedicated target. The irradiated solution is transfered to a Neptis synthesis module vi a a target switch system. The synthesis, or more accurately the purification of [^{13}N]ammonia was done by using a modified [^{18}F] NaF method and cassette, from Ora (Neuville, Belgium) and ABX (Radeberg, Germany) respectively, using the Ora Neptis Mosaic-RS synthesis module. The target solution was pushed through a QMA, in order to trap eventual anionic impurities before the [^{13}N]ammonia is captured on a waters CM cartridge. After washing with sterile water, the CM cartridge is flushed with saline and the purified [^{13}N]ammonia is collected in a product vial, via a sterile filter. The QMA and CM cartridges are flushed with sterile water, and the process can be repeated for a new batch of target solution.
Results: An experiment was set up, to examine how many batches we could produce using the same synthesis cassette. A full QC analysis, including HPLC identification, half life, HPGe spectroscopy, pH and endotoxin was performed on each batch. Sterility was performed on a pool of all batches. For each cassette we ran 9 sub-batches, including QC, and the experiment was repeated three times. It was evident from the data that a total of 5 sub-batches could successfully be produced from each cassette., with good results. A clear trend emerged that from sub batch 6 and onward, the ammonia was no longer captured on the CM cartridge and the final product activity was very low. We found this drop in activity to correlate with a clear drop in the pH, and pH did in fact fail for the latter batches.
Conclusion: A fast and convenient method has been made to yielded [^{13}N]ammonia in good result, all within pH.Eur specifications for a total of up to 5 sub-batches, for all three cassettes. The method described was made, based on our experience with the ISAR system (GE Healthcare)(1). A similar method was also reported by Fakhri et al.

References

1. 1 Frank C, Winter G, Rensei F, Samper V, Brooks AF, Hockley BG, Henderson BD, Rensch C, Scott PJH. Development and implementation of ISAR, a new synthesis platform for radiopharmaceutical production. EJNMMI Radiopharm Chem. 2019 Sep 18;4(1);p1-24.
2. 2 Yokell, DL, Rice, PA, Neelamegam, Fakhri G. Development, validation and regulatory acceptance of improved purification and simplified quality control of [^{13}N]Ammonia. EJNMMI radiopharm. chem. 2020; 5, p1-11

PP41

Exploring the therapeutic efficacy of [^{177}Lu]Lu-DOTA-trastuzumab in trastuzumab-resistant HER2 + lesions

Liliana Santos[1,2,3*], Ivanna Hrynchak[1], Hugo Ferreira[2,3], José Sereno[1], Célia Gomes[2,3], Antero Abrunhosa[1]
[1]CIBIT/ICNAS – Institute for Nuclear Sciences Applied to Health, University of Coimbra, Portugal. [2]iCBR—Institute for Clinical and Biomedical Research, Faculty of Medicine, University of Coimbra, Portugal. [3]CIBB—Center for Innovative Biomedicine and Biotechnology Consortium, University of Coimbra, Portugal
[*]**Corresponding author**: lsantos@icnas.uc.pt

EJNMMI Radiopharmacy and Chemistry 2024, **9(1)**: PP41
Aim: The prognosis for HER2 + breast cancer patients has been notably enhanced by HER2-targeted therapies, including the monoclonal antibody trastuzumab. Despite this advancement, the emergence of resistant metastatic lesions, especially in advanced stages such as brain metastasis, poses a challenge to the efficacy of these treatments. To address this limitation, we investigated the therapeutic potential of trastuzumab labeled with the β-emitting radionuclide lutetium-177 (^{177}Lu).
Materials and methods: Trastuzumab was radiolabeled with ^{177}Lu ($t_{1/2}$ = 6.7 days; 79.3% β^-; E = 0.13 MeV) using a DOTA-based bifunctional chelator. The labeling efficiency and stability of [^{177}Lu]Lu-DOTA-trastuzumab in biological fluids were assessed. Cell surface HER2 density and sensitivity to both trastuzumab and [^{177}Lu]Lu-DOTA-trastuzumab were characterized in HER2 + breast cancer cell lines and their brain-tropic derivatives. Swiss nude mice were injected orthotopically into the mammary gland with HER2 + breast cancer cells. Primary tumour growth was monitored by magnetic resonance imaging (MRI) until reaching an appropriate volume. Subsequently, mice were intravenously administered either trastuzumab or [^{177}Lu]Lu-DOTA-trastuzumab, and the therapeutic efficacy was assessed.
Results: The radiolabeling process of trastuzumab with ^{177}Lu achieved a robust radiolabeling yield exceeding 93% (93.2 ± 6.2%, n = 6) and demonstrated outstanding stability in biological fluids for a duration of up to 168 h. Despite expressing similar levels of HER2, brain-tropic cells exhibited heightened resistance to trastuzumab compared to their parental cell line. However, these brain-tropic cells demonstrated sensitivity to [^{177}Lu]Lu-DOTA-trastuzumab, as indicated by reduced clonogenic survival, DNA damage, and γH2AX foci. In mice with resistant breast cancer lesions, the response to trastuzumab therapy was limited, whereas a significant reduction in tumor size was observed in mice treated with [^{177}Lu]Lu-DOTA-trastuzumab.
Conclusion: Our findings demonstrate the enhanced therapeutic efficacy of [^{177}Lu]Lu-DOTA-trastuzumab in treating trastuzumab-resistant HER2 + lesions.

PP42

Sequential labeling of Silk Fibroin Nanoparticles with Technetium-99m and Indocyanine Green for in vivo SPECT NIR-I/II imaging: Towards photothermal theranostic nanoprobes

Mª de la Luz Bravo-Ferrer Moreno[1], Andrea Blesa Jiménez[1], Carmen Belén Otero Alonso[1], María Alejandra Asensio Ruiz[1,2], Antonio Abel Lozano-Pérez[2,3], María Teresa Martínez Martínez[1,2].
[1]Servicio de Radiofarmacia, Hospital Clínico Universitario Virgen de la Arrixaca, Murcia, Spain. [2]Instituto Murciano de Investigación Biosanitaria (IMIB)-Arrixaca, Murcia, Spain. [3]Departamento de Biotecnología

Genómica y Mejora Vegetal, Instituto Murciano de Investigación y Desarrollo Agrario y Medioambiental, Murcia, Spain.
EJNMMI Radiopharmacy and Chemistry 2024, **9(1)**: PP42

Aim: Recently, there has been a great interest in near infrared(NIR) induced thermotherapy for cancer treatment due to excellent tissue penetration, high efficiency and minimal invasiveness (1). NIR thermotherapeutic nanoprobes have raised as potential tools, enhancing the stability and effect of a photothermal drug in a selective and biocompatible nanoformulation. The aim of this work is to carry out dual labeling of silk fibroin nanoparticles(SFN) with the radioisotope technetium-99m (^{99m}Tc) and the fluorescent agent indocyanin green(ICG).
Materials and methods: ^{99m}Tc-labeled ICG-SFNs were obtained by two-step direct labeling. In a first step, 1 mg of SFNs (4×10^{11} nanoparticles/mg; Zave = 148.8 ± 1.8nm; PdI = 0.107 ± 0.008; Zpot = -27.4 ± 1.9 mV) were labeled with ~ 37 MBq of sodium [^{99m}Tc]Tc-pertechnetate reduced with stannous chloride in hydrochloric acid as previously described (2).Once the ^{99m}Tc-labeled SFNs were centrifuged, the pellet was suspended in 1.5 mL of a solution containing 2.4 µg of ICG and incubated for 30 min. Subsequently, the ^{99m}Tc-labeled ICG-SFNs were recovered by centrifugation, the absorbance of the supernatant was measured in a spectrophotometer at 780 nm, and the pellet was suspended in water for injection. Radiochemical Purity (RCP%) before and after ICG labeling was analyzed by instant-Thin Layer Chromatography (iTLC). Radiolabeling efficiency (RLE%), Encapsulation Efficiency (EE%) and Drug Loading Content (DLC%) were calculated by using formulae described elsewhere (2, 3). Characterization of ^{99m}Tc-labeled ICG-SFNs with Dynamic Light Scattering (DLS) was performed after a decay period of at least 12 τ½.
Results: After initial labeling of the SFNs with ^{99m}Tc(n = 18), RLE(%) of 94.31 ± 0.87 and RCP(%) of 98.08 ± 2.93 were obtained. The EE(%) was of 97.95 ± 1.07 and DLC of 2.54 ± 0.03 µg of ICG/mg ^{99m}Tc-ICG-SFNs. After the labeling with ICG, the RCP was 99.57 ± 0.46%, showing no release of technetium from the nanoparticles during the second step of labeling. The hydrodynamic characteristics of the nanoparticles remained relatively stable after the dual labeling, with the zeta potential stable (Zpot = -28.6 ± 2.32mV) but a decreasement in diameter (Zave = 143.8 ± 1.32nm) and an increasement in polidispersity (PdI = 0.130 ± 0.025) of no statistical significance when compared with the unloaded nanoparticles.
Conclusion: A direct, reproducible and feasible method of dual labeling of silk nanoparticles with ^{99m}Tc and ICG has been implemented without modifying the hydrodynamic characteristics of the nanoparticles.

References

1. Biao-Qi C., Ranjith Kumar K., Geng-Yi, H., Da-Yun Y., Guo-Ping, L. Pei, W., Shi-Bin W., Yu Shrike Z., and Ai-Zheng C. Supercritical Fluid-Assisted Fabrication of Indocyanine Green-Encapsulated Silk Fibroin Nanoparticles for Dual-Triggered Cancer Therapy *ACS Biomaterials Science & Engineering* 2018 4 (10), 3487–3497. https://doi.org/10.1021/acsbiomaterials.8b00705
2. Asensio Ruiz M.A.; Alonso García Á.; Bravo-Ferrer Moreno M.d.l.L.; Cebreiros-López I.; Noguera-Velasco J.A.; Lozano-Pérez A.A.; Martínez Martínez T. In Vitro Hemocompatibility and Genotoxicity Evaluation of Dual-Labeled [^{99m}Tc]Tc-FITC-Silk Fibroin Nanoparticles for Biomedical Applications. *Pharmaceuticals* 2023, 16, 248. https://doi.org/10.3390/ph16020248
3. Ruiz-Alcaraz, A.J.; Núñez-Sánchez, M.Á.; Asensio Ruiz, M.A.; Martínez-Sánchez, M.A.; Oliva-Bolarín, A.; Martínez Martínez, T.; Pérez Cuadrado, J.J.; Ramos-Molina, B.; Lozano-Pérez, A.A. Optimizing the Preparation of Silk Fibroin Nanoparticles and Their Loading with Polyphenols: Towards a More Efficient Anti-Inflammatory Effect on Macrophages. *Pharmaceutics* 2023, 15, 263. https://doi.org/10.3390/pharmaceutics15010263

PP43

^{211}At-labeling of trans-cyclooctenes and cis-cyclooctenes with astatine-211 using electrophilic and nucleophilic reactions

Maarten Vanermen[1,2], Tim Van den Wyngaert[1], Pieter Van der Veken[2], François Guérard[3], Filipe Elvas[1,2]
[1]Molecular Imaging and Radiology (MIRA), University of Antwerp, Antwerp, Belgium. [2]Laboratory of Medicinal Chemistry, University of Antwerp, Antwerp, Belgium. [3]Nantes Université, Inserm, CNRS, Université d'Angers, CRCI2NA, Nantes, France
EJNMMI Radiopharmacy and Chemistry 2024, **9(1)**: PP43

Aim: Fibroblast Activating Protein (FAP) is a widely recognized cancer biomarker. [1] Motivated by the success of imaging radioligands, radionuclide therapies targeting FAP are currently being extensively investigated. However, relatively short retention and fast washout of radioactivity from the tumor, and inadequate pharmacokinetics of current FAP-ligands represent major limitations for radioligand therapy. [2] Therefore, this study proposes a pretargeting strategy to improve FAP radionuclide therapy. In this respect, we developed trans-cyclooctenes (TCOs) radiolabeled with the α-emitter, astatine-211 (^{211}At).
Materials and methods: We have synthesized TCO and cis-cyclooctene (CCO) precursors with either boronic acids or tributyltin leaving groups, primarily using CCO for optimization of the reaction conditions. Besides precursors, we produced the iodinated cold References (as astatine surrogate). The TCOs were synthesized using a known procedure, followed by amide coupling of the TCO or CCO amines using EDC, HOBt and DIPEA to yield the precursors or References [3].
Astatination of the CCO tributyltin precursor was performed via electrophilic destannylation with ^{211}At along with NCS in methanol solution at ambient temperature. For comparative purposes, we employed a CCO boronic acid precursor using a nucleophilic substitution reaction in the presence of nucleophilic ^{211}At and a copper(II) catalyst. TCO was also astatinated electrophilically from boronic acid precursor with NBS or KI in methanol/water at room temperature. [4] Radiochemical conversions (RCC) were determined using HPLC C18 column and radio-TLC. Reaction mixtures were purified with C18 SPE cartridges. Radiolabeled compounds will be further reacted with a tetrazine-FAP ligand and used in cell uptake experiments.
Results: Tributyltin yielded 99% [^{211}At]At-CCO by electrophilic approach while boronic acid yielded the product nucleophilically with 84-96% RCC. Since TCO is sensitive to copper and the tributyltin precursor is toxic, we pursued the TCO employing the boronic acid with electrophilic labeling. [5] The NBS-method resulted in a lower RCC of 37%, while the KI-method was more effective, achieving 75% and a decay-corrected yield of 68%, after purification. To confirm the stability of the TCO during astatination, a reaction with a model tetrazine was conducted. A new radioactive peak corresponding to the dihydropyridazine reaction product could be observed.
Conclusion: The boron-astatine electrophilic substitution reaction is an efficient method for ^{211}At-labeling of TCOs. [^{211}At]At-CCO is promising for pretargeted therapy using tetrazine-conjugated ligands. These astatinated radioligands will be further evaluated in cell uptake experiments using FAP-positive cells.

References

1. REVIEWS AND COMMENTARY • REVIEW. [cited 2024 Jan 23]; Available from: https://doi.org/10.1148/radiol.220749
2. Lindeman SD, Mukkamala R, Horner A, Tudi P, Booth OC, Huff R, et al. Fibroblast Activation Protein-Targeted Radioligand Therapy for Treatment of Solid Tumors. J Nucl Med [Internet]. 2023 [cited 2024 Jan 16];64:759–66. Available from: https://doi.org/10.2967/jnumed.122.264494.
3. Adhikari K, Dewulf J, Vangestel C, Van der Veken P, Stroobants S, Elvas F, et al. Characterization of Structurally Diverse ^{18}F-Labeled d-TCO Derivatives as a PET Probe for Bioorthogonal Pretargeted Imaging. ACS Omega [Internet]. 2023 [cited 2023 Dec 5];8:38,262. Available from: https://pubs.acs.org/doi/full/10.1021/acsomega.3c04597
4. Shirakami Y, Watabe T, Obata H, Kaneda K, Ooe K, Liu Y, et al. Synthesis of [^{211}At]4-astato-L-phenylalanine by dihydroxyboryl-astatine substitution reaction in aqueous solution. Scientific Reports 2021 11:1 [Internet]. 2021 [cited 2023 Dec 4];11:1–7. Available from: https://www.nature.com/articles/s41598-021-92476-6
5. Rossin R, Van Den Bosch SM, Ten Hoeve W, Carvelli M, Versteegen RM, Lub J, et al. Highly reactive trans-cyclooctene tags with improved stability for diels–alder chemistry in living systems. Bioconjug Chem [Internet]. 2013 [cited 2023 Dec 4];24:1210–7. Available from: https://pubs.acs.org/doi/full/10.1021/bc400153y

PP44

The role of radiopharmaceutical [^{99m}Tc]Tc-MIBI in the evaluation of parathyroid adenoma and osteoporosis in young patients—a case report supporting its integration into standard clinical practice

Ismet Bajrami[1,2,3], Fakir Spahiu[2,3], Ylli Kaçiu[3], Emilija Janevik[2], Elena Drakalska[2], Sinisa Stojanoski[4], Armend Jashari[2,3*]
[1]University of Business and Technology UBT-Higher Education Institution Republic of Kosovo. [2]Faculty of Medical Science "Goce Delcev" University Stip, Republic of North Macedonia. [3]Nuclear Medicine Department in Clinical University Centre of Kosovo. [4]Institute of Pathophysiology and Nuclear Medicine "Acad Isac S. Tadzer", Faculty of Medicine University of "Ss. Cyril and Methodius", Skopje North Macedonia
*__Corresponding author__: armendjashari@yahoo.com

EJNMMI Radiopharmacy and Chemistry 2024, **9(1)**: PP44

Aim: This study aims to evaluate the sensitivity and specificity of [^{99m}Tc]Tc-MIBI as a radiopharmaceutical and parathyroid scintigraphy as a diagnostic tool for identifying parathyroid adenomas.
The patient presented in this paper as a case report can serve as confirmation of the effectiveness of the implementation of this method and supports its integration into our standard clinical practice.
Materials and methods: Data were obtained from a 32-year-old male patient reported to our department with generalized skeletal pain using a SPECT gamma camera and after injection of [^{99m}Tc]Tc-MIBI radiopharmaceutical at a dose of 555 MBq.
The patient was first referred to our department for a bone scan. A full body scan showed multiple foci suggestive of metabolic bone disease. A parathyroid scintigraphy was performed which revealed suspected adenoma which with biopsy-confirmed parathyroid adenoma.
Results: The parathyroid scintigraphy revealed the intensive focal accumulation of the [^{99m}Tc]Tc-MIBI in the left distal lobe of thyroid grand. The patient undergo surgery—lobectomiam gl. thyroidea lat sin et parathyroidectomiam lat. sin. HP findings were: adenoma glandula parathyroides lat. sin.
The bone pain was stopped after surgery and the level of the parathormone PTH was decreased. The patient recovered after surgery and released from hospital with osteoporotic therapy.
Conclusion: The SPECT camera-based evaluation of patients with recurrent or persistent hyperparathyroidism can provide valuable insights to prevent osteoporosis and other complications associated with untreated parathyroid adenoma. The high sensitivity and specificity of [^{99m}Tc]Tc-MIBI scintigraphy, combined with routine preoperative SPECT localization, are increasingly becoming standard practices.
Keywords: Tc99m-MIBI, Scintigraphy, Radiopharmaceutical, Diagnostic tool, Sensitivity

References

1. Petra Petranović Ovčariček, Luca Giovanella, Ignasi Carrió Gasset, Elif Hindié, Martin W.Huellner, Markus Luster, Arnoldo Piccardo, Theresia Weber, Jean-Noël Talbot & Frederik Anton Verburg European Journal of Nuclear Medicine and Molecular Imaging volume 48, pages2801–2822 (2021
2. Gary JR Cook, Micheal N Maisey, Keith E Britton and Vaseem Chengazi Fourth edition pages
3. M.M. Khalil (ed.), Basic Sciences of Nuclear Medicine, DOI:https://doi.org/10.1007/978-3-030-65245-6, # Springer Verlag Berlin Heidelberg 2011
4. Shankar Vallabhajosula, Ph.D. Molecular Imaging-Radiopharmaceuticals for PET and SPECT
5. Bennett S. Greenspan1, Gary Dillehay2, Charles Intenzo3, William C. Lavely, Michael O'Doherty,
6. Christopher J. Palestro 6, William Scheve 7, Michael G. Stabin 8, Delynn Sylvestros 7, and Mark Tulchinsky SNM Practice Guideline for Parathyroid Scintigraphy

PP45

In-hospital production and quality control of radiotracer [^{68}Ga]Ga-NODAGA-Exendin-4 on Trasis EasyOne synthesizer

Sonja Van den Block[1,2], Julien Masset[3], Charles Vriamont[3], Sophie Bourgeois[2],Vicky Caveliers[1,2]
[1]Vrije Universiteit Brussel (VUB), Molecular Imaging and Therapy Research Group (MITH), Laarbeeklaan 103, 1090 Brussels, Belgium. [2]Vrije Universiteit Brussel (VUB), Universitair Ziekenhuis Brussel (UZ Brussel), Nuclear Medicine Department,, Laarbeeklaan 101, 1090 Brussels, Belgium. [3]Trasis, Liège, Belgium.

EJNMMI Radiopharmacy and Chemistry 2024, **9(1)**: PP45

Aim: [^{68}Ga]Ga-NODAGA-Exendin-4 is a promising radiopharmaceutical for positron emission tomography (PET) in pancreatic β-cell imaging to non-invasively detect, diagnose, and preoperatively localize insulinomas [1]. Exendin-4 is a peptide analogue of glucagon-like peptide-1 (GLP-1) and binds with similar affinity to the GLP-1 receptor which is highly expressed in human insulinomas. The synthesis protocol of [^{68}Ga]Ga-NODAGA-Exendin-4 was reported earlier [2] but in this work we aimed at synthesizing the radiotracer in an automated production process on a Trasis EasyOne synthesizer in a hospital-based radiopharmacy.
Materials and methods: ^{68}Ge/^{68}Ga-generator Galli Eo™ (IRE-Elit Radiopharma, Fleurus, Belgium) was used to produce the radionuclide, and was connected to the EasyOne synthesis module (Trasis SA, Ans, Belgium). The chemicals, reagents and consumables for the radiolabelling procedure were commercially provided as single use kits (Trasis SA, Ans, Belgium). EDTA-Tween solution was obtained from ABX advanced biochemical compounds (Radeberg, Germany). The GMP grade precursor peptide Lys^{40}(NODAGA)-Exendin-4 (Acetate) was purchased from piCHEM GmbH (Raaba-Grambach, Austria). The radiolabelling was optimized using different incubation temperatures and times in combination with variable starting masses of the peptide. Quality control methods included visual inspection of the final product, determination of pH, radiochemical and radionuclide identity, radiochemical purity (RCP) by reverse phase high pressure liquid chromatography (RP-HPLC) and instant thin layer chromatography (iTLC), colloid detection by iTLC, bacterial endotoxins by limulus amebocyte lysate (LAL)-test, and filter integrity test. The ^{68}Ge-breakthrough of the generator was tested periodically. Sterility testing of the final product was done after conditional release, verifying the absence of microorganisms, essential for final release.
Results: The optimized automated synthesis of [^{68}Ga]Ga-NODAGA-Exendin-4 was performed with the following parameters: 10µg of precursor and incubation time of 15 min at 85°C. Acetate buffer was used during the labelling step, guaranteeing a stable pH while limiting the formation of ^{68}Ga-colloids. It resulted in a sterile final product > 500MBq with a RCP > 95%, comprising both oxidized and non-oxidized [^{68}Ga]Ga-NODAGA-Exendin-4, as the oxidized form of the tracer does not impact its quality [3,4]. Results show an apparent molar activity > 250GBq/µmol and a decay corrected (DC) overall radiochemical yield (RCY) of 81,6 ± 3,8% (n = 3). Three validation batches confirmed both the robustness of the synthesis process and the reproducibility in production yield and quality of the radiotracer.
Conclusion: [^{68}Ga]Ga-NODAGA-Exendin-4 was successfully synthesized on a Trasis EasyOne using the IRE ^{68}Ge/^{68}Ga-generator Galli Eo™, making the radiopharmaceutical available to a broader community. It can be used for application in clinical settings, routine productions, and translation to a GMP facility for further use in clinical trials.

References

1. Boss M, Buitinga M, Jansen TJP, Brom M, Visser EP, Gotthardt M. PET-based human dosimetry of ^{68}Ga-NODAGA-exendin-4, a tracer for β-cell imaging. Journal of Nuclear Medicine. 2020 Jan 1;61(1):112–6.

2. Tokgöz S, Boss M, Prasad S, Shah P, Laverman P, van Riel M, et al. Protocol for Clinical GLP-1 Receptor PET/CT Imaging with [^{68}Ga]Ga-NODAGA-Exendin-4. In: Methods in Molecular Biology. Humana Press Inc.; 2023. p. 143–53.
3. Janota B, Karczmarczyk U, Laszuk E, Garnuszek P, Mikołajczak R. Oxidation of methionine—Is it limiting the diagnostic properties of ^{99m}Tc-labeled exendin-4, a glucagon-like peptide-1 receptor agonist? Nuclear Medicine Review. 2016 Jul 29;19(2):104–10.
4. Jodal A, Lankat-Buttgereit B, Brom M, Schibli R, Béhé M. A comparison of three $^{67/68}$Ga-labelled exendin-4 derivatives for β-cell imaging on the GLP-1 receptor: the influence of the conjugation site of NODAGA as chelator. EJNMMI Res. 2014 Jun 22;4(1):1–10.

PP46

Manufacturing of investigational medicinal products under GMP conditions using the example of a radiopharmaceutical kit PSMA-T4 for labeling with technetium-99m

Anna Drapsa[1], Barbara Janota[1], Agnieszka Sawicka[1], Marcin Radzik[1], Wioletta Wojdowska[1], Piotr Garnuszek.[1]
[1]National Centre for Nuclear Research Radioisotope Centre POLATOM, Otwock, Poland.
EJNMMI Radiopharmacy and Chemistry 2024, **9(1)**: PP46

Aim: An investigational medicinal product (IMP) is defined as „a pharmaceutical form of an active substance or placebo being tested or used as a reference in a clinical trial, including products already with a marketing authorization but used or assembled (formulated or packaged) in a way different from the authorised form, or when used for an unauthorised indication, or when used to gain further information about the authorised form". The production of IMPs should be carried out in accordance with the GMP guidelines for IMPs (EU GMP Guide, Annex 13 and Annex 1 containing the principles of manufacturing sterile medicinal products). For each IMP quality documentation should be developed, including specifications, process validation, and analytical method validation. Significant parameter determining the safety of IMP is stability testing, which forms the basis for determining the expiration date.
This work presents the process of developing a new IMP on an example of PSMA-T4 radiopharmaceutical kit for preparation of ^{99m}Tc-labelled tracer for SPECT imaging loco-regional metastases and/or local relapse in patients with prostate cancer.
Materials and methods: As part of the development research, the composition of the PSMA-T4 kit was optimised, as well as the radiolabelling procedure. The PSMA-T4 one-vial kit formulation contains 23µg PSMA-T4 (net) and excipients: EDDA, tricine, $SnCl_2 \times 2H2O$ and phosphate buffer. To confirm that the manufacturing process is effective and reproducible, three validation batches were produced. Stability tests were performed for these batches: long-term, accelerated, transport conditions and photostability study. Following successful process validation, two batches of the PSMA-T4 kit were made and submitted for clinical trials.
Results: All the batches used for process validation complied with the acceptance criteria. Stability tests showed that the PSMA-T4 kit met the specification throughout its assumed 12-month shelf life when stored at 2-8oC. The results of first-in-human clinical trials showed that [^{99m}Tc]Tc-PSMA-T4 tracer demonstrated high sensitivity and specificity, which indicated potential usefulness of this radiopharmaceutical [1, 2]. The PSMA-T4 kit is currently during commercial clinical trials conducted in three clinical centres (ClinicalTrials.gov Identifier: NCT05847166).
Conclusion: The quality and manufacturing requirements for IMP are exactly the same as for a registered medicinal product. The requirements set for IMP manufacturers aim to ensure the safety of participants and the credibility of clinical data obtained in the course of a clinical trial.
The clinical impact and accessibility of ^{99m}Tc-tracers for the prostate specific membrane antigen (PSMA) and other targets would be greatly enhanced by the availability of a simple, 1-step PSMA-T4 kit-based labeling process.

References

1. Sergieva S, Mangaldgiev R, Dimcheva M, Nedev K, Zahariev Z, Robev B. SPECT-CT Imaging with [^{99m}Tc]PSMA-T4 in patients with Recurrent Prostate Cancer. Nucl. Med. Rev. 2021; 24(2):70–81.
2. Ćwikła J. B., Roslan M, Skoneczna I, Kempińska-Wróbel M, Maurin M, Rogowski W, Janota B, Szarowicz A, Garnuszek P. Initial Experience of Clinical Use of [^{99m}Tc]Tc-PSMA-T4 in Patients with Prostate Cancer. A Pilot Study. Pharmaceuticals. 2021; 14 (11), 1107.

PP50

Pharmacoeconomic analysis as a tool for more objective insight into the idea of introducing new radiopharmaceuticals

Katerina Kolevska[1,2*], Marija Atanasova Lazareva[1,2], Maja Chochevska[1,2], Maja Velichkovska[1], Filip Jolevski[1], Emilija Janevik-Ivanovska[2], Guenka Petrova[4], Ana Ugrinska[1,3], Bistra Angelovska.[2]
[1]University Institute of Positron Emission Tomography, Skopje, North Macedonia. [2]Faculty of Medical Sciences, Goce Delcev University, Stip, North Macedonia. [3]Faculty of Medicine, Ss. Cyril and Methodius University, Skopje, North Macedonia. [4]Faculty of Pharmacy, Medical University-Sofia, Bulgaria.
[*]**Corresponding author**: katerina.kolevska@ugd.edu.mk

EJNMMI Radiopharmacy and Chemistry 2024, **9(1)**: PP50
Aim: A pharmacoeconomic analysis was conducted within the framework of a feasibility study for establishing in-house production of zirconium-89 radioisotope and ^{89}Zr-based radiopharmaceuticals. The objective was to assess the cost–benefit ratio of utilizing ^{89}Zr-labeled trastuzumab PET/CT for testing patients with breast cancer instead of the biopsy method.
Materials and methods: An economic feasibility assessment was performed, encompassing financial and pharmacoeconomic analysis. A cost analysis was carried out to calculate the cost of in-house production of zirconium-89 radioisotope and ^{89}Zr-labeled trastuzumab radiopharmaceutical at the University Institute for Positron Emission Tomography (UI PET) and compare the costs of radioisotope production with the costs of purchasing a readymade product. The production process was simulated based on literature data.
A cost–benefit analysis was applied to assess the cost–benefit ratio of either testing patients with ^{89}Zr-labeled trastuzumab PET/CT or biopsy as the comparison alternatives. Unit costs were sourced from an intentional marketing analysis, institute data review and analysis of the National Health Insurance Fund tariff costs. The result was measured with the number of tested patients with both alternatives.
Results: The cost analysis has demonstrated that the cost of an in-house prepared radioisotope is lower compared to the cost of a purchased radioisotope, thus the in-house production of zirconium-89 radioisotope is more profitable than its purchase. In terms of ^{89}Zr-labeled trastuzumab, the cost analysis estimated approximately the cost of producing this radiopharmaceutical in three cases: production for 4, 7 and 10 patients.
The net benefits of using the ^{89}Zr-labeled trastuzumab are higher than using biopsy. The cost–benefit ratio assessed by cost–benefit analysis differs in the three analysed cases, and it is 3.8, 2.4 and 1.84 for radiopharmaceutical production for 4, 7 and 10 patients respectively.
Conclusion: Pharmacoeconomic analysis results, as part of a feasibility study for establishing radioisotope production, are not single determinants for the overall feasibility estimation, but also the results of other analyses should be considered. Aspects that should be taken into account when establishing the production of new radioisotopes and radiopharmaceuticals are the production technology that will be used, the unique characteristics of a given radioisotope, as well as the number of planned patients per production, which would optimize the use of production capacities.

PP51

Application of autoradiography to study radionuclide distribution in 3D culture models

Catarina I. G. Pinto[1*], Laura Ordas[2], Joana F. Guerreiro[1*], Sophie Poty[2], Jean-Pierre Pouget[2], Filipa Mendes[1, 3]
[1]C[2]TN – Centro de Ciências e Tecnologias Nucleares, Instituto Superior Técnico, Universidade de Lisboa, Lisboa, Portugal. [2]Institut de Recherche en Cancérologie de Montpellier (IRCM), Institut National de la Santé et de la Recherche Médicale (INSERM) Unité 1194, Université de Montpellier, Institut Régional du Cancer de Montpellier (ICM), Montpellier, France. [3]DECN – Departamento de Engenharia e Ciências Nucleares, Instituto Superior Técnico, Universidade de Lisboa, Lisboa, Portugal.
[*]**Corresponding mail**: catarina.pinto@tecnico.ulisboa.pt

EJNMMI Radiopharmacy and Chemistry 2024, **9(1)**: PP51

Aim: Nowadays, advanced cell culture models have been brought to the spotlight due to their capacity to better mimic in vivo tumor features, which grant them an increased clinical translatability in comparison to conventional monolayer cultures. An example of these advanced models is the multicellular tumor spheroid, a 3D culture able to reproduce the metabolic and proliferative gradients of in vivo tumors [1, 2]. Considering the complexity of in vivo 3D tumors, and in the preclinical setting, models like spheroids, it is important to evaluate the ability of radiopharmaceuticals under development to penetrate through these structures. A possible solution to this question is a classical technique, commonly used to visualize radionuclides, named autoradiography. In fact, autoradiography includes a set of techniques that allow imaging of beta-emitting radionuclides present in a sample. There are two main detection systems: energy storage systems and particle-counting systems. The first are based on the measurement of the amount of energy emitted by the radionuclides, while the second are based on the measurement of the number of beta particles being emitted [3]. The main applications of these techniques in biological studies include whole-body autoradiography, receptor autoradiography, high-resolution gel analysis, and DNA sequencing among others. In the present work, we further add a new application to this technique by studying the penetration of simple radiocompounds, [^{177}Lu]$LuCl_3$, [^{68}Ga]$GaCl_3$ and [^{64}Cu]$CuCl_2$, in spheroids derived from prostate and glioblastoma cell lines, characterized by different compactness among them.

Materials and methods: Here, we performed autoradiography using a particle-counting system, in particular a solid membrane detector, to study the distribution of ^{177}Lu, ^{68}Ga, and ^{64}Cu radionuclides with different types of decay (β^-, β^+, or both) in spheroid slices derived from prostate cancer (22RV1, DU145, and LNCaP), glioblastoma (T98G, U87, and U373) and a non-tumoral prostate (RWPE) cell line.

Results: Overall, the image quality is dependent on the spheroids' compactness and on the type of emission of the radionuclide under evaluation. Nonetheless, the results obtained revealed that all radionuclides could successfully penetrate through the spheroids, being uniformly distributed among the spheroid slices.

Conclusion: The present work reinforced the utility of autoradiography as a tool to image the distribution of radionuclides in advanced culture models, as the case of spheroids, in a simple and rapid fashion that allows for real-time analysis of the signal emitted by the radionuclides.

Acknowledgments
This work was supported by Fundação para a Ciência e Tecnologia (FCT), Portugal, through the grant UID/Multi/04349/2019 to C2TN, the PhD Fellowship 2020.07119.BD to CIGPinto. FCT and Campus France are also acknowledged for Program PESSOA grant 2021.09137.CBM to FMendes and 47890XB to JPPouget.

References

1. Engrácia DM, Pinto CIG, Mendes F. Cancer 3D models for metallodrug preclinical testing. Int J Mol Sci. 2023; 24(15):11,915.
2. Pinto CIG, Bucar S, Alves V, Fonseca A, Abrunhosa AJ, da Silva CL, et al. Copper-64 chloride exhibits therapeutic potential in three-dimensional cellular models of prostate cancer. Front Mol Biosci. 2020; 7:609,172.
3. Barthe N, Maîtrejean S, Carvou N, Cardona A. Chapter 9—High-resolution beta imaging. In: L'Annunziata MF, editor. Handbook of Radioactivity Analysis: Volume 2 (Fourth Edition). Academic Press; 2020. P. 669–727.

Current address [+] CIISA—Centro de Investigação Interdisciplinar em Sanidade Animal, Faculdade de Medicina Veterinária, Universidade de Lisboa, Lisboa, Portugal and Laboratório Associado para Ciência Animal e Veterinária (AL4AnimalS).

PP52

Validation of an in-house process for the production of Sodium ^{18}F-fluoride radiopharmaceutical

Marija Atanasova Lazareva[1,2*], Maja Chochevska[1,2], Katerina Kolevska[1,2], Maja Velichkovska[1], Filip Jolevski[1], Ana Ugrinska[1,3], Emilija Janevik Ivanovska.[2]
[1]University Institute of Positron Emission Tomography, Skopje, North Macedonia. [2]Faculty of Medical Sciences, Goce Delcev University, Stip, North Macedonia. [3]Faculty of Medicine, Ss. Cyril and Methodius University, Skopje, North Macedonia.
[*]**Corresponding author**: marija.atanasova@ugd.edu.mk

EJNMMI Radiopharmacy and Chemistry 2024, **9(1)**: PP52

Aim: An original in-house method for the synthesis of Sodium ^{18}F-fluoride radiopharmaceutical ([^{18}F]NaF) was designed and developed. The process validation of [^{18}F]NaF radiopharmaceutical production was performed with the aim of confirming the reproducibility of the process to produce a final product with consistent quality.

Materials and methods: The protocol for process validation was developed following the recommendations outlined in FDA Guidance for Industry Process Validation: General Principles and Practices and EANM Guidance on validation and qualification of processes and operations involving radiopharmaceuticals. Three consecutive batches of [^{18}F]NaF were produced on different days under the same predetermined conditions.

The production process (synthesis and dispensing) was carried out on the dispensing module Clio, using a modified single-use kit for dispensing. The modification involved installing a Y-connector and QMA cartridge on the kit. The quality of the final product should be in accordance with [^{18}F]NaF monograph of European Pharmacopeia.

The tested parameters were approximate pH value (pH strips), identification (half-life determination and difference in retention times), chemical and radiochemical purity (ion-exchange HPLC isocratic method with radiodetector and conductivity detector serial connected), radionuclidic purity (gamma-ray spectrometry), bacterial endotoxins (chromogenic LAL method) and sterility.

Results: The results of tested quality parameters for the three batches were within the defined acceptance criteria. The difference in retention times was 33.18, 32.76 and 32.82 s, and the measured half-life was 1.80,1.84 and 1.82 h. The approximate pH value was 6.5–7.0 for each batch. No chemical and radiochemical impurities were detected in the three batches. Only ^{18}F-fluoride peaks were detected on the radiochromatograms, while no fluoride peaks were observed on the chromatograms obtained from the conductivity detector.

Radionuclidic purity testing showed a very low percentage of radionuclide impurities (0.0000883, 0.00000171 and 0.000001633%), which indicates a high radionuclidic purity.

The results from the bacterial endotoxins testing were < 5 EU/mL for each batch and all tested samples were found to be sterile.

Conclusion: The process validation results confirmed that the in-house designed production process for manufacturing [^{18}F]NaF radiopharmaceutical is capable of consistently producing a product that fulfils the quality requirements defined in the European Pharmacopoeia monograph (Ph. Eur. 01/2008:2100).

PP53

Preliminary evaluation of a novel Temozolomide-based molecule radiolabeled with ^{99m}Tc as a theranostic agent against glioblastoma

Evangelia-Alexandra Salvanou[1], Stavroula G. Kyrkou[2], Vasileios-Panagiotis Bistas[2], Vasiliki Zoi[3], Maria Giannakopoulou[3], George A. Alexiou[3],

Athanasios P. Kyritsis[3], Savvas Thalasselis[4], Andreas G. Tzakos[2*], Penelope Bouziotis[1*]
[1]Institute of Nuclear & Radiological Sciences & Technology, Energy & Safety, INRASTES, NCSR "Demokritos", 15,341, Athens, Greece. [2]University of Ioannina, Department of Chemistry, Section of Organic Chemistry and Biochemistry, 45,110, Ioannina, Greece. [3]Neurosurgical Institute, University of Ioannina, 45,500 Ioannina, Greece. [4]SYN INNOVATION LABORATORIES SA, Athens, Greece.
[*]**Corresponding author**: atzakos@uoi.gr; bouzioti@rrp.demokritos.gr

EJNMMI Radiopharmacy and Chemistry 2024, **9(1)**: PP53

Aim: Glioblastoma is the most common and aggressive type of primary brain tumor in adults, accounting for 50% of malignant brain tumors (1). Standard of care includes surgery, radiotherapy, and chemotherapy with temozolomide (TMZ), however with a median overall survival of 15–20 months (2). Consequently, the development of a sensitive diagnostic or theranostic tool for the early detection and treatment of this type of cancer is crucial. Tetrofosmin (TF) radiolabeled with Technetium-99m (^{99m}Tc) is extensively used for glioblastoma SPECT imaging (3). The present work aims to develop an innovative theranostic molecule based on TF and TMZ that will be able to provide targeted imaging and therapy against glioblastoma.

Materials and methods: An analog of bis[(2-pyridyl)methyl]amine was synthesized by starting with tert-Butyl (4-aminobutyl) carbamate and 2-pyridinecarboxyaldehyde (4). The final therapeutic compound (SP2F) was created by amide coupling with TMZ acid following processing and purification by High Performance Liquid Chromatography (HPLC). The analog was characterized by NMR spectroscopy and mass spectrometry. Cell viability was evaluated by the trypan blue exclusion assay in T98 and U87 cell lines up to 72h. Radiolabeling of SP2F was accomplished via the $[^{99m}Tc][Tc(CO)_3(OH_2)_3]^+$ precursor at 40°C for 45min. Radiolabeling yield was assessed with HPLC. In vitro stability was evaluated at room temperature (RT) and serum up to 24h post-radiolabeling. Ex vivo biodistribution of the [^{99m}Tc]Tc-SP2F was investigated at 1, 4 and 24h post-injection and compared to ex vivo biodistribution with [^{99m}Tc]Tc-TF.

Results: The yield after purification of the final therapeutic compound was 30%. The IC50 value of SP2F and TMZ in T98 human glioma cells was 62 μM and 330 μM, respectively, while in U87 cells IC50 was 60 μM and 50 μM. Radiolabeling yields > 90% were achieved without further purification. [^{99m}Tc]Tc-SP2F was stable at RT and serum up to 24h post-radiolabeling. The ex vivo biodistribution of [^{99m}Tc]Tc-SP2F in comparison to [^{99m}Tc]Tc-TF was demonstrated in normal CFW mice.

Conclusion: An analog of TMZ and bis-2-picolylamine has been developed. Beyond its inherent cytotoxic properties, this molecule serves the extremely significant function of monitoring the transfer of the cytotoxic drug TMZ to cancer cells. Facile and robust radiolabeling of the SP2F with the ^{99m}Tc carbonyls precursor was accomplished. Preliminary ex vivo biodistribution results in comparison to [^{99m}Tc]Tc-TF have demonstrated the diagnostic potential of SP2F. Therapeutic efficacy studies in glioblastoma xenografts will follow in order to assess the therapeutic potential of this molecule.

References

1. Schaff LR, Mellinghoff IK. Glioblastoma and Other Primary Brain Malignancies in Adults: A Review. JAMA. 2023 Feb 21;329(7):574–87.
2. Rong L, Li N, Zhang Z. Emerging therapies for glioblastoma: current state and future directions. J Exp Clin Cancer Res. 2022 Apr 15;41(1):142.
3. Alexiou GA, Xourgia X, Gerogianni P, Vartholomatos E, Kalef-Ezra JA, Fotopoulos AD, et al. ^{99m}Tc-Tetrofosmin Uptake Correlates with the Sensitivity of Glioblastoma Cell Lines to Temozolomide. World J Nucl Med. 2017;16(1):45–50.
4. Kasten BB, Ma X, Cheng K, Bu L, Slocumb WS, Hayes TR, et al. Isothiocyanate-Functionalized Bifunctional Chelates and fac-[MI(CO)3] + (M = Re, ^{99m}Tc) Complexes for Targeting uPAR in Prostate Cancer. Bioconjug Chem. 2016 Jan 20;27(1):130–42.

PP54

PSMA-targeted Radioconjugates Bearing a DNA Intercalator for Enhanced Auger Therapy of Prostate cancer

Joana F. Santos[1], Rita Julião[1], Catarina D. Silva[1*], Célia Fernandes[1,2], Francisco Silva[1], Paula Raposinho[1,2], Filipa Mendes[1,2], Margarida Sobral[3,4*], Rafael P. Silveira[3], Ana M. Urbano[3,5], Paulo J. Oliveira[3], António Paulo[1,2]
[1]C2TN Centro de Ciências e Tecnologias Nucleares, Instituto Superior Técnico, Universidade de Lisboa, Estrada Nacional 10 (km 139,7), 2695–066 Bobadela LRS, Portugal. [2]Departamento de Engenharia e Ciências Nucleares, Instituto Superior Técnico, Universidade de Lisboa, Portugal. [3]Molecular Physical Chemistry R&D Unit, Department of Life Sciences, University of Coimbra, Portugal. [4]CNC-Center for Neuroscience and Cell Biology, UC-Biotech, Cantanhede, Portugal. [5]Center of Investigation in Environment, Genetics and Oncobiology, University of Coimbra, Portugal.
[*]**Corresponding author**: catarinadsilva@tecnico.ulisboa.pt; msobral@cnc.uc.pt

EJNMMI Radiopharmacy and Chemistry 2024, **9(1)**: PP54

Aim: Prostate Specific Membrane Antigen (PSMA) derivatives having the Glu-urea-Lys binding motif were labeled with different imaging and therapeutic radionuclides, emerging as promising tools for the theranostics of prostate cancer (PCa). This research effort led to the development of the beta minus emitter [^{177}Lu]Lu-PSMA-617 (PluvictoTM), approved by the FDA for targeted radionuclide therapy of prostate cancer [1]. However, the use of beta minus emitters in targeted radionuclide therapy (TRT) has some limitations, such as nephrotoxicity and beta radiation resistance. To overcome these limitations, TRT with Auger electron (AE) emitters is considered a possible alternative because AEs have a high linear energy transfer (LET) within a nanometric range and can cause highly lethal and selective effects in target tumor cells, particularly if placed near the DNA in the cell nucleus [2,3]. Having this in mind, we have designed and synthesized dual-targeting ^{111}In-complexes bearing a PSMA inhibitor and an acridine orange (AO) intercalator to promote specific uptake by prostate cancer cells and the selective accumulation in their nucleus. In this way, we expected to obtain AE emitting radioconjugates with the ability to induce selective and enhanced radiobiological effects in PSMA(+) PCa cells, opening new avenues for the design of radiotherapeutics for PCa theranostics.

Materials and methods: DOTA-based chelators bearing PSMA-617 and AO groups were synthesized and labeled with ^{111}In. The preclinical evaluation of the resulting radioconjugates included cellular uptake, internalization and PSMA-blocking assays in cell lines expressing different levels of PSMA, as well as the evaluation of radiobiological effects (e.g., clonogenic survival) in the same cell lines.

Results: The ^{111}In-complexes were obtained with high radiochemical yield and purity presenting high in vitro stability. The dual-targeted ^{111}In-complexes displayed high cellular uptake and internalization in the PSMA-positive PC3 PIP cells while presenting a negligible internalization in the PSMA-negative PC3 Flu cells. The specificity of PSMA targeting was further confirmed by blocking studies. The performed radiobiological studies indicated that the dual-targeted radioconjugates compromise cellular viability in a dose-dependent manner, pointing out for more enhanced radiobiological effects when compared with the single-targeted congeners.

Conclusion: The dual-targeted ^{111}In-complexes exhibited high and specific internalization in PSMA + PCa cells and extensive radiotoxicity in the same cell lines revealing their potential for Auger therapy of PCa cancer. Further cell studies are underway to fully ascertain the mechanisms underlying the observed radiobiological effects with prospects to proceed to therapeutic assays in PSMA(+) tumor-bearing mice.

Acknowledgments
This work was funded by Fundação para a Ciência e Tecnologia, Portugal (projects UID/Multi/04349/2019 and PTDC /MED-QUI/1554/2020). The authors acknowledge Prof M. Pomper (Johns Hopkins Medical School, Baltimore, USA) for the kind gift of the PC3 PIP-Flu cell lines.

Joana F. Santos acknowledges the PhD grant PRT/BD/154612/2023. Catarina D. Silva acknowledges the PhD grant PRT/BD/154625/2023. Margarida Sobral acknowledges the PhD grant 2021.06783.BD.

References

1. Hennrich U, Eder M, [^{177}Lu]Lu-PSMA-617 (PluvictoTM): The First FDA-Approved Radiotherapeutical for Treatment of Prostate Cancer. Pharmaceuticals. 2022, 15; 1292.
2. Bolcaen J, Gizawy M, Terry S, Paulo A, Cornelissen B, Korde A, Engle J, Radchenko V, Howell R. Marshalling the Potential of Auger Electron Radiopharmaceutical Therapy. J. Nucl. Med. 2023; 64: 1344–1351.
3. Santos J, Braz M, Raposinho P, Cleeren F, Cassels I, Leekens S, Cawthorne C, Mendes F, Fernandes C, Paulo A. Synthesis and Preclinical Evaluation of PSMA-Targeted ^{111}In-Radioconjugates Containing a Mitochondria-Tropic Triphenylphosphonium Carrier. Mol. Pharmaceutics. 2024; 21: 216 — 233.

PP55

Therapeutic Efficacy of [^{177}Lu]Lu-DMSA-SPIONs in a Mouse CT26 and 4T1 Xenograft Model

Dragana Stanković[1*], Magdalena Radović[1], Marija Mirković[1], Zorana Milanović[1], Aljoša Stanković [2], Milica Mijović[3], Miloš Ognjanović[1], Drina Janković[1], Aleksandar Vukadinović[1], Bratislav Antić[1], Sanja Vranješ-Đurić[1], Miroslav Savić[4], Željko Prijović.[1]
[1]Laboratory for radioisotopes,„VINČA" Institute of Nuclear Sciences—National Institute of the Republic of Serbia, University of Belgrade, Belgrade, Serbia. [2]University Clinical Centre of the Republic of Srpska, Banja Luka, Bosnia and Herzegovina. [3]Faculty of Medicine, University of Priština, Kosovska Mitrovica, Serbia. [4]Faculty of Pharmacy, University of Belgrade, Belgrade, Serbia.
[*]**Corresponding author**: dragana.s@vin.bg.ac.rs

EJNMMI Radiopharmacy and Chemistry 2024, **9(1)**: PP55
Abstract published here: https://www.mdpi.com/1999-4923/15/7/1943

PP56

NOAR—Network for Optimized Astatine-211 labeled Radiopharmaceuticals EU COST Action CA19114

Jean-Francois Gestin[1], Emma Aneheim[2], Penelope Bouziotis[3], Petra Kolenc[4], Marek Pruzynski[5], Antero Abrunhosa[6], Emilija Janevik-Ivanovska[7], Andreas I. Jensen[8], Sture Lindegren[9], Joelle Gaschet[10], Stig Palm[9], François Guerard[10], Laurent Navarro[11], Dana Niculae[12*]
[1]Université de Nantes, Inserm, CNRS, Centre de Recherche en Cancérologie et Immunologie Nantes—Angers (CRCINA)—UMR 1232, ERL 6001, F-44000 Nantes, France. [2]Department of Medical Radiation Sciences, Institute of Clinical Sciences, the Sahlgrenska Academy, University of Gothenburg; 41,345 Gothenburg, Sweden. [3]Radiochemical Studies Laboratory, INRASTES, National Center for Scientific Research Demokritos, Aghia Paraskevi 15,341 Athens, Greece. [4]Department of Nuclear Medicine, University Medical Centre Ljubljana, 1000 Ljubljana, Slovenia. [5]Institute of Nuclear Chemistry and Technology, Dorodna 16, 03–195 Warsaw, Poland. [6]ICNAS/UC, Institute for Nuclear Sciences Applied to Health, University of Coimbra, 3000–548 Coimbra, Portugal. [7]Goce Delcev University, Faculty of Medical Sciences, Stip, Republic of North Macedonia. [8]Center for Nanomedicine and Theranostics (The Hevesy Laboratory), DTU Health Technology, Technical University of Denmark (DTU), Ørsteds Plads 345C, 2800 Lyngby, Denmark. [9]Department of Medical Radiation Sciences, Institute of Clinical Sciences, the Sahlgrenska Academy, University of Gothenburg; 413 45 Gothenburg, Sweden. [10]Université de Nantes, CNRS, Inserm, CRCINA, 44,000, Nantes, France. [11]Precirix, Brussels, Belgium. [12]Radiopharmaceutical Research Centre, Horia Hulubei National Institute for Physics and Nuclear Engineerig, Magurele, 077125, Romania.
EJNMMI Radiopharmacy and Chemistry 2024, **9(1)**: PP56

Aim: COST project Network for Optimized Astatine-labeled Radiopharmaceuticals (NOAR) brings together European and international laboratories of excellence, Astatine-211 production centers, hospitals, industry and patient associations, and thus covering the entire innovation value chain.
The main goal is to demonstrate that Astatine-211, promising radionuclide used for targeted alpha therapy (TAT), can be established as the standard for the treatment of cancerous tumors.
The project implementation includes: European network of astatine-211 nodes, defining better therapeutic strategies through harmonized protocols, exchange of good practices for production and quality control.
Materials and methods: The COST-NOAR action ensures efficient interdisciplinary, cross-sectoral and international exchange of knowledge, effective networking within all stakeholders, promoting the medical application of Astatine-211, significantly increase fundamental and applied knowledge of TAT technology.
Results: The results so far show that the projected goals through the 5-working groups have already generated interest in the development of the production of radiopharmaceuticals, dosimetry, preclinical and clinical research, ensuring critical mass that raises the capacity for further collaboration and expertise to establish a worldwide network dedicated to Astatine-211.
An important contribution is training a new generation of early career researchers and PhD students, promoting interdisciplinary competences through international mobility.
Conclusion: The implementation of ATNodes results in strong collaboration between researchers from COST member countries, and also international partner countries, in order to share expertise and establish a worldwide network devoted to astatine-211. The Action provides insights into European research landscape, favoring better organization models and particular emphasis on training and mobility of a new generation of young researchers and PhD students.

Reference

1. https://astatine-net.eu/

PP57

Automated production of [^{68}Ga]Ga-deferoxamine on two different synthesis modules for bacterial infection imaging

Martin Kraihammer[1,2*], Milos Petrik[3], Christine Rangger[1], Hubertus Haas[4], Irene Virgolini[1], Clemens Decristoforo.[1]
[1]Department of Nuclear Medicine, Medical University of Innsbruck, Innsbruck, Austria.[2]Institute of Nuclear Medicine and Endocrinology, Kepler University Hospital, Linz, Austria. [3]Institute of Molecular and Translational Medicine, Faculty of Medicine and Dentistry, Palacky University, Olomouc, Czech Republic. [4]Institute of Molecular Biology, Biocenter, Medical University of Innsbruck, Innsbruck, Austria.
[*]**Corresponding author**: martin.kraihammer@i-med.ac.at

EJNMMI Radiopharmacy and Chemistry 2024, **9(1)**: PP57
Aim: Nosocomial bacterial infections, especially with drug-resistant pathogens, are a growing concern in clinical practice worldwide. Among other species, Staphylococcus aureus, Klebsiella pneumoniae and Pseudomonas aeruginosa are causing infectious diseases associated with high mortality. Early diagnosis and accurate localization of these infections could improve patient outcome and would allow to monitor antibacterial treatment more precisely.
Deferoxamine (DFO B) belongs to a group of biomolecules called siderophores, which show high binding affinity for iron, among other metals. These low-molecular weight (< 1 kDa) substances play a pivotal role in the iron metabolism of most fungal and bacterial species, including human pathogenic microorganisms. Labelling siderophores with Ga-68 could enable precise localisation of pathogens within the body, a concept already proven in preclinical PET imaging of S. aureus and P. aeruginosa mouse infection models with [^{68}Ga]Ga-deferoxamine1. This study aimed to establish automated production of [^{68}Ga]Ga-deferoxamine on two different synthesis modules for clinical trial application.
Materials and methods: Automated synthesis was performed on two different synthesis modules: 1) Modular-Lab PharmTracer module (Eckert & Ziegler Radiopharma GmbH, Germany) and 2) GRP 3V module (Scintomics Molecular Applied Theranostics Technologies GmbH,

Germany) in combination with a GalliaPharm ^{68}Ge/^{68}Ga generator (Eckert & Ziegler Radiopharma GmbH, Germany). Radiolabelling of 100 µg of deferoxamine in an acetic acid/sodium acetate buffer system with post-labelling solid phase extraction (SPE) purification and sterile filtration was conducted.
The final products were characterised by TLC and RP-HPLC, among other test methods, according to Pharmacopeial standards for other ^{68}Ga-radiopharmaceuticals. Validation of the production processes was performed with four master batches for each synthesis module.
Results: Sufficient activity yield for both production processes was achieved (405.9 ± 26 MBq for PharmTracer vs. 443.2 ± 133 MBq for GRP 3V) using a single ^{68}Ge/^{68}Ga generator.
Quality control for various parameters according to Pharmacopeial standards of radiopharmaceuticals met all pre-defined specifications and showed stability over 2 h post production. Radiochemical purity measured by radio-HPLC was > 95% for all master batches (n = 4 for each synthesis module).
Conclusion: Radiolabelling of deferoxamine with Ga-68 can easily be performed under mild reaction conditions with the two described automated synthesis approaches, enabling cost-efficient and reproducible in-house production for patient use. A clinical trial is currently ongoing (EudraCT No. 2020-002868-3).

Reference

1. Petrik M, Umlaufova E, Raclavsky V, Palyzova A, Havlicek V, Pfister J, Mair C, Novy Z, Popper M, Hajduch M, Decristoforo C. ^{68}Ga-labelled desferrioxamine-B for bacterial infection imaging. Eur J Nucl Med Mol Imaging. 2021; 48(2):372-382.

PP58

First automatic multidose injection of the [^{177}Lu]Lu-ITG-PSMA-1 in Bosnia and Herzegovina

Aljoša Stanković[1,2]
[1]Clinical department of nuclear medicine and thyroid gland disease, University clinical centre of the Republic of Srpska, Banja Luka, Bosnia and Herzegovina. [2]Medical faculty, University of Banja Luka, Banja Luka, Bosnia and Herzegovina.
EJNMMI Radiopharmacy and Chemistry 2024, **9(1)**: PP58

Aim: [^{177}Lu]Lu-ITG-PSMA-1 is a therapeutic agent used for radioligand therapy (RLT) indicated for the treatment of metastasized castration-resistant prostate cancer (mCRPC).[1][2] From September 2022. the clinical department of nuclear medicine in Banja Luka has started with the synthesis and application of this agent. After the synthesis using the automatic module, [^{177}Lu]Lu-ITG-PSMA-1 was manually diluted to 100 ml with saline and infused intravenously within 30 min. This route of application brought high radiation exposure to the patient but also to the medical staff. Procurement of injector IRIS® Comecer gave the possibility to automatically inject high-volume therapeutic radiopharmaceuticals with minimal radiation exposure. In comparison to automatic injections of ^{177}Lu-DOTA peptides using this device, there was no data for the application of [^{177}Lu]Lu-ITG-PSMA-1.[3].
Materials and methods: The [^{177}Lu]Lu-ITG-PSMA-1 was initiated for a 65-year-old male patient with mCRPC by an interdisciplinary tumor board decision. The labeling was performed in an automatic module with 8 GBq of [^{177}Lu]$LuCl_3$ solution and 115 µg of the peptide. After synthesis, the activity in the product vial was measured in a dose calibrator and it was 7,7 GBq/20mL. Sufficient patient hydration was ensured by intravenous infusion of 250 ml of saline starting 30 min in advance.
Results: Since the software allowed injection of a maximum of 5 mL per cycle, the application needed to be performed through 4 cycles (1850 MBq per cycle). Patency of the patient administration set was done with 2 mL of saline, followed by 10 ml saline flush (flow rate of 10 ml/min) after every cycle. The total injection time was 10 min and the total volume of the dose was 81 mL. There was no adverse reaction during application and staff were at a safe distance from the patient. After application, the product vial was taken out from the injector and remained activity was 0,3 GBq, which confirmed the given dose (7,4 GBq) and precision of the device. The patient did not have any side effects during the isolation period (24h) and one planar post-therapeutic emission scan ruled out extravasation and confirmed physiological tracer biodistribution.
Conclusion: Use of the automatic multidose injector for [^{177}Lu]Lu-ITG-PSMA-1 is safe and convenient for the patient. Moreover, radiation exposure of the employees will be significantly reduced for future application cycles of this novel therapeutic radiopharmaceutical.

References

1. Kratochwil C, Fendler WP, Eiber M, Hofman MS, Emmett L, Calais J, et al. Joint EANM/SNMMI procedure guideline for the use of ^{177}Lu-labeled PSMA-targeted radioligand-therapy (^{177}Lu-PSMA-RLT). Eur J Nucl Med Mol Imaging. 2023;50(9):2830–45.
2. Schuchardt C, Zhang J, Kulkarni HR, Chen X, Müller D, Baum RP. Prostate-Specific Membrane Antigen Radioligand Therapy Using ^{177}Lu-PSMA I&T and ^{177}Lu-PSMA-617 in Patients with Metastatic Castration-Resistant Prostate Cancer: Comparison of Safety, Biodistribution, and Dosimetry. J Nucl Med. 2022 Aug 1];63(8):1199–207.
3. Tylski P, Pina-Jomir G, Bournaud-Salinas C, Jalade P. Tissue dose estimation after extravasation of ^{177}Lu-DOTATATE. EJNMMI Phys. 2021 Dec 1;8(1).

PP59

Unlocking the potential of ^{45}Ti for PET-imaging: the formation and evaluation of the Ti-DOTA complex

Eduard Pogorilyy[1], Tamal Roy[1], Erwan Le Roux[1*]
[1]Department of Chemistry, University of Bergen, Bergen, Norway.
[*]**Corresponding author:** Erwan.LeRoux@uib.no

EJNMMI Radiopharmacy and Chemistry 2024, **9(1)**: PP59
Aim: Among the relatively efficient radiometals, the radionuclide titanium-45 isotope, stands out as a radionuclide of interest for its beneficial qualities in Positron Emission Tomography (PET).[1] This isotope is notable for its high positron emission rate (85%) coupled with a relatively low average kinetic energy of positrons, leading to both reduced radiation doses for patients and enhanced image resolution. Additionally, its half-life of ca. 3.1 h is advantageous in clinical settings, allowing for imaging procedures to be conducted several hours post-injection, thereby simplifying logistical considerations, for instance. The production of ^{45}Ti in substantial quantities is feasible through the ^{45}Sc(p,n)^{45}Ti reaction.[2]
Materials and methods: The expansion of the collection of chelators capable of efficiently binding non-radioactive Ti^{4+} ions indeed represent a significant scientific objective.[1] In this work, we present the proof-of-concept that the ligand DOTA (1,4,7,10-tetraazacyclododecane 1,4,7,10-tetraacetic acid) can form a complex with the Ti^{4+} ion (Fig. 1). Formation of the Ti-DOTA complex was confirmed through a range of advanced analytical methods that together validated both the successful formation and detailed analysis of the Ti-DOTA complex.

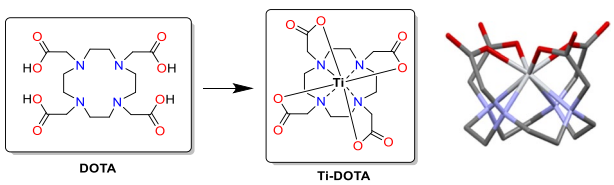

Fig. 1 Synthesis of nonradioactive titanium complex of DOTA.
Following the production and detailed examination of the complex, we conducted a series of in vitro metal competition studies, as the result, it was observed a low level of demetallation of Ti-DOTA complex. This evaluation demonstrated that Ti-DOTA complex is highly suitable for use in PET-imaging.

Acknowledgements
This research was funded by the Trond Mohn Foundation, project no. TMS2019TMT07 "Centre for PET tracer development".

References

1. Boros E., Packard A. B. Radioactive Transition Metals for Imaging and Therapy. Chem. Rev. 2019; 119: 870–901.
2. Costa P., Metello L. F., Alves F., Naia M. D. Cyclotron Production of Unconventional Radionuclides for PET Imaging: the Example of Titanium-45 and Its Applications. Instruments 2018; 2:8.

PP60

Automated fluorine-18 radiolabelling via alkyne-azide cycloaddition reaction on dual peptide-functionalized liposomes surface for in vivo PET imaging

Marco N Iannone[1*]; Marcelo Kravicz[2]; Stefano Stucchi[1,2]; Elisa Vino[1]; Elia A Turolla[1,2]; Antonia Antoniou[3]; Arianna Amenta[3]; Paolo Rainone[2,4]; Silvia Valtorta[4–6]; Sara Pellegrino[7]; Daniele Passarella[7]; Rosa Moresco[1,2,4,5]; Pierfausto Seneci[3]; Francesca Re[2]; Sergio Todde[1,2]
[1]Tecnomed Foundation, University of Milano-Bicocca, via Pergolesi 33, 20,900 Monza, Italy. [2]School of Medicine and Surgery, University of Milano-Bicocca, via Raoul Follereau 3, 20,854 Vedano al Lambro (MB), Italy. [3]Chemistry Department, University of Milan, Via Golgi 19, 20,133 Milan, Italy. [4]Nuclear Medicine Department, San Raffaele Scientific Institute IRCCS, Via Olgettina 48, 20,132 Milan, Italy. [5]Institute of Molecular Bioimaging and Physiology (IBFM), National Research Council (CNR), Via F.lli Cervi 93, 20,054 Segrate, Italy. [6]National Biodiversity Future Center (NBFC), Piazza Marina 61, 90,129, Palermo, Italy. [7]Pharmaceutical Sciences Department, University of Milan, Via Golgi 19, 20,133 Milan, Italy.
[*]**Corresponding author**: marco.iannone@unimib.it

EJNMMI Radiopharmacy and Chemistry 2024, **9(1)**: PP60

Aim: Due to their valuable combination among drug delivery, controlled release and specificity toward a target organ/tissue, liposomes are considered promising agents for imaging with positron emission tomography (PET).
Radiolabeling of liposomes surfaces, functionalized with suitable chelators, is generally performed using radiometals [1] but radiolabeling with fluorine-18 may be useful for short kinetic and biodistribution studies.
Here we report an automated procedure for the radiolabeling of liposome surface with fluorine-18 via copper(I)-catalysed (CuAAC) and "copper-free" alkyne-azide cycloaddition approaches. Liposomes were also functionalized with a peptide deriving from the receptor-binding domain of apolipoprotein E (mApoE) and with a metalloproteinase (MMP)-sensitive lipopeptide (MSLP), for further use in biodistribution studies aimed to evaluate their biodistribution in vivo in orthotopic mouse models of glioma with PET.
Materials and methods: m_A-DOPE and m_{CA}-DOPE were synthesized in-house, while liposomes were formulated from stock solutions of cholesterol and sphingomyelin and functionalized using suitable amounts of the requested peptides.
Radiolabelling procedures have been performed using a commercially available automated radiosynthesis system (Trasis-AllinOne). [^{18}F]fluoroazide was prepared following a previously published procedure [2].
PET biodistribution studies were performed on an orthotopic glioma model (Gli36ΔEGFR).
Results: The liposome surface was functionalized with two dioleoylphosphatidylethanolamine modified constructs bearing a terminal alkyne (m_A-DOPE) or a cyclooctyne (m_{CA}-DOPE) (Fig. 1) and reacted with fluorine-18 labelled azide (Fig. 1) through a "click" cycloaddition reaction.
In case of m_A-DOPE functionalized liposome, bio-orthogonal copper(I)-catalyzed cycloaddition (CuAAC) occurred at room temperature, and liposome **[^{18}F]1** (Fig. 1, approach 1) was obtained in ready-to-inject formulation (RCYndc = 9.6 ± 0.8%, radiochemical purity > 95%, overall radiosynthesis time of 126 min).
Liposome **[^{18}F]2** (Fig. 1) was obtained by reacting [^{18}F]fluoroazide with m_{CA}-DOPE functionalized liposome formulation heating at 40–50 °C in a "copper free" cycloaddition approach (Fig. 1, approach 2) (RCYndc = 5.6 ± 0.9%, purity > 95%, overall radiosynthesis time of 129 min).
The latter was chosen to radiolabel a m_{CA}-DOPE, mApoE and MSLP functionalized liposome (RCYndc = 4.2 ± 1.0%, purity > 95%, overall radiosynthesis time of 129 min) in order to investigate the in vivo uptake in an orthotopic mouse model of glioma (Gli36ΔEGFR cell line) by PET/CT. The results showed higher uptake in the tumor for mApoE and MSLP-functionalized liposomes.

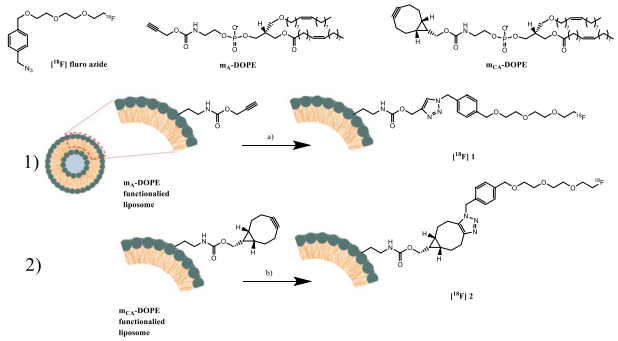

Fig. 1 *Liposome surface radiolabelling approaches:* (**a**) [^{18}F]fluoroazide, $CuSO_4 \cdot 5H_2O$, ascorbic acid, rt, 20 min, ~ 76%. (**b**) [^{18}F]fluoroazide, 40–50 °C, 30 min, ~ 40%.

Conclusion: In conclusion, we have implemented a fully automated method for the radiolabelling with fluorine-18 of liposome surface by CuAAC and copper-free click chemistry. Moreover, a mApoE and MSLP-functionalized derivatives showed interesting tumor/background biodistribution ratio that prompted for further characterization.

References

1. Man F., Gawne P.J., de Rosales R.T.M., *Adv. Drug Deliv. Rev.* **2019**, *143*, 134.
2. Iannone M.N., Stucchi S., Turolla E.A. et al., *J Label Compd Radiopharm,* **2022**,65:48–62.

PP61

Development of [^{18}F]AlF-RESCA-FSH as a diagnostic probe for ovarian cancer.

Maria Kominia[1]*, Kavya Prasad[1], Philip Elsinga[1], Bart Cornelissen[1], Erik de Vries[1], Inês Antunes.[1]
[1]Department of Nuclear Medicine and Molecular Imaging, University of Groningen, University Medical Center Groningen, Groningen, The Netherlands.
[*]**Corresponding author**: m.kominia@umcg.nl

EJNMMI Radiopharmacy and Chemistry 2024, **9(1)**: PP61

Aim: Ovarian cancer (OC) is one of the leading causes of cancer-related death among women[1]. The follicle-stimulating hormone (FSH) receptor is a transmembrane G protein-coupled receptor that is highly expressed in OC cells and tumor-associated vasculature. However, its expression in non-malignant tissue and inflammation is limited[2], suggesting that FSH receptors could be a potential target for imaging OC. To this aim, we developed [^{18}F]AlF-RESCA-FSH and performed preliminary in vitro binding studies.
Materials and methods: Synthesis of [^{18}F]AlF-RESCA-FSH was performed manually. An [^{18}F]AlF^{2+} solution was freshly prepared by adding ca. 200 MBq [^{18}F]fluoride in 400 µL NaCl 0.9% to 50 nmol $AlCl_3$ in 100 µL of NaOAc buffer (0.1 M, pH 4.5). This solution was added to the activated chelator RESCA-TFP (50 nmol, 15 min, RT). The resulting [^{18}F]AlF-RESCA-TFP was purified using an HLB cartridge, after which was conjugated to human recombinant FSH (50 µg, 50°C, 30 min, pH 8.4) and purified using a PD10 cartridge. This conversion was monitored by ITLC (eluent 30%ACN/Water) and SEC UPLC (ACQUITY UPLC Protein BEH SEC Guard Column, 200Å, 1.7 µm, 4.6 mm X 30 mm and Acquity UPLC Protein BEH SEC, 125A, 1.7 µm, 4.6 × 150 mm, 10% IPA in 50 mM sodium phosphate, 250 mM sodium chloride, flow = 0.2 mL/

min). In-vitro cellular uptake of [^{18}F]AlF-RESCA-FSH was performed in OVCAR3 cells (FSHR-(+), as confirmed by Western Blot) in the presence or absence of recombinant FSH.
Results: The final product [^{18}F]AlF-RESCA-FSH, was formed at room temperature with 1.05 ± 0.55% conversion (based on [^{18}F]fluoride). The radiochemical purity based on UPLC and ITLC was > 95% within 90 min of the total synthesis time. Preliminary in-vitro experiments with [^{18}F]AlF-RESCA-FSH in OVCAR3 cells (n = 2, p = 0.723) showed no reduction of the tracer's uptake when blocked with 0.5 µg of FSH. However, when blocked with 2 µg of FSH, the uptake of [^{18}F]AlF-RESCA-FSH in OVCAR3 cells was significantly reduced by 42% (n = 1, p = 0.0004).
Conclusion: We were able to conjugate the [^{18}F]AlF-RESCA-TFP complex to recombinant FSH. Preliminary in-vitro data suggests the selectivity of [^{18}F]AlF-RESCA-FSH towards FSH receptors. Further studies are warranted to improve its production and to confirm its selectivity.

References

1. Momenimovahed Z, Tiznobaik A, Taheri S, Salehiniya H. Ovarian cancer in the world: epidemiology and risk factors. Int J Womens Health. 2019;11:287–299.
2. Papadimitriou, K., Kountourakis, P., Kottorou, A.E. et al. Follicle-Stimulating Hormone Receptor (FSHR): A Promising Tool in Oncology?. Mol Diagn Ther 2016; 20:523–530.

PP62

Design and evaluation of Cu(II)-HMPAO complex as a representative model for assessing the potential of ^{64}Cu radiopharmaceutical

Marija Mirković[1,*], Ferdinand Belaj[2], Marko Perić[1], Dalibor Stanković[1,3], Magdalena Radović[1], Zorana Milanović[1], Sanja Vranješ-Đurić[1], Drina Janković[1], Ilija Cvijetić[3], Ljiljana E. Mihajlović-Lalić.[4]
[1]Laboratory for radioisotopes,„VINČA" Institute of Nuclear Sciences—National Institute of the Republic of Serbia, University of Belgrade, Belgrade, Serbia. [2]Institute of Chemistry, University of Graz, Graz, Austria. [3]Faculty of Chemistry, University of Belgrade, Belgrade, Serbia. [4]Innovative Centre Faculty of Chemistry Belgrade, Belgrade, Serbia.
[*]**Correspoding author:** mmarija@vin.bg.ac.rs

EJNMMI Radiopharmacy and Chemistry 2024, **9(1)**: PP62
Aim: Considering the biological properties of the Cu(II) complexes and the properties of hexamethylpropylene amine oxime (HMPAO) ligand employed in medical applications [1–3], we synthesized the Cu(II) complex with meso-HMPAO ligand as a model to estimate the potential of ^{64}Cu radiopharmaceutical.
Materials and methods: The synthesis of the Cu(II)-HMPAO complex (Fig. 1) follows a general procedure, wherein the metal precursor, copper(II) acetate monohydrate, is dissolved in MeOH and reacts with a hot MeOH ligand suspension in a 1:1 molar ratio. The complex's structure was analyzed using FTIR, cyclic voltammetry, and X-ray technique. Additionally, we explored the interactions of the synthesized metal complex with deoxyribonucleic acid (DNA) and human serum albumin (HSA).

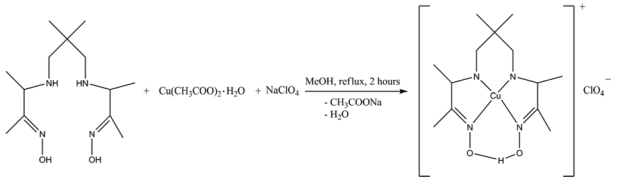

Fig. 1 Reaction scheme for synthesis Cu(II)-HMPAO complex.
Results: A new copper complex with meso-HMPAO ligand was synthesized via a reaction of methanolic solutions of the metal precursor and meso-HMPAO refluxed for 2 h. The crystalline purple product was precipitated by adding a proper amount of counterion. Isolated crystalline precipitate was air-stable, partially soluble in water and EtOH, soluble in polar (DMSO, MeOH, and CH_3CN) but insoluble in nonpolar solvents (toluene and benzene). From the characterization methods, HMPAO has been shown to act as a tetradentate ligand that coordinates through the nitrogen atoms of the oxime and amine groups. The results of cyclic voltammetry of copper(II) acetate monohydrate, meso-HMPAO, and Cu(II)-HMPAO complex show that the formation of the complex strongly affects the redox behavior of the electroactive groups. Electrochemical analysis confirmed the binding between the complex and DNA molecule (Fig. 2A). The fluorescence titration experiments revealed a moderate binding affinity of the [Cu-HMPAO] ClO_4 complex to HAS (Fig. 2B). To investigate the binding mode of Cu(II)-HMPAO complex to HSA, molecular docking simulations were performed. The two representative docking solutions are displayed in Fig. 2C. These findings clarify that Cu(II)-HMPAO complex exhibits partial accessibility to the tryptophan fluorophore, given that the highest-affinity binding site is more than 20 Å away from Trp214.

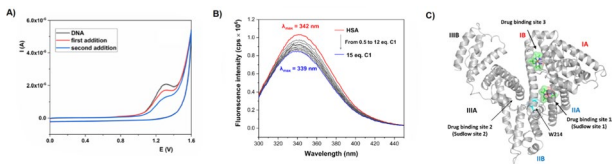

Fig. 2 A) Changes in guanine from DNA oxidation current after the addition of Cu(II)-HMPAO complex. B) The changes in the fluorescence emission spectrum of HSA upon the addition of Cu(II)-HMPAO complex. C) The binding modes of Cu(II)-HMPAO complex (green surface) on HSA. Trp214 is displayed as blue sticks with a blue transparent surface..
Conclusion: We conceived, synthesized, and characterized a complex involving copper and hexamethylpropylene amine oxime (HMPAO) ligand. Electrochemical assessments validated the interaction between the complex and DNA molecules. Simultaneously, spectroscopic findings suggested that the Cu(II)-HMPAO complex exhibits moderate binding affinity with human serum albumin (HSA), indicating its potential for efficient transport and storage within the human body. The experimental outcomes provide the impetus for further exploration of this complex, either as a promising anticancer agent or for its potential application in nuclear medicine as a ^{64}Cu radiopharmaceutical.

References

1. Holcman K, Rubiś P, Stępień A, Graczyk K, Podolec P, Kostkiewicz M. The Diagnostic Value of ^{99m}Tc-HMPAO-Labelled White Blood Cell Scintigraphy and ^{18}F-FDG PET/CT in Cardiac Device-Related Infective Endocarditis—A Systematic Review. J. Pers. Med. 2021; 11: 1016.
2. Roddie M E, Peters A M, Danpure H J, Osman S, Henderson B L, Lavender J P, Carroll M J, Neirinckx R D, Duncan Kelly J. Inflammation: imaging with Tc-99m HMPAO-labeled leukocytes. Radiology 1988; 166: 767–772.
3. Yeo J M, Lim X, Khan Z, Pal S. Systematic review of the diagnostic utility of SPECT imaging in dementia. Eur. Arch. Psychiatry Clin. Neurosci. 2013; 263: 539–552.

PP63

Using Epin boronic esters as substrates improves the copper-mediated ^{18}F-fluorination of arenes

Anna M. Doze[1,2*], Maria Kominia[1], Simon N. Blok[1], Gert Luurtsema[1], Wiktor Szymanski[3,4], Ben L. Feringa[2], Philip H. Elsinga.[1]
[1]Department of Nuclear Medicine and Molecular Imaging, University of Groningen, University Medical Centre Groningen, 9713 GZ Groningen, The Netherlands. [2]Centre of Systems Chemistry, Stratingh Institute for Chemistry, Faculty for Science and Engineering, University of Groningen, 9747 AG Groningen, The Netherlands. [3]Department of Medicinal Chemistry, Photopharmacology and Imaging, Groningen Research Institute of Pharmacy, University of Groningen, Antonius Deusinglaan 1, 9713 AV, Groningen, The Netherlands. [4]Department of Radiology, University of Groningen, University Medical Centre Groningen, 9713 GZ Groningen, The Netherlands.
[*]**Corresponding author**: a.m.doze@umcg.n

EJNMMI Radiopharmacy and Chemistry 2024, **9(1)**: PP63

Aim: A highly promising and emerging method for the ^{18}F-labelling of arenes is the copper-catalyzed radiofluorination of pinacol boronic acid ester (Bpin)-structures, introduced by the Gouveneur group. [1] This method tolerates a wide range of functional groups, enabling its application for a variety of aromatic systems including clinically relevant radiotracers. Despite the success of this copper-mediated radiofluorination, this method also has several limitations. These include modest or fluctuating radiochemical yields, practical challenges in purification and stability of the Bpin-structures and challenges in the purification of the radiolabeled product from the hydrodeborylated precursor. [2] In this work, we explore the copper-mediated radiofluorination of arenes based on an alternative boronic ester structure. These 1,1,2,2-tetraethylene glycol ester (Epin)-precursors have been reported to be more stable, easier to purify and to be more reactive in Suzuki coupling reactions. [3] We aimed to investigate whether these Epins are also better candidates for the copper-mediated ^{18}F-radiofluorination.

Materials and methods: Various Epin- and Bpin- derived structures, bearing both electron-withdrawing and electron-donating substituents, were synthesized and characterized. Their stabilities were tested using liquid-chromatography coupled with mass spectrometry (LCMS). Subsequently, the radiolabeling of the Epin-precursors was compared to that of the traditionally employed Bpin-precursors. For this, dry [^{18}F] fluoride was dissolved in dimethylacetamide (DMA), added to a mixture of Epin- or Bpin-precursor and Cu(OTf)2(py)4 in DMA and stirred for 20 min at 120 oC. The labelling was evaluated using radio-TLC and radio-HPLC.

Results: In general, purification of the Epin-precursors using silica gel chromatography was easier than the corresponding Bpin-precursors. The Epin-precursors were also found to be more stable in water. For example, the Bpin-precursor for 4-fluoro-1-pyrrolidine was fully degraded after 40 min in water/acetonitrile (1:1), while the Epin-precursor was still intact (> 95%). The use of Epin-precursor also led to significantly higher radiochemical conversion of 68 ± 10% (n = 5), compared to the Bpin precursor (5 ± 3%). Correspondingly, the radiochemical yield was significantly higher (43% vs 2%). Also for other examples, the Epin-precursors led to better radiochemical conversions and yields. Notably, in many cases the reaction mixtures of the Epin precursors led to cleaner HPLC chromatograms, suggesting the presence of lower amounts of the difficult-to-separate hydrodeborylated precursor.

Conclusion: This study demonstrates that Epin-precursors are more stable than the corresponding Bpin-precursors and that therefore their ^{18}F-fluorination occurs with higher and more reproducible yields. Therefore, we conclude that Epin-precursors can offer a good alternative for Bpin-precursors in copper-mediated radiofluorination studies.

References

1. Tredwell M, Preshlock SM, Taylor NJ, Gruber S, Huiban M, Passchier J, et al. A general copper-mediated nucleophilic.^{18}F-fluorination of arenes. Angew. Chem. Int. Ed. 2014; 53 (30):7751–55
2. Orlovskaya V, Fedorova O, Kuznetsova O, Krasikova R. Cu-mediated radiofluorination of aryl pinacolboronate esters: alcohols as solvents with application to 6-L-[.^{18}F]FDOPA synthesis. Eur. J. Org. Chem. 2020; 2020 (45):7079–7086
3. Oka N, Yamada T, Sajiki H, Akai S, Ikawa T. Aryl boronic esters are stable on silica gel and reactive under Suzuki–Miyaura coupling conditions. Org. Lett. 2022; 24 (19), 3510–3514

PP64

Effects of the conjugation method on the stability of a ^{161}Tb-labeled antibody

Camille Van Laere[1,2], Tomas Opsomer[2], Koen Vermeulen[2], Maarten Ooms[2], Frederik Cleeren[1*]

[1]Department of Pharmaceutical and Pharmacological sciences, KU Leuven, Leuven, Belgium. [2]Belgian Nuclear Research Centre (SCK CEN), Mol, Belgium.

***Corresponding author**: Frederik.cleeren@kuleuven.be

EJNMMI Radiopharmacy and Chemistry 2024, **9(1)**: PP64

Aim: Antibodies are generally modified with a bifunctional chelator by random conjugation to lysins using isothiocyanates or activated esters to form thiourea and amide bonds, respectively. Prior research has suggested that the use of isothiocyanates may compromise the stability of the conjugate in NaCl-containing buffers. This is attributed to the radiation-induced formation of hypochlorite which can disrupt the integrity of the thiourea bond [1,2]. Here, we present findings on the stability of a radiolabeled monoclonal antibody (mAb) within phosphate buffered saline (PBS) and human serum. In addition, we introduce a novel bifunctional chelator 3p-*C*-NETA-PEG$_4$-TFP, designed to improve the radiolabeling efficiency and stability of the radiopharmaceutical.

Materials and methods: p-NCS-Bz-DOTA-GA (5 eq.) was conjugated to a mAb (1 eq., 500 µL, 0.05 M $NaHCO_3$, pH 8.5, 2 h, 25°C) and purified using Amicon Centrifugal Filter Units (MWCO 30 kDa). The purified conjugate (10 µM; 0.1 M CH_3COONa, pH 4.7) was radiolabeled with [^{161}Tb]$TbCl_3$ (100 MBq, 50 mM HCl) at 40 °C for 1 h. Radiochemical yields were determined by iTLC-SG eluted with sodium citrate buffer (0.1 M, pH 5.8) and radio-SEC analysis. Next, the stability was evaluated in human serum and PBS at 37 °C.

The 3p-*C*-NETA precursor was synthesized according to a previously published protocol [3]. The 3p-*C*-NETA (1 eq., 500 µL acetonitrile) was added in droplets to a solution of DIPEA (1.5 eq.) and bis-PEG$_4$-TFP (1.5 eq., 500 µL acetonitrile). The resulting mixture was stirred at 60 °C for 48 h and purified with HPLC.

Results: DOTA-GA-conjugated mAb was radiolabeled with [^{161}Tb]$TbCl_3$ with a radiochemical yield of 98.0 ± 0.3% and a specific molar activity of 2.5 MBq/nmol. The radiopharmaceutical showed reduced stability in PBS (Fig. 1), probably due to cleavage of the thiourea bond by the presence of Cl^- in the buffer [1,2]. The construct was however more stable in serum which was hypothesized to be attributed to the sulfur atoms present in serum proteins scavenging the hypochlorite. 3p-C-NETA-PEG$_4$-TFP, a compound with a different random lysine coupling method was successfully synthesized and will be tested further.

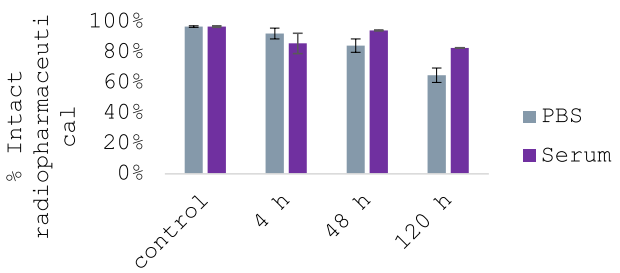

Fig. 1 In vitro stability of a ^{161}Tb-labeled mAb.

Conclusions: The [^{161}Tb]Tb-DOTA-GA-mAb was stable in serum up to 48 h, but not in PBS, probably due to instability of the thiourea bond in presence of Cl^-. Other random lysine coupling methods will be tested to find the most stable one. Finally, we are in the process of evaluating the bifunctional chelator 3p-*C*-NETA-PEG$_4$-TFP to improve radiolabeling efficiency and stability.

References

1. Chomet M, Schreurs M, Bolijn MJ, Verlaan M, Beaino W, Brown K, et al. Head-to-head comparison of DFO* and DFO chelators: selection of the best candidate for clinical ^{89}Zr-immuno-PET. Eur J Nucl Med Mol Imaging. 2021 Mar;48(3):694–707.
2. Vugts DJ, Klaver C, Sewing C, Poot AJ, Adamzek K, Huegli S, et al. Comparison of the octadentate bifunctional chelator DFO*-pPhe-NCS and the clinically used hexadentate bifunctional chelator DFO-pPhe-NCS for 89Zr-immuno-PET. Eur J Nucl Med Mol Imaging. 2017;44(2):286–95.
3. Ahenkorah S, Murce E, Cawthorne C, Ketchemen JP, Deroose CM, Cardinaels T, et al. 3p-C-NETA: A versatile and effective chelator for development of AI ^{18}F-labeled and therapeutic radiopharmaceuticals. Theranostics. 2022;12(13):5971–85.

PP65

Liquid target production of zirconium-89 for antibody labelling

Agnieszka Chmura[1,2], Andrzej Czudek[1], Artur Tomasik[1], Anna Kastelik-Hryniewiecka[1], Karolina Miszczyszyn[1], Łukasz Sochaczewski[3], Małgorzata Żółtowska[3], Renata Mikolajczak[3], Fredrik Y Frejd[4], Marika Nestor[4], Gabriela Kramer-Marek[1,5]
[1]Division of Radiopharmacy and Preclinical PET Imaging, National Research Institute of Oncology, Gliwice, Poland. [2]Silesian University of Technology, Gliwice, Poland. [3]National Centre for Nuclear Research, Radioisotope Centre POLATOM, Otwock, Poland. [4]Department of Immunology, Genetics and Pathology, Uppsala University, Uppsala, Sweden. [5]Division of Radiotherapy and Imaging, The Institute of Cancer Research, London, UK.
EJNMMI Radiopharmacy and Chemistry 2024, **9(1)**: PP65

Aim: The utilisation of immuno-PET radioconjugates targeting specific cell-surface markers represents a transformative shift in guiding patient management [1]. Among the various radioisotopes, zirconium-89 (^{89}Zr) is the most frequently used in immuno-PET due to its near-ideal physical and chemical properties. The production of ^{89}Zr using liquid target (LT) systems can expand the availability of this isotope for cyclotron facilities. Therefore, we have produced ^{89}Zr using a cyclotron (IBA, Cyclone 18/9) by irradiating the aqueous solution of yttrium nitrate (Y(NO3)3·6H2O). Subsequently, the isotope was used to radiolabel an anti-CD44v6 monoclonal antibody for the detection of this highly overexpressed marker in head and neck squamous cell carcinoma (HNSCC) [2].
Materials and methods: The target material was prepared using two different concentrations of an aqueous solution of yttrium (III) nitrate (99,8%) (1,5 and 0,3 g/ml) in 0,8M nitric acid. The material was loaded into the niobium insert of LT (IBA) on Cyclone 18/9 (IBA) cyclotron and irradiated with proton beam with energies ~ 18MeV and ~ 13,4 MeV. Extraction and purification of ^{89}Zr was carried out in 3 steps on Reform-Plus APS-3300 (Bioscan) synthesis module with Zr-resin columns (Triskem). The final radionuclide purity was measured by gamma spectrometer with HPGe detector. The isotopes impurities were measured using ICP-OES (Perkin Elmer) and TXRF (Bruker). Afterwards, the ^{89}Zr was used for labelling of anti-CD44v6 mAb. Radiochemical purity was determined with TLC (Raytest). The specificity of radioconjugate binding was assessed in vitro using cell lines with different CD44v6 expression (A431, SCC25 and UMSCC74b).
Results: Irradiation with proton beam with energy < 14MeV (n = 9) led to the production of ^{89}Zr with high radionuclide purity > 99%. The purification yield markedly increased by decreasing yttrium (III) nitrate concentration in the target material. The main radionuclide impurities were ^{88}Zr and ^{88}Y. ICP-OES and TXRF (Fig. 1A and 1B) confirmed the presence of the Zn and Y in product (n = 4). The radioconjugate ([^{89}Zr]Zr-DFO-CD44v6) was produced with a radiochemical purity (RCP) > 99%. The [^{89}Zr]Zr-DFO-CD44v6 specificity binding studies showed a correlation between the cell-associated radioactivity and the level of CD44v6 expression in the selected cell lines (Fig. 1C).

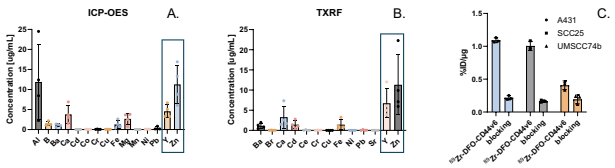

Fig. 1 (**A**) Isotopes concentration in the final product (n = 4) confirmed by ICP-OES and (**B**) TXRF for samples with 1,5 g/ml of yttrium (III) nitrate. (**C**) Specificity of the radioconjugate binding in vitro.
Conclusion: We demonstrated the feasibility of producing and purifying ^{89}Zr in-house using IBA cyclotron on a liquid target and confirmed successful radiolabelling of CD44v6 mAb with the isotope.

References

1. De Lucas ÁG, Lamminmäki U, López-Picón FR. ImmunoPET Directed to the Brain: A New Tool for Preclinical and Clinical Neuroscience. Biomolecules. 2023;13(1):164.
2. Hassn Mesrati M, Syafruddin SE, Mohtar MA, Syahir A. CD44: A Multifunctional Mediator of Cancer Progression. Biomolecules. 2021;11(12):1850.

PP66

Copper-61: From Bench to Bedside

Nicole Schubert[1*], Francesco De Rose[1], Leila Jaafar.[1]
[1]Nuclidium AG, Im Erasmushaus, Basel, Switzerland.
[*]**Corresponding author**: info@nuclidium.com.

EJNMMI Radiopharmacy and Chemistry 2024, **9(1)**: PP66
Aim: In recent years, many new radiopharmaceuticals and radionuclides have been developed for positron emission tomography (PET), focusing on metal radioisotopes due to their versatile chemistry and beneficial physical properties.
Materials and methods: Copper-61 is a highly desirable radionuclide for labelling PET tracers in pre-clinical and clinical settings. It has a half-life of 3.33 h and is a favourable positron emitter (61% β+, Emax = 1.216 MeV). The moderate half-life of 3.33 h provides an advantage over the current clinical standard, gallium-68 ($T_{1/2}$ = 68 min), allowing PET scans to be conducted at later timepoints after injection. This results in improved diagnostic performance due to higher image contrast and better tumour-to-background ratios over time compared to ^{68}Ga-labelled tracers.
Results: We present a method for producing the radiopharmaceutical precursor [^{61}Cu]$CuCl_2$ with high specificity, radionuclide purity and yield from irradiated nickel targets. Additionally, we demonstrate the synthesis of [^{61}Cu]Cu-NuriPro, a PSMA-targeting PET radiotracer, and its successful application in first-in-human experiments.
The irradiated nickel targets are transferred from a standard medical cyclotron to a hot cell, where the fully automated purification process is carried out. First, the solid target is dissolved in acid, and the solution is then transferred to a FASTlab chemistry module, where sequential ion exchange resins are used to purify the [^{61}Cu]CuCl2. The produced [^{61}Cu]CuCl2 has a radiochemical purity of 99.999%.
Conclusion: Our [^{61}Cu]Cu-NuriPro first-in-human imaging detected multifocal metastatic prostate cancer, bringing hope for better cancer diagnosis and treatment. Our team carefully evaluated various factors, including radiochemical yield, radiochemical purity, and stability, which play a crucial role in the production, distribution, and clinical viability of PET tracers. These exci;ng results demonstrate the immense potential of ^{61}Cu-labelled radiotracers for PSMA-targeted imaging and present opportunities for developing other ^{61}Cu-labelled agents for various clinically valuable targets.

Publisher's Note